

Modeling of Miniaturized, Multiband and Ultra-Wideband Fractal Antenna

Sikiru Olayinka Zakariyya

Submitted to the
Institute of Graduate Studies and Research
in partial fulfilment of the requirements for the Degree of

Master of Science
in
Electrical and Electronic Engineering

Eastern Mediterranean University
September 2015
Gazimağusa, North Cyprus

Approval of the Institute of Graduate Studies and Research

Prof. Dr. Serhan iftioęlu
Acting Director

I certify that this thesis satisfies all the requirements as a thesis for the degree of Master of Science in Electrical and Electronic Engineering.

Prof. Dr. Hasan Demirel
Chair, Department of Electrical and Electronic Engineering

We certify that we have read this thesis and that in our opinion it is fully adequate in scope and quality as a thesis for the degree of Master of Science in Electrical and Electronic Engineering.

Asst. Prof. Dr. Rasime Uyguroęlu
Supervisor

Examining Committee

1. Prof. Dr. Hasan Demirel

2. Prof. Dr. Abdullah Y. Oztoprak

3. Asst. Prof. Dr. Rasime Uyguroęlu

ABSTRACT

Due to advancements in communication technology, there is an increase in the demand of small size, low cost, multiband and wideband antennas. With a view to address these demands, a fractal design was employed in this study. Despite the advantages provided by these antennas, miniaturization and performance enhanced further by using a partial ground plane. This research work presents an antenna which is based on the well-known Sierpinski Carpet fractal with iteration factor of $1/3$. The antenna was designed up to third iteration with a view of achieving miniaturization. A simple antenna was designed for purpose of comparison, by using a simple rectangular slot at the middle of the patch and a 34.88% size reduction was achieved at the same resonant frequency. This is achieved by introducing defected ground structure into the design which gives the antenna wideband behaviour with bandwidth of 442MHz at centre frequency of 2.45GHz.

A multiband square patch antenna using third order Sierpinski Carpet was designed to operate at 1.88GHz alongside a new circular fractal antenna up to third iteration with a partial ground structure to achieve ultra wideband behaviour with a bandwidth of 8.18GHz at centre frequency of 2.54GHz. The designed antenna was simulated using three dimensional finite integration time domain commercial software microwave studio. The objective of this thesis to design a fractal antenna with small size, multiband and wideband behaviour was largely met.

Keywords: Miniaturized, Multiband and Ultra Wideband antenna, Fractal geometries, Partial Ground Structure.

ÖZ

İletişim teknolojisindeki gelişmeler ile, küçük boyutlu, düşük maliyetli, çok bantlı ve geniş bantlı anten taleplerinde büyük bir artış olmuştur. Bu talepleri karşılamak üzere yapılan bu çalışmada fraktal anten tasarımları gerçekleştirilmiştir. Fraktal antenlerin sağladığı bu avantajlara rağmen, performansının artırılması ve boyutlarının küçültülmesi için kısmi yer düzlemi uygulamak gerekmiştir. Bu çalışma, 1/3 yineleme faktörü ile bilinen Sierpinski Halı fractal anten tasarımına dayalı bir tasarım içermektedir. Anten, minyatür anten elde etmek amacıyla üçüncü yineleme faktörüne (iterasyon) kadar tasarlanmıştır. Karmaşık yapıları ile bilinen fraktal antenlerin performansı ile karşılaştırma maksatlı basit bir anten tasarlanmış ve aynı rezonans frekansında antenin boyutunda %34.88 küçülme sağlanmıştır. Tasarımda, arızalı zemin yapısı kullanılarak, geniş band davranışı gösteren 442MHz'lik bir bant elde edilmiştir.

Bu çalışmada, 1.88GHz frekansında üçüncü dereceden kare Sierpinski Halı ile kısmi yer düzlemlili, dairesel fraktal anten tasarımı gerçekleştirilmiştir. İki durum için de anten çok band ve çok geniş band elde etmek için üçüncü iterasyona kadar tasarlanmıştır. Kısmi yer düzlemi ile ultra geniş band davranış gösteren dairesel fraktal anten, 2.54GHz merkez frekansında 8.18GHz'lik bir bant genişliğine sahiptir. Çalışma tam-dalga benzetim programı kullanılarak yapılmıştır.

Bu tezin amacı olan, küçük boyutu, çok bantlı ve geniş bantlı davranış gösteren bir fraktal anten tasarımı büyük ölçüde gerçekleştirilmiştir.

Anahtar Kelimeler: minyatür, Çok Bantlı ve Ultra Geniş Bantlı anten, Fraktal geometri, Kısmi yer düzlemi

ACKNOWLEDGEMENT

All praise is due to Allah Subhanahu Watahala for his blessing and guidance. I sincerely express my gratitude to my supervisor Assist. Prof. Dr. Rasime Uyguroğlu whose encouragement, patience, advice and guidance has made this work possible and also for giving me the opportunity to carry out this thesis under her guidance. My gratitude also goes to Prof. Dr. Abdullah .Y. Oztoprak for his endless advice and guidance.

To all the staff of the Department of Electrical and Electronics Engineering, those whom we had contact with directly or indirectly I say a big thank you to you all for all the knowledge and advice I gained from you.

My deepest gratitude goes to my family and Engineer Abdulwahab for their prayers, encouragement, and financial support. May Allah reward you all for me.

To all my friends in Nigeria and TRNC, thank you all for all the prayers, motivations and encouragement.

TABLE OF CONTENTS

ABSTRACT	iii
ÖZ	iv
ACKNOWLEDGEMENT	vi
LIST OF TABLES	ix
LIST OF FIGURES	x
LIST OF SYMBOLS /ABBREVIATIONS	xiii
1 INTRODUCTION	1
1.1 Thesis Objective	2
1.2 Thesis Contribution	2
1.3 Thesis Organization.....	2
2 PLANAR ANTENNAS AND FRACTAL ANTENNAS.....	3
2.1 Antenna Definition	3
2.2 Antenna Parameters.....	3
2.3 Patch Antenna.....	5
2.3.1 Advantage of Patch Antenna	5
2.3.2 Disadvantage of Patch Antenna.....	6
2.3.3 Feeding Techniques:	6
2.3.4 Microstrip Line Feed	6
2.3.5 Coaxial Probe Feeding.....	7
2.3.6 Aperture Coupling	8
2.3.7 Proximity Couple Fed.....	8
2.4 Literature Survey of Fractal Antenna	9

2.4.1 Koch Curve	10
2.4.2 Sierpinski Gasket	10
2.4.3 Sierpinski Carpet.....	11
3 MINIATURIZATION OF PATCH ANTENNA	17
3.1 Sierpinski Fractal Miniaturized Rectangular Patch Antenna Design	17
3.1.1 Edge Fed Sierpinski Carpet First Iteration	23
3.1.2 Edge Fed Sierpinski Carpet Second Iteration	26
3.1.3 Edge Fed Sierpinski Carpet Third Iteration.....	29
3.2 Using a Single Slot to Design Miniaturized Patch Antenna.....	31
3.2.1 Modified Miniaturized Patch Antenna With U Slot Ground To Increase Bandwidth.....	36
4 SIERPINSKI CARPET FRACTAL FOR MULTIBANDS APPLICATIONS	41
4.1 Antenna Design	41
4.1.1 Sierpinski Carpet First Iteration.....	46
4.1.2 Sierpinski Carpet Second Iteration	50
5 CIRCULAR FRACTAL ANTENNA WITH PARTIAL GROUND PLANE.....	57
5.1 Antenna design	57
5.2 Circular Fractal with Partial Ground Plane.	70
6 CONCLUSION AND FUTURE WORK.....	79
6.1 Conclusion.....	79
6.2 Future Work	80
REFERENCES.....	81

LIST OF TABLES

Table 2.1: Dimension of Edge Fed Sierpinski Miniaturized Antenna [9].....	15
Table 3.1: Edge Fed Sierpinski Carpet Design Parameters.....	19
Table 3.2: Edge Fed Sierpinski Carpet Size Reduction.....	19
Table 3.3: Performance of the Edge Fed Miniaturized Patch Antenna.....	39
Table 3.4: Comparison of Results.....	39
Table 4.1: Result of Multiband Square Patch Antenna first iteration.....	47
Table 4.2: Result of Multiband Square Patch Antenna second iteration.....	53
Table 4.3: Result of Multiband Square Patch Antenna third iteration.....	54
Table 5.1: Circular Fractal first Iteration Performance.....	62
Table 5.2: Circular Fractal second Iteration Performance.....	65
Table 5.3: Circular Fractal Third Iteration Performance.....	68
Table 5.4: Performance of the Proposed Antenna.....	73

LIST OF FIGURES

Figure 2.1: Microstrip Line Feed.....	7
Figure 2.2: Coaxial probe feed.....	7
Figure 2.3: Aperture coupling feed.....	8
Figure 2.4: Proximity couple feed.....	9
Figure 2.5: Koch curve iteration.....	10
Figure 2.6: Sierpinski gasket fractal iteration.....	11
Figure 2.7: Sierpinski carpet fractal iteration.....	11
Figure 2.8: Sierpinski carpet fractal antenna in third iteration [4].....	12
Figure 2.9: Edge fed sierpinski carpet miniaturized antenna [9].....	15
Figure 3.1: Edge feed MPA geometry.....	20
Figure 3.2: Edge fed MPA reflection coefficient.....	21
Figure 3.3: Edge fed MPA simulated in HFSS.....	22
Figure 3.4(a): 3D radiation pattern.....	23
Figure 3.4(b): Polar plot radiation pattern.....	23
Figure 3.5: Edge fed sierpinski carpet first iteration.....	24
Figure 3.6: First iteration SCF reflection coefficient.....	25
Figure 3.7(a): 3D radiation pattern of first iteration.....	26
Figure 3.7(b-c): Far field polar plot at first iteration.....	26
Figure 3.8: Sierpinski carpet second iteration model.....	27
Figure 3.9: Second iteration SCF reflection coefficient.....	28
Figure 3.10(a-b): Far field polar plot of second iteration.....	28
Figure 3.10(c): 3D plot of second iteration radiation pattern.....	29
Figure 3.11: Sierpinski carpet third iteration.....	29

Figure 3.12: Third iteration SCF reflection coefficient.....	30
Figure 3.13(a): 3D radiation pattern of third iteration.....	30
Figure 3.13(b-c): Polar plot of third iteration.....	31
Figure 3.14: Modified miniaturized patch antenna.....	32
Figure 3.15: Return loss plot for the new modified miniaturized MPA.....	33
Figure 3.16(a) 3D radiation pattern of the new modified miniaturized MPA.....	33
Figure 3.16(b-c) Polar plot of the new modified miniaturized MPA.....	34
Figure 3.17(a): Lg-5.....	35
Figure 3.17(b): Lg-10.....	35
Figure 3.17(c): Lg-15.....	35
Figure 3.17(d): Lg-20.....	35
Figure 3.18: Return loss plot for various ground length.....	36
Figure 3.19: Front and back view of the new proposed U slit ground SCF.....	37
Figure 3.20: Return loss plot for the U slit ground miniaturized MPA.....	37
Figure 3.21(a-b): Polar plot radiation pattern at 2.45GHz.....	38
Figure 3.21(c):3D radiation pattern at 2.45GHz.....	38
Figure 4.1: MPA geometry.....	42
Figure 4.2: MPA reflection coefficient.....	43
Figure 4.3: MPA reflection coefficient simulated in IE3D.....	44
Figure 4.4(a): 3D radiation pattern.....	45
Figure 4.4(b): Polar plot radiation pattern.....	45
Figure 4.5: Sierpinski carpet first iteration.....	46
Figure 4.6: First iteration SCF reflection coefficient.....	47
Figure 4.7(a-e): Far field polar plot of first iteration.....	48
Figure 4.8: Sierpinski carpet second iteration.....	50

Figure 4.9: Second iteration SCF reflection coefficient.....	51
Figure 4.10(a-f): Far field polar plot of second iteration.....	52
Figure 4.11: Sierpinski carpet third iteration model.....	53
Figure 4.12: Third iteration SCF reflection coefficient.....	54
Figure 4.13(a-f): Far field polar plot of third iteration.....	55
Figure 5.1(a-e): Circular patch fractal iteration.....	59
Figure 5.2: Return loss plot of zero iteration.....	60
Figure 5.3: Polar plot radiation pattern for zero iteration.....	61
Figure 5.4: Return loss for first iteration.....	61
Figure 5.5(a-f): Polar plot diagram for the first iteration.....	63
Figure 5.6: Return loss for the second iteration.....	64
Figure 5.7(a-f): Polar plot radiation pattern for second iteration.....	66
Figure 5.8: Return loss for the third iteration.....	67
Figure 5.9(a-f): Polar plot radiation pattern for third iteration.....	69
Figure 5.10: Circular fractal third iteration with partial ground plane.....	71
Figure 5.11: Return loss plot for partial ground third iteration.....	71
Figure 5.12: Proposed Partial ground plane model.....	72
Figure 5.13: Return loss plot for proposed partial ground plane design.....	72
Figure 5.14(a-f): Radiation pattern of the proposed partial ground plane design.....	75
Figure 5.15: Square and circular patch antenna without iteration.....	77
Figure 5.16: Third iteration SCF and proposed PG Circular fractal.....	78

LIST OF SYMBOLS /ABBREVIATIONS

c	Light Speed
D	Antenna Directivity
F	Frequency of Operation
H	Substrate Thickness
L	Patch Length
L_{eff}	Effective Length of Patch
L_g	Ground Plane Length
P_{in}	Input Power
P_{rad}	Radiation Power
S11	Reflection coefficients
W	Patch Antenna Width
W_g	Ground Plane Width
ΔL	Increment Length
ϵ_0	Free Space Permittivity
ϵ_r	Dielectric Constant
ϵ_{eff}	Effective Dielectric Permittivity
η	Antenna Efficiency
λ	Wavelength
π	PI
BGS	Band Gap Structure
CFA	Circular Fractal Antenna
CST	Computer Simulation Technology

DGS	Defected Ground Structure
FDTD	Finite Difference Time Domain
FEM	Finite Element Method
FR4	Flame Retardant 4
GPF	Giuseppe Peano Fractal
GPS	Global Positioning System
HFG	Hilbert Fractal Geometry
HFSS	High Frequency Structures Simulators
KSF	Koch Snowflake Fractal
MKF	Minkowski Fractal
MPA	Microstrip Patch Antenna
MSL	Microstrip Line
PG	Partial Ground
PGS	Partial Ground Structure
RF	Radio Frequency
SCA	Sierpinski Carpet Antenna
SCF	Sierpinski Carpet Fractal
UWB	Ultra Wide Band
Wi-Fi	Wireless Fidelity
WLAN	Wireless Local Area Network

Chapter 1

INTRODUCTION

Communication systems are growing rapidly with increase in technology. These systems operate at more than one frequency band which suggest there is a need for small antennas capable of resonating at multiple band [1]. To realize such communication systems with a low profile, one of the critical factors is the antenna size. Hence, many different kinds of techniques have been applied to a patch antenna such as the use of substrate with high dielectric constant, use of reactive loading and antenna electrical length increment by optimizing its shape [2]. Microstrip antenna possesses some attractive characteristics which include smaller volume, lighter weight, low profile and lower cost of production. But there are two serious limitations when microstrip antenna is applied in variety areas. The one is low gain, the other one is narrow bandwidth [3]. Small antennas with capability of resonating at different bands of frequencies are generally in great demand. One of the techniques to reduce area of patch is to make use of fractal geometry [4]. The application of the fractal geometry to conventional patch antenna structures optimizes the shape of the antennas in order to increase their electrical length, which thus reduces their overall size [5]. The design of fractal geometry can be in different shapes. The most commonly used shapes are Minkowski Loop, Koch Island, Sierpinski Carpet and the Sierpinski Gasket [6].

1.1 Thesis Objective

The objective of this thesis is to design and simulate fractal antennas to achieve size reduction, multiband and ultra-wideband operation.

1.2 Thesis Contribution

Fractals geometries and partial ground technique have been applied to achieve small size, multi band and ultra-wideband antenna with bandwidth of 8.18GHz at centre frequency of 2.54GHz.

1.3 Thesis Organization

Overview of the thesis was done in Chapter 1 which provides the needs for microstrip antenna, uses of fractals in antenna design. Chapter 2 demonstrates various antenna properties and terms associated with it such as radiation pattern, gain, and bandwidth. A small discussion was done on the advantage and disadvantage of patch antenna and on the feeding techniques. Also, the most commonly used fractal geometries were discussed. Chapter 3 describes the design process and simulation results of Sierpinski Carpet fractal antenna. Section 3.2 describes the modified miniaturized patch antenna with defected ground structure. In chapter 4, a multiband antenna using third iteration Sierpinski Carpet fractals was designed. Chapter 5, section 5.1 includes the designs and simulation of a circular fractal antenna with partial ground structure for multiband and ultra-wideband applications. Chapter 6 discuss the conclusion and future work.

Chapter 2

PLANAR ANTENNAS AND FRACTAL ANTENNAS

2.1 Antenna Definition

According to IEEE an antenna is defined as a means of receiving or radiating radio waves [1]. Heinrich Hertz in 1886 designed the first antenna called dipole antenna. The dipole antenna has a centre fed element and also two conductors which is used for transmitting and also receiving radio frequency. The result of removing one of the two conductors of the dipole antenna is the monopole antenna. The monopole antenna was developed in 1896 by Marconi; these antennas were the simplest forms. Overtime, antennas have been used in different applications such as military, medical, aviation and also in navigation, GPS, and mobile etc.

2.2 Antenna Parameters

Radiation Pattern: A radiation pattern defines the variation of the power radiated by an antenna as a function of the direction away from the antenna. The radiation pattern is represented as a function of the directional coordinates and in most cases it is determined in the far field.

Antenna Efficiency: The efficiency of an antenna relates the amount of power entering the antenna as input and the power radiated or dissipated within the antenna. An antenna will have high efficiency if most of the input power is radiated whereas an antenna where most of the power are either reflected away due to mismatch or absorbed as loss will have low efficiency. The antenna efficiency (or radiation

efficiency) can be written as the ratio of the radiated power to the input power of the antenna:

$$\eta = \frac{P_{radiated}}{P_{input}} \quad (2.1)$$

Directivity: Directivity of an antenna is defined as “the ratio of the maximum radiation intensity in a given direction from the antenna to the radiation intensity averaged over all directions.

$$D = 4\pi \frac{U}{P_{rad}} = 4\pi \frac{\text{radiation intensity}}{\text{total radiated power}} \quad (2.2)$$

Antenna Gain: Antenna Gain is same as the directivity when the antenna is lossless. But in the case of losses, antenna gain (G) can be related to directivity (D) by:

$$G = \eta D \quad (2.3)$$

Bandwidth: Bandwidth describes the range of frequencies over which the antenna can properly operate. Often, the desired bandwidth is one of the determining parameters used to decide upon an antenna.

Input Impedance: The input impedance consists of imaginary and real part and it is the ratio of voltage at input terminal of antenna to the current.

VSWR: The VSWR stands for (voltage standing wave ratio) which shows how much power is reflected from the antenna. It is a function of reflection coefficient. If

the reflection coefficient is given by Γ , then the **VSWR** is defined by the following formula:

$$VSWR = \frac{1+|\Gamma|}{1-|\Gamma|} \quad (2.4)$$

The reflection coefficient is also known as S_{11} or return loss.

2.3 Patch Antenna

Microstrip or patch antennas are becoming more and more helpful due to the ease of being able to be printed directly onto a circuit board. Microstrip antennas are getting very widespread among the portable market such as phone market. Patch antennas are less expensive, have a low profile and are easily fabricated. Microstrip antennas received sizeable attention beginning within the 1970s; although the idea of a microstrip antenna can be traced to 1953 [1] and a patent in 1955. Microstrip antennas consist of a very thin ($t \ll \lambda_0$, where λ_0 is the free-space wavelength) metallic strip (patch) placed a small fraction of a wavelength ($h \ll \lambda_0$, usually $0.003\lambda_0 \leq h \leq 0.05\lambda_0$) above a ground plane. There are numerous substrates that can be used for the design of microstrip antennas, and their dielectric constants are usually in the range of $2.2 \leq \epsilon_r \leq 12$. For good antenna performance, thicker substrates with dielectric constant within the lower end range are desired because they provide larger bandwidth and better efficiency [1].

2.3.1 Advantage of Patch Antenna

Compact and difficult to crack

Size reduction for portable system is easily achieved

It can achieve multiband mode of operation

By changing the feed position, circular and linear polarization can be made

They are conformable to both planar and non planar structure

They have low weight and low profile

2.3.2 Disadvantage of Patch Antenna

Their power handling capacity is low

In the feed structure of arrays, they have large ohmic loss

Surface wave excitation

Lower efficiency

Narrow bandwidth

Low gain

2.3.3 Feeding Techniques:

One of the very important steps in antenna design is how the antenna is fed; this is done so that the antenna can operate at full power of transmission. Several methods are available for feeding microstrip antenna. Commonly used feeding techniques are:

1. Coaxial feed
2. Microstrip line
3. Proximity coupling
4. Aperture coupling.

2.3.4 Microstrip Line Feed

The microstrip line feeding is one of the simplest feeding technique in which a conducting strip is connected directly with the radiating patch element. This could be seen as extension of the patch. It has the advantage of ease of fabrication. But this feeding technique also has its draw back as the thickness of the substrate increases, feed radiation and spurious wave also increases thereby limiting the bandwidth (typically 2–5%).

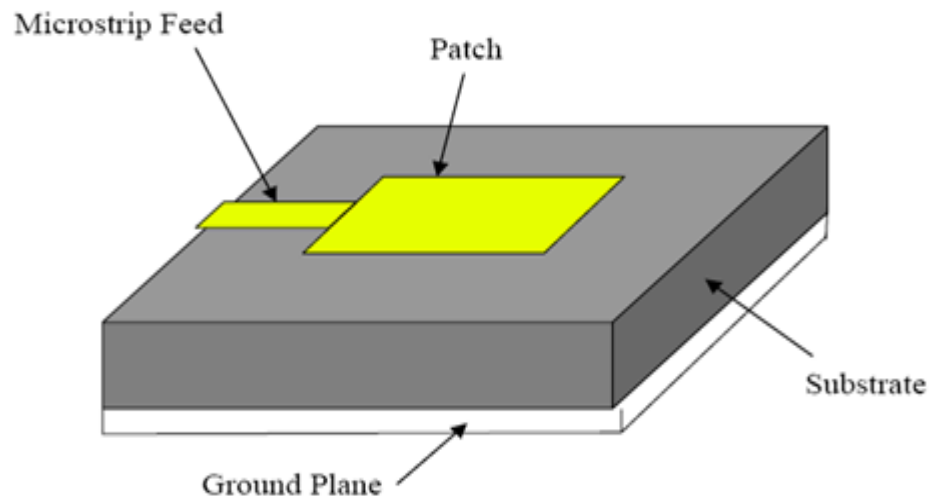


Figure 2.1: Microstrip Line Feed [23]

2.3.5 Coaxial Probe Feeding

Coaxial probe feeding is a feeding technique where the outer and inner conductor of the coaxial cable is attached to the ground plane and radiating patch of the antenna respectively. It exhibits the advantage of ease of fabrication, spurious radiation is lower and matching is easy. But it has a drawback of narrower bandwidth and also difficulty when modelling a thicker substrate.

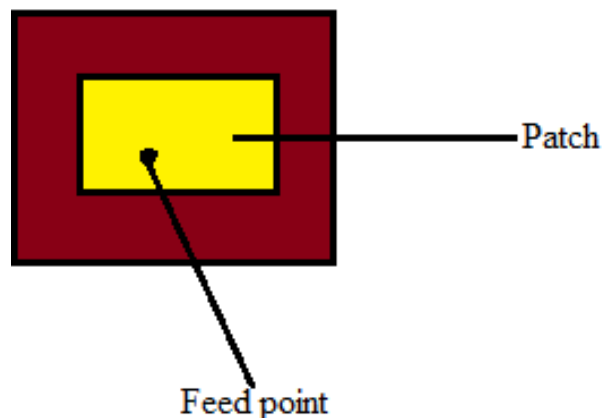


Figure 2.2: Coaxial probe feed

2.3.6 Aperture Coupling

In this feeding technique, a ground plane is used in separating two substrates. High dielectric substrate is used at the bottom substrate while the top substrate uses a thick low dielectric constant. In the middle is the ground plane which minimizes interference and isolate the feed from radiation element. An advantage of this technique is the allowance of independent optimization of feed mechanism element.

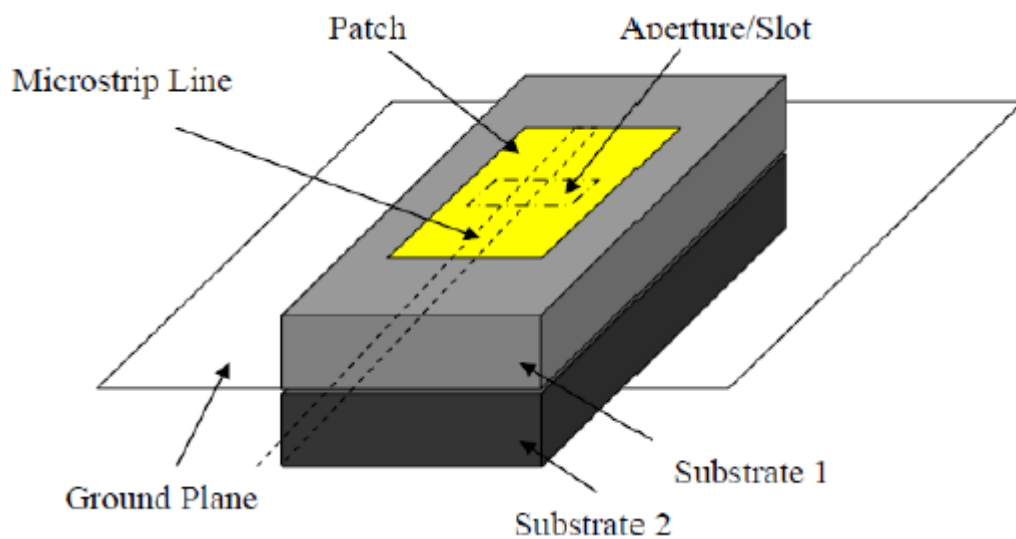


Figure 2.3: Aperture coupling feed [23]

2.3.7 Proximity Couple Fed

This kind of technique has low spurious radiation and somewhat easy to model although it is difficult to fabricate. This technique has the largest bandwidth as high as 13%.

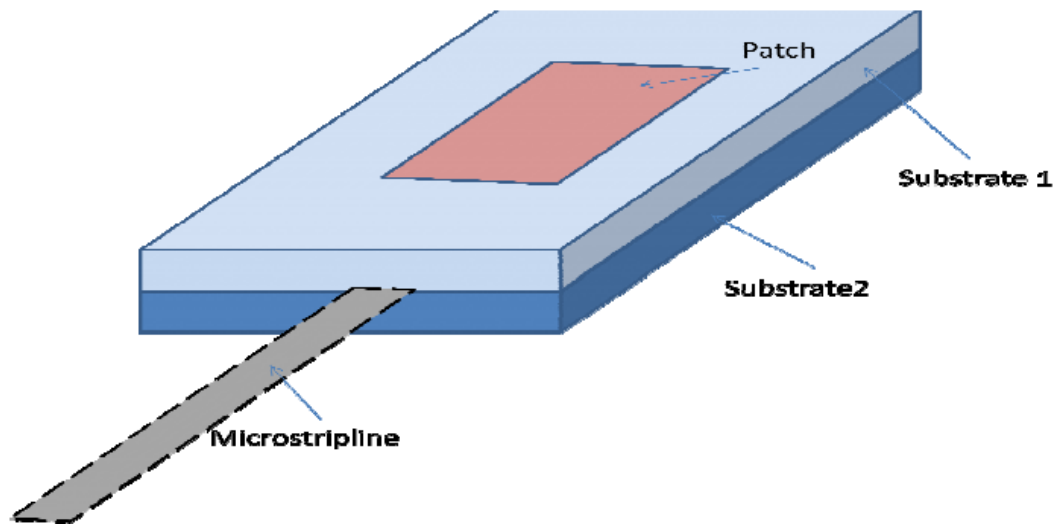


Figure 2.4: Proximity couple feed [26]

2.4 Literature Survey of Fractal Antenna

Fractals in 1975 were defined as a way of classifying structures whose dimensions were not whole numbers by Benoit Mandelbrot. Fractal shapes usually consist of copies of themselves but with different scales, and have no specific size.

In modern wireless communication systems there is great demand for antenna with low profile, wide bandwidth, and ability to operate in a multiband for different applications. Conventional antenna mostly resonate at a single or double frequency band [2] which is not suitable for the current modern wireless requirement of where an antenna is needed for different application and different band. This urges researchers to find a new way in designing antenna; using of fractals geometry in antenna design has proven to be one of the new ways of designing antenna. Various areas have employed the use of fractals to create new types of antenna.

Many fractals geometry have been found useful in antenna development. The most commonly used fractals include:

2.4.1 Koch Curve

The Von Koch curve was initially presented by the Swedish mathematician Helge Von Koch. The Koch curve was created to demonstrate how to construct a continuous curve that did not have some tangent line. It is built by starting with a straight line. The line is divided into three parts. The centre part was substituted by a regular triangle with the base detached. This process is repeated on every straight line on going in an infinite procedure resulting in a curve with no smooth sections.

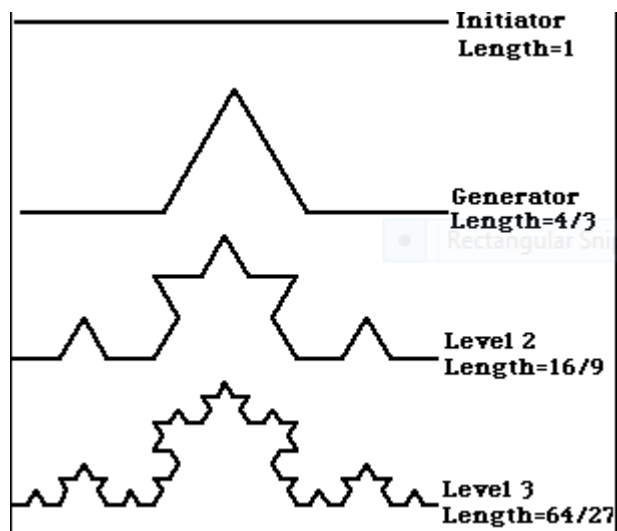


Figure 2.5: Koch curve iteration [25]

2.4.2 Sierpinski Gasket

The method used in creating the Sierpinski Gasket involves creating a triangle which serves as the initiator then cutting out the middle piece in the triangle which results in three triangles of smaller size which is called the first iteration. The process is continuing for the other iteration. The Sierpinski Gasket is one of the most widely used fractal geometry.

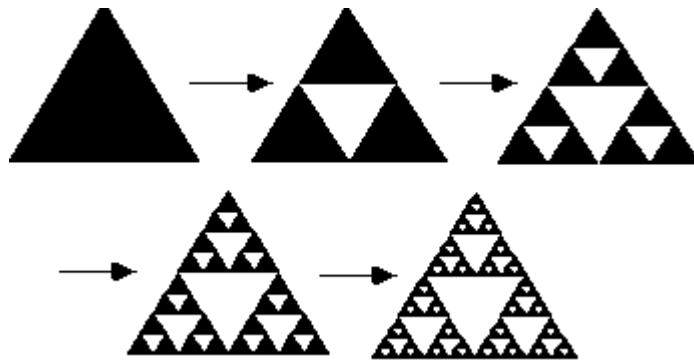


Figure 2.6: Sierpinski Gasket fractal iteration [25]

2.4.3 Sierpinski Carpet

The method used in creating the Sierpinski carpet involves creating a rectangle which serves as the initiator then cutting out the middle piece in the rectangle which results in three rectangles of smaller size. The process is continuing for the other iteration. The Sierpinski Carpet use same procedure as the Gasket but in this case a square or rectangle is used.

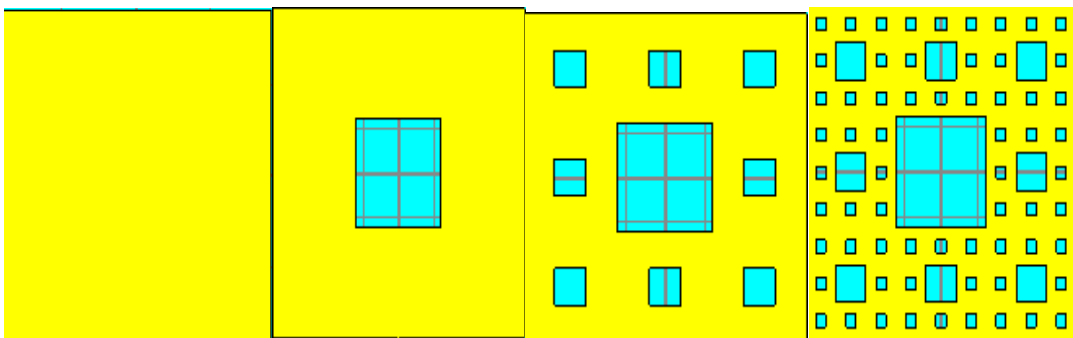


Fig 2.7: Sierpinski Carpet fractal iteration

2.4.3.1 Sierpinski Carpet Fractal Antenna in Third Iteration

N. Lu and X. Xu [4] designed and simulate a square patch antenna using Sierpinski Carpet. FR-4 substrate of relative permittivity 4.4 was used in the fabrication. The gasket was mounted upside down over a 210mmX210mm square conductor ground plane. The size of the main patch is 72X72mm. In other words, the main patch is $1/3$

of the substrate, the second patch is $1/3$ of the main one, the third patch is $1/3$ of the second one. The feeding point is 16mm far from the centre of the substrate. The structure is fed through 1.56mm diameter 50 ohms coaxial probe with an SMA connector on the bottom side of the plane. HFSS13.0 software was used to analyse the antenna. First resonance frequency occurs at 1GHz, second at 3GHz and third at 9GHz. The antenna was simulated respectively at 0.5-15GHz, 2.5-3.5GHz and 8.5-9.5 GHz. The antenna exhibits good radiation and impedance matching characteristics in the first two bands. The impedance matching of this antenna at high frequency is worse than at low frequency because the second and the third patch are excited by parasitic coupling [4].

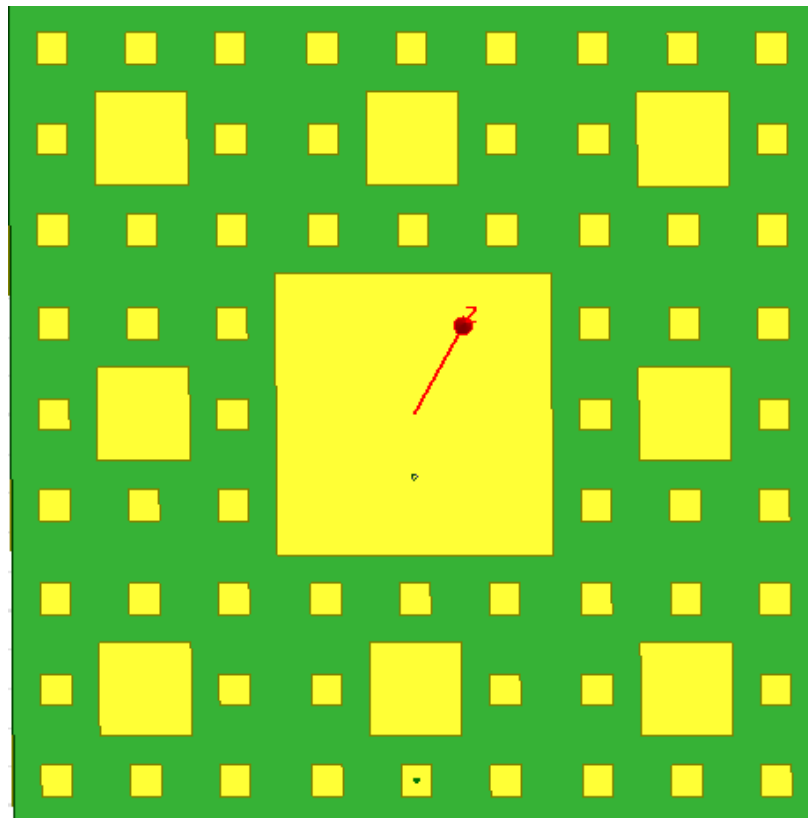


Figure 2.8: Sierpinski Carpet fractal antenna in third iteration [4]

2.4.3.2 Analysis of Modified Sierpinski Carpet Fractal for UWB Applications

The ultra-wideband (UWB) system has become emerging research topic in the field of modern wireless communications since Federal Communication Commission (FCC) band 3.1GHz- 10.6GHz declared in Feb.2006. In a UWB antenna system, the system was designed with the help of rectangular patch consisting of two steps and partial ground plane which can be used to achieve wide band characteristics [2]. B. Shi et'al [2] designed a planar microstrip antenna with modified Sierpinski carpet fractal for UWB characteristics. The designed antenna covers the UWB range of 2.2GHz to 10.3GHz achieving impedance bandwidth of 129.6%. Simulation was carried out in HFSS V10. The design was printed on FR-4 substrate with a thickness of 1.8mm, permittivity of 4.4 and dielectric loss of 0.02 with compact dimension of 40mmX50mm. Coplanar waveguide is used to feed the antenna. The result shows that third iteration is better than the first and second iteration in bandwidth.

2.4.3.3 A 2.45 GHz Sierpinski Carpet Edge Fed Microstrip Patch Antenna for WPT Rectenna

Wireless power transmissions (WPT) have become an interesting topic for energy transmission in the future. Antenna is one of the most important components of WPT. Microstrip patch antennas have been used greatly in the rectenna for wireless power transmission [6]. T.Shanmuganatham and K.Ramasamy designed Sierpinski carpet edge fed microstrip antenna to reduce the size of the antenna in the rectenna of WPT system. The antenna was designed at 2.45GHz using edge fed on a FR-4 material as the substrate. The return loss for the simulated antenna for first two iterations is -25.63db and -18db for the first and second iteration respectively. Without having effect on the antenna performance, significant size reduction was achieved.

2.4.3.4 Small Size Edge-Fed Sierpinski Carpet Microstrip Patch Antenna

W. Chen and G. M. Wang proposed a novel technique to apply fractal theory to reduce size of the patch antenna by loading the patch surface with capacitive load. The antenna was designed at 1.8GHz using an edge fed on a FR-4 material which has permittivity of 4.3 with 1mm as the height. Results obtained from measurement and simulations indicate that the patch antenna size can be reduced to 33.9% of the conventional counterpart without degrading the antenna performance such as return loss and radiation pattern [7].

2.4.3.5 Fractal Antenna for Multiband Applications

R. Mohanamuruli and T. Shanmuganatham simulate a planar antenna with Microstrip feed Sierpinski carpet fractal geometry for multiband applications. The multiband behaviour was analysed through two fractal iterations. Self similarity property of fractal technology was applied in the antenna design to reduce the physical size, increase bandwidth and gain. The antenna was designed on FR-4 material which has a thickness of 1.59 mm. A square patch of 37 mm was used as the initial generator; microstrip line was used in feeding the antenna. The simulated result shows that the antenna is suitable for 1.8/5.59/5.78/6.4/6.63/7.84 GHz wideband applications [8].

2.4.3.6 Design of 2.45 GHz Sierpinski Fractal Based Miniaturized Microstrip Patch Antenna

Fractal geometry has a space filling property [9]. This property was employed by S. Shrestha et'al to achieve patch antenna size reduction. The feed was placed at the edge of the radiating patch. Sierpinski iteration process was performed on the antenna up till third iteration. The antenna was designed to operate at 2.45GHz and the frequency of operation was retained after third iteration thereby achieving size

reduction without affecting the performance of the antenna. The antenna structure is shown in Figure 2.9

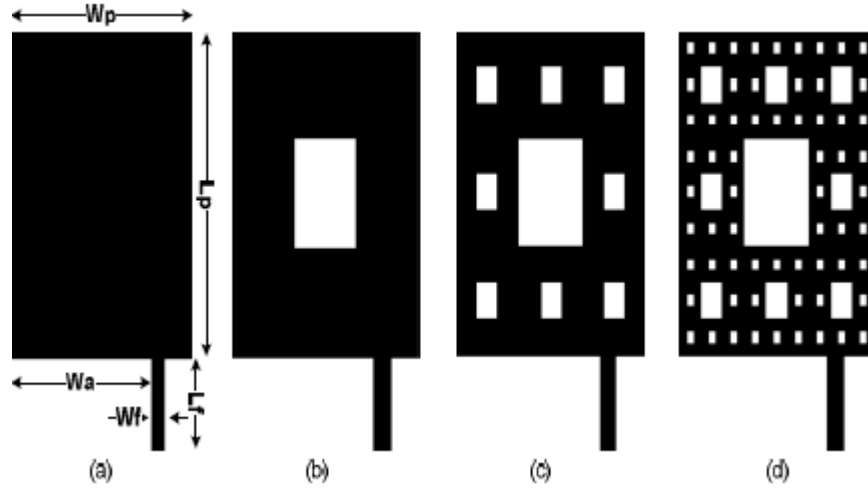


Figure 2.9: Edge fed Sierpinski Carpet miniaturized antenna [9]

The dimensions of the antenna are presented in Table 2.1.

Table 2.1: Dimension of edge fed sierpinski miniaturized antenna [9]

Antenna	W_p (mm)	L_p (mm)	W_a (mm)	W_f (mm)	L_f (mm)
Generator	27	34.41	21.3	2	10
Iteration 1	23.58	34.41	18	2.3	10
Iteration 2	23.66	32.4	18	1.9	10
Iteration 3	23.66	32.4	18	1.9	10

2.4.3.7 Slotted Circular Microstrip Antenna with DGS for Wireless Applications

R. Saini, and D. Parkash, designed a circular microstrip antenna which is mainly for WLAN/WIMAX applications which occupy the frequency band of 5.2GHz and 5.8GHz. The antenna was designed on low cost FR4 material which has relative permittivity of 4.4 and substrate thickness of 1.6mm. The ground plane and also the patch were loaded with slot in other to enhance the antenna performance and widen

the bandwidth. 50 ohms coplanar waveguide which has a feed length of 8.875mm and 4.1mm as the width was used in feeding the patch [10]. The designed antenna was able to achieve up till 2.46GHz of bandwidth in the band of 4.97GHz-7.43GHz [10].

2.4.3.8 Bandwidth Enhancement of a Wide Slot Using Fractal-Shaped Sierpinski

Y. J. Sung proposed a technique for enhancing the microstrip line fed wide slot antenna based on fractal shape. By introducing a Sierpinski fractal into a wide slot, a broadband characteristic was achieved without changing the antenna size. The antenna was fabricated on a low cost FR-4 substrate of relative permittivity 4.4 and thickness of 1.6mm. The three-dimensional finite integration time domain (FITD) software package Microwave Studio by CST was used in simulating the antenna. The measured result shows that the second iteration Sierpinski slot has a bandwidth of 64% with frequency range of 1.96 GHz to 3.78 GHz [11].

Previous work by various researchers using fractal geometries includes Performance Enhancement of Sierpinski Carpet Fractal Antenna using Computational techniques [12], Bandwidth Enhancement of Modified Square Fractal Patch Antenna using Gap Coupling [13], Modified Hilbert Fractal Geometry for UWB wireless Communication [14], Miniaturization of MPA using Giuseppe Peano Geometries [15], Sectorial Sierpinski Gasket Fractal Antenna for Wireless LANs [16], Minkowski fractal Patch antenna for Size and Radar Cross Section Reduction [17], High-Directivity Fractal Antenna using KSF [18]

Chapter 3

MINIATURIZATION OF PATCH ANTENNA

3.1 Sierpinski Fractal Miniaturized Rectangular Patch Antenna

Design

A miniaturized compact antenna was designed. In the first stage of the design, the antenna was designed based on the well-known Sierpinski Carpet fractal with iteration factor of 1/3. The antenna was designed up till third iteration to achieve miniaturization. A new approach was designed using a simple slot at the middle of the patch to achieve a 34.88% size reduction at the same resonating frequency. The second stage of the design involves incorporating a defected ground structure. This was carried out in order to achieve bandwidth increment [10] and it was realized by cutting a U slit in the ground plane. The antenna was built on a FR-4 lossy material which has permittivity of 4.7 and loss tangent of 0.019. The height of the substrate is 1.6mm. Multiband antenna was also designed using the same procedure of the third order iteration of Sierpinski Carpet. The dimension of the patch was calculated using transmission line model [1].

According to the given equation, the width of the patch can be calculated:

$$W = \frac{c}{2f_0} \sqrt{\frac{2}{\epsilon_r + 1}} \quad (3.1)$$

Where W represents the width, f_o the resonating frequency, and ϵ_r the relative dielectric constant.

The effective dielectric constant is obtained by:

$$\epsilon_{reff} = \frac{\epsilon_r+1}{2} + \frac{\epsilon_r-1}{2} \left(1 + \frac{12h}{w}\right)^{-1} \quad (3.2)$$

Due to the fringing effect, the patch dimension along its length is extended on each side by a distance ΔL which is given by:

$$\Delta L = 0.412h \frac{(\epsilon_{reff}+0.3)(W/h+0.264)}{(\epsilon_{reff}-0.258)(W/h+0.8)} \quad (3.3)$$

Where h is the height of the substrate.

The actual length is given by:

$$L = L_{eff} - 2\Delta L \quad (3.4)$$

Where $L_{eff} = \frac{c}{2f_o\sqrt{\epsilon_{reff}}}$ is the effective length which is also known as the electrical length of the patch antenna and its closely related to the resonant frequency. Increasing the length of the rectangular patch antenna reduces the resonant frequency.

Using the above equations and substituting the known parameters, the dimension of the patch antenna can easily be calculated.

Table 3.1 shows the dimensions of the designed antenna in (mm) using FR-4 substrate with dielectric constant of 4.7 and thickness of 1.6mm at the centre frequency of 2.45GHz where W_p , L_p , W_a , W_f and L_f corresponds to width of the patch, length of the patch, distance from edge of patch to the feed point, width and length of the feed as shown in figure 2.9.

Table 3.1: Edge fed Sierpinski Carpet design parameters

Antenna	W_p (mm)	L_p (mm)	W_a (mm)	W_f (mm)	L_f (mm)	Area (mm) ²
Without iteration	27	34.41	21.3	2	10	929.07
1 st iteration	23.58	34.41	18	2.3	10	811.38
2 nd iteration	23.66	32.4	18	1.9	10	766.58
3 rd iteration	23.66	32.4	18	1.9	10	766.58
Modified approach	20.86	29	18	2.1	10	604.94

Table 3.2: Size Reduction

Antenna	Area(mm) ²	Area Reduction
Without Iteration	929.07	
1 st iteration	811.38	12.67%
2 nd iteration	766.58	17.49%
3 rd iteration	766.58	17.49%
Modified approach	604.94	34.88%

Miniaturization methods on fractal antenna involves the process whereby some parts of the main patch structure has been removed. The microstrip patch antenna is etched

as a Sierpinski Carpet fractal in order to obtain compact size antenna using different order of iteration. The initial stage of Sierpinski Carpet involves dividing the rectangular patch into nine smaller congruent rectangles in which the central rectangle is removed. The remaining eight rectangles in the further iteration are divided into nine more congruent rectangles and removing the central rectangles from each rectangle. Other iteration follows the same procedure [9].

The antenna has been fed by using a microstrip line technique due to its simplicity. The antenna has a best performance when the transmission line is placed at a point where the current does not face obstruction. The proposed antenna feed position is slightly moved away from the centre of the patch for better performance and impedance matching [9]. Figure 3.1 shows the patch antenna model.

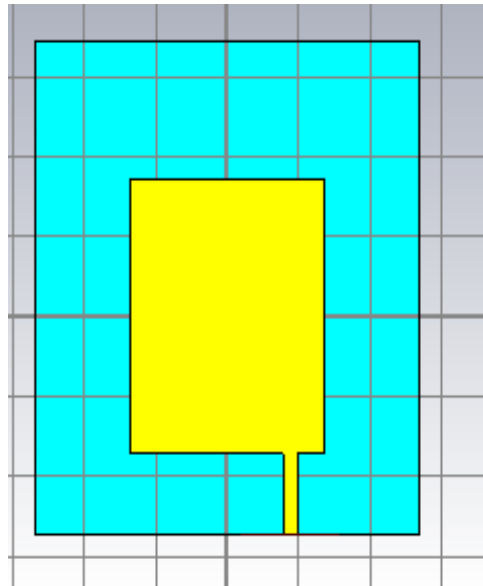


Figure 3.1: Edge fed MPA geometry

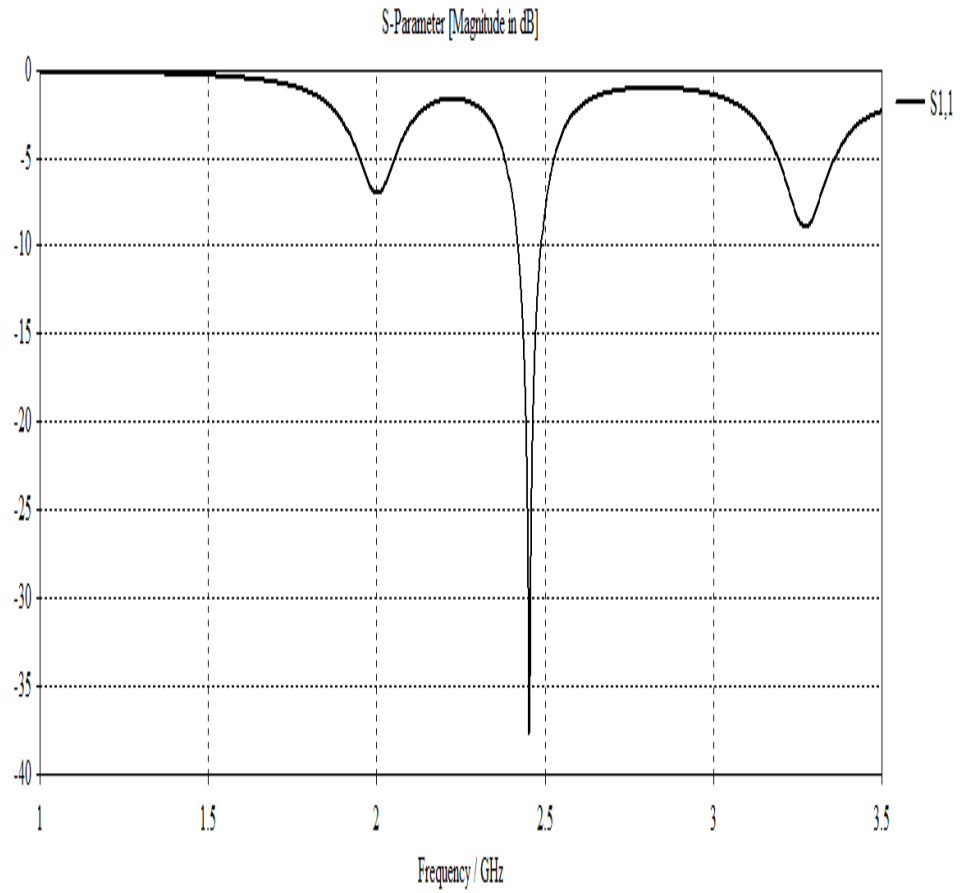


Figure 3.2: Edge fed MPA reflection coefficient

Simulated result was compared with the same antenna designed by S. Shrestha et'al.

The result is shown in Figure 3.3.

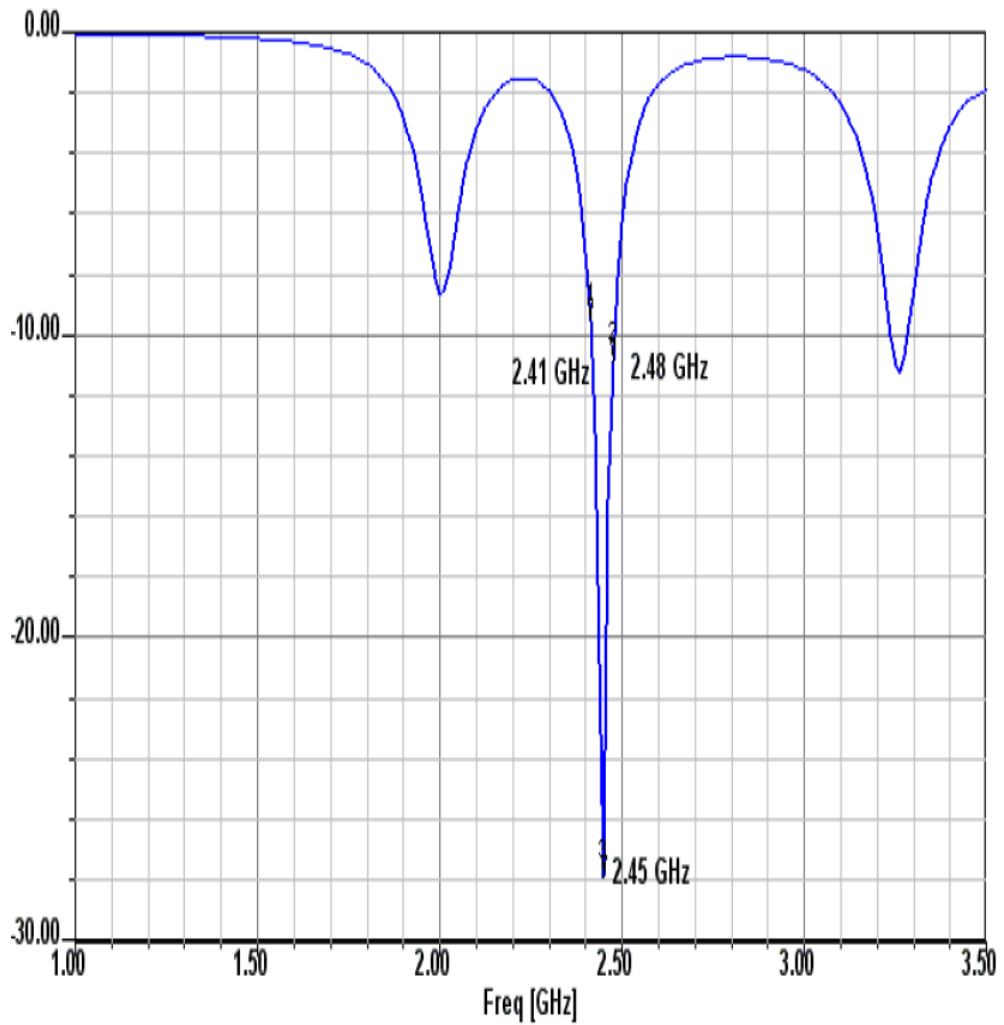


Figure 3.3: Edge fed MPA simulated by S. Shrestha et'al

From Figure 3.2, the antenna has resonant frequency at 2.45 GHz with return loss of -37dB. The 3D and polar plot radiation pattern of the antenna is shown in Figure 3.4(a-c) which shows that the antenna has a gain of 3.64dB. In the H- plane, the direction of the main lobe is 0° while the E- plane has main lobe direction of 3° .

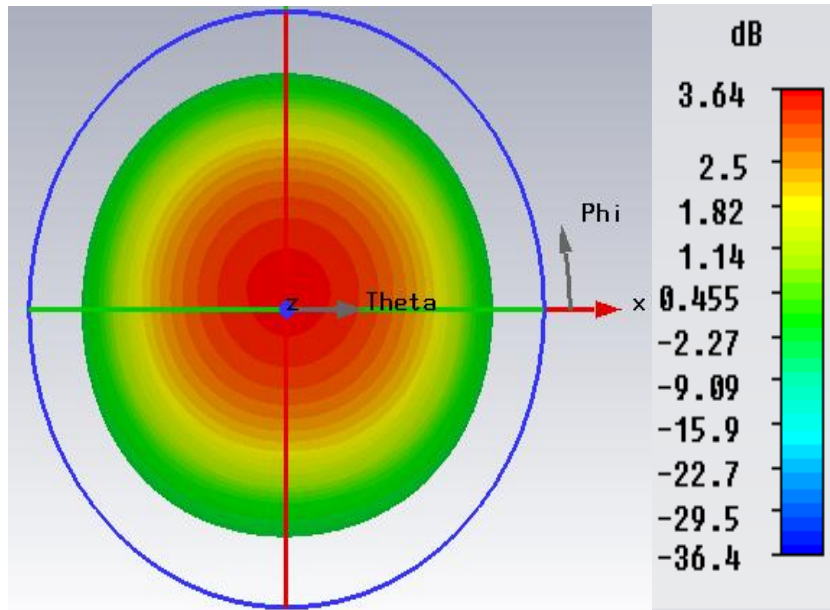
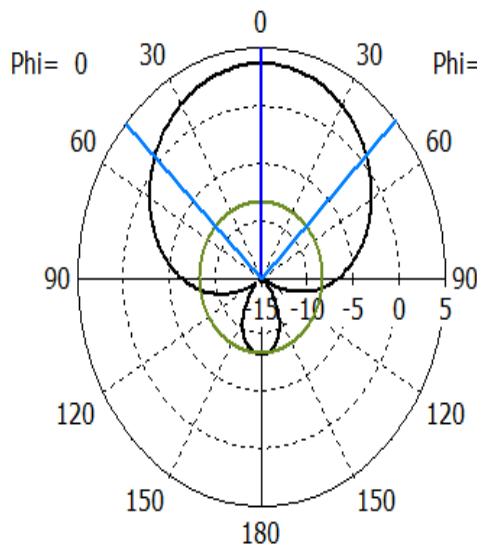
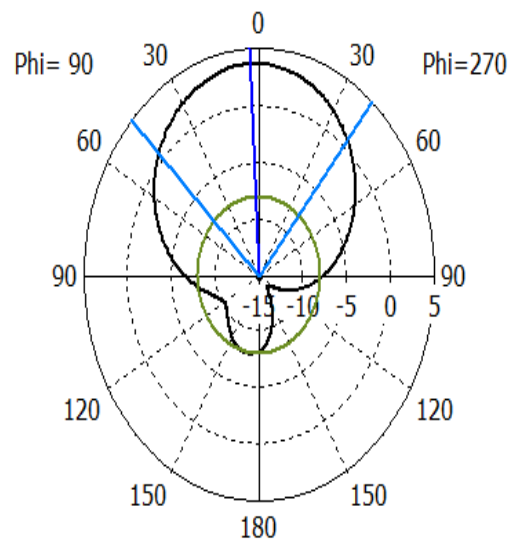


Figure 3.4(a): 3D radiation pattern



Theta / Degree vs. dB

Figure 3.4(b): H- plane radiation pattern



Theta / Degree vs. dB

Figure 3.4(c): E- plane radiation pattern

3.1.1 Edge Fed Sierpinski Carpet First Iteration

The Sierpinski Carpet geometry in the first iteration with the iteration factor of $1/3$ was applied to the antenna to achieve size reduction. This involves dividing both the length and width of the patch by 3 to achieve the first iteration. To achieve the same

resonant frequency as the original patch designed previously, the width of the patch was adjusted by trying different values until optimum value was achieved while keeping the length constant. The structure is shown in Figure 3.5.

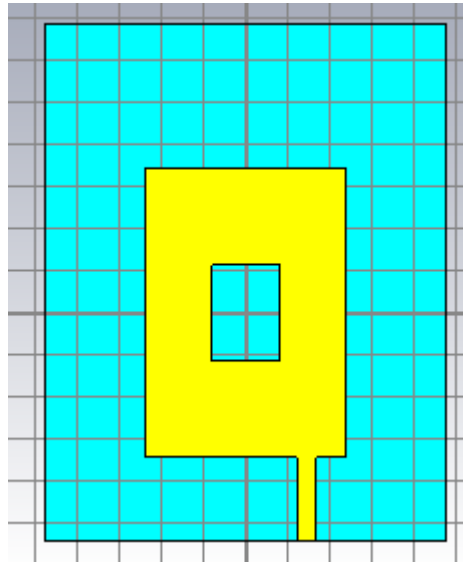


Figure 3.5: Edge fed Sierpinski Carpet first iteration

From Figure 3.5, the empty space shows the first iteration. The plot of return loss of the designed antenna is shown in Figure 3.6.

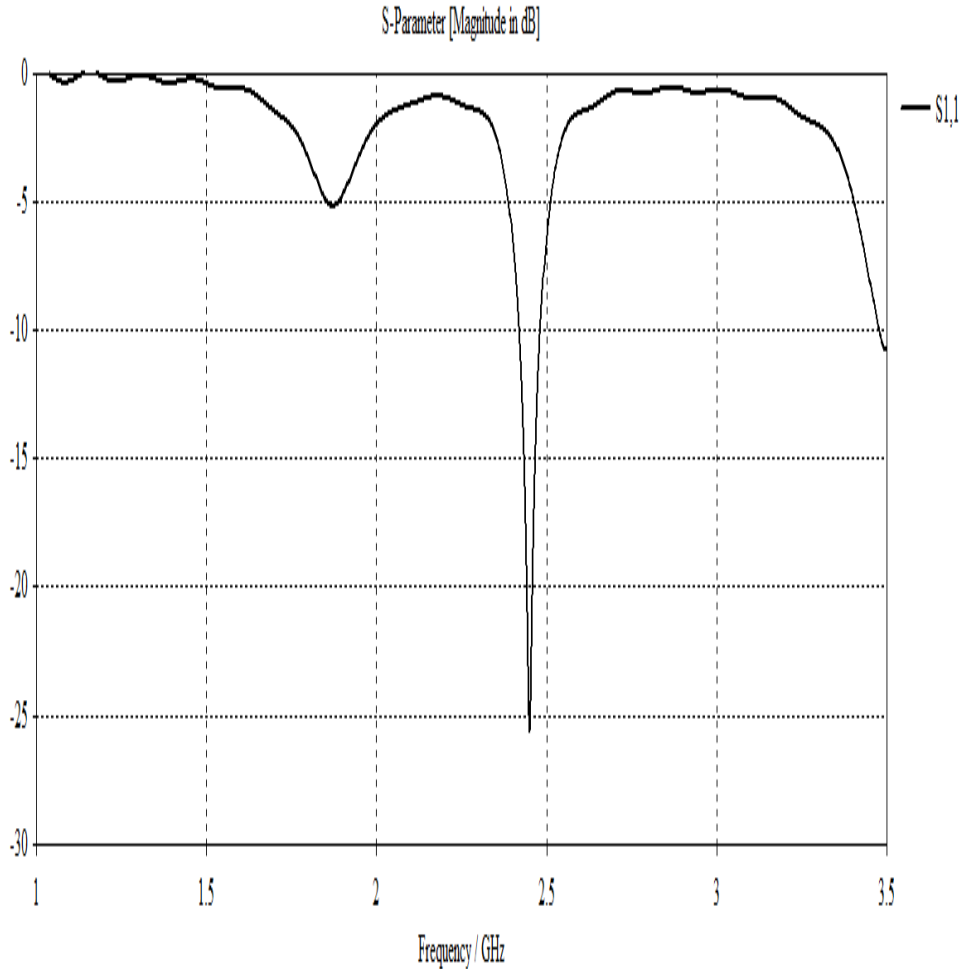


Figure 3.6: First iteration SCF reflection coefficient

From Figure 3.6, it was observed that the antenna is resonating at 2.45GHz with return loss of -25dB after the first iteration. This shows that the resonant frequency of the antenna remain the same after the first iteration while the size has been reduced by 12.67%. The 3D and polar plot radiation pattern of the antenna is shown in Figure 3.7(a-c) which shows that the antenna has a gain of 2.41dB. In the H- plane, the direction of the main lobe is 0° while the E- plane has main lobe direction of 2° . The reduction in gain can be as a result of reduction in the antenna size since the area of antenna is proportional to the gain.

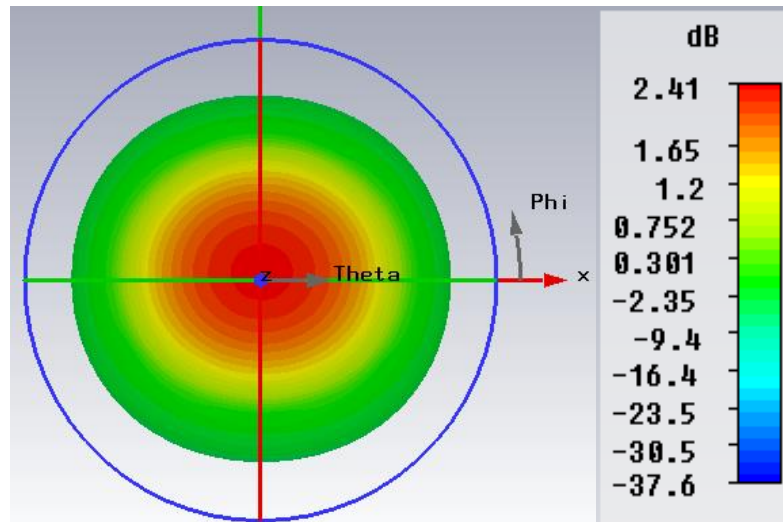


Figure 3.7(a): 3D radiation pattern of first iteration

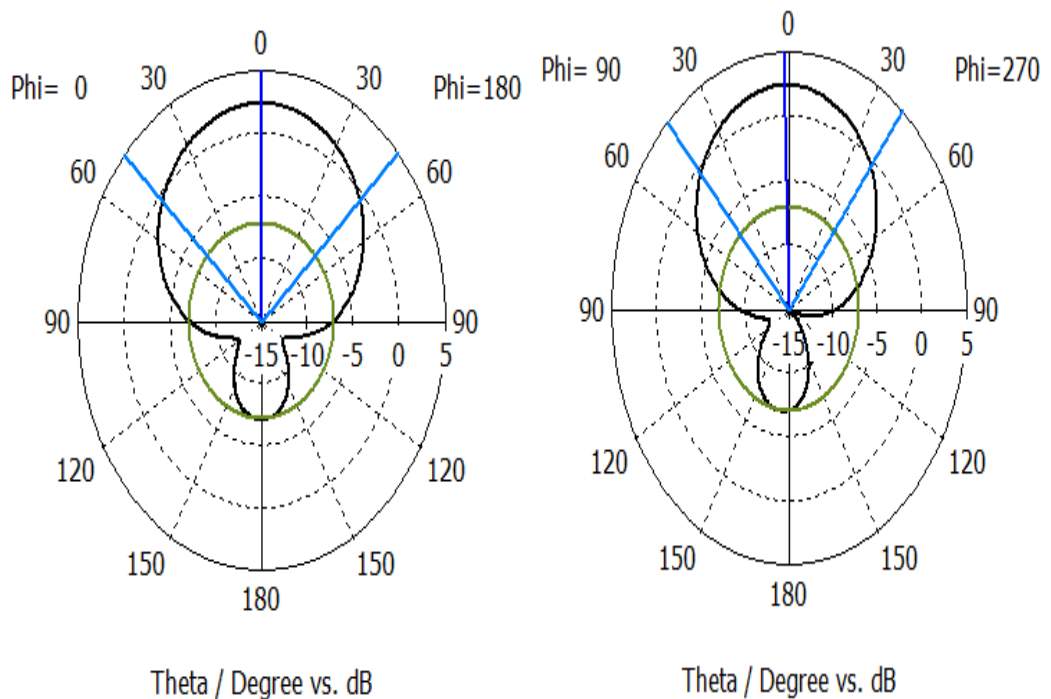


Figure 3.7(b): H- plane radiation pattern

Figure 3.7(c): E- plane radiation pattern

3.1.2 Edge Fed Sierpinski Carpet Second Iteration

Following the design procedure described previously, the second iteration is shown in Figure 3.8.

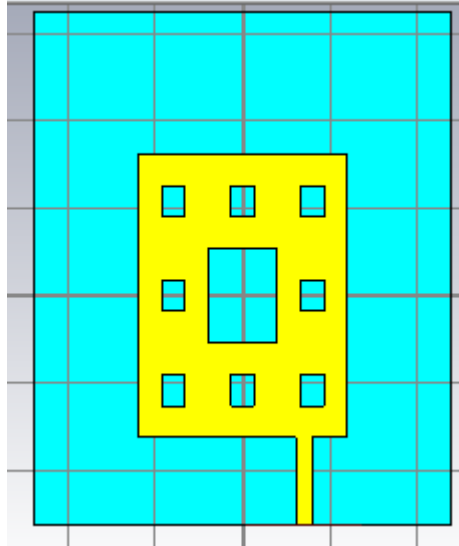


Figure 3.8: Sierpinski Carpet second iteration model

The length and width of the patch were slightly adjusted while keeping the feed position constant as in first iteration. The width of the feed was slightly reduced to achieve better matching since the size of the antenna is different from the previous iteration. From the return loss plot in Figure 3.9, the antenna is resonating at 2.45GHz with return loss of -29dB. This shows that the antenna retains its resonating point after second iteration while antenna size further reduced. Figure 3.10(a-c) shows the 3D and polar plot radiation pattern of the antenna in second iteration. From the result, the antenna has similar radiation pattern as the main patch with a gain of 2.25dB. In the H- plane, the direction of the main lobe is 0° while the E- plane has main lobe direction of 2° .

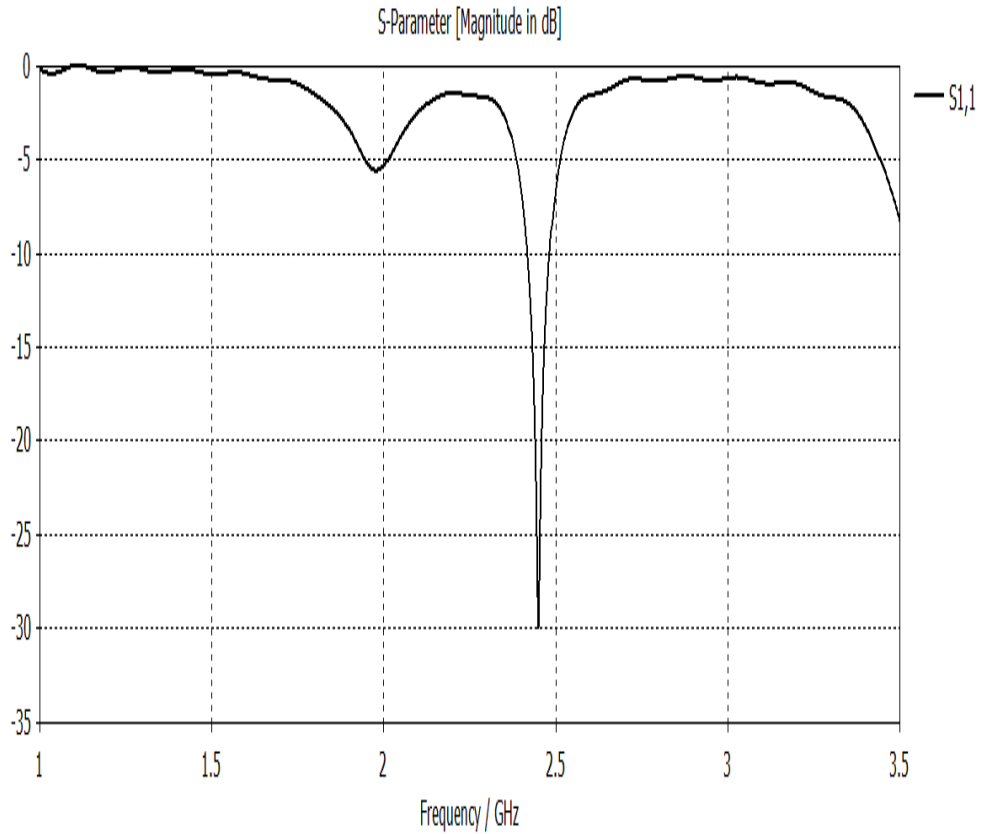


Figure 3.9: Second iteration SCF reflection coefficient

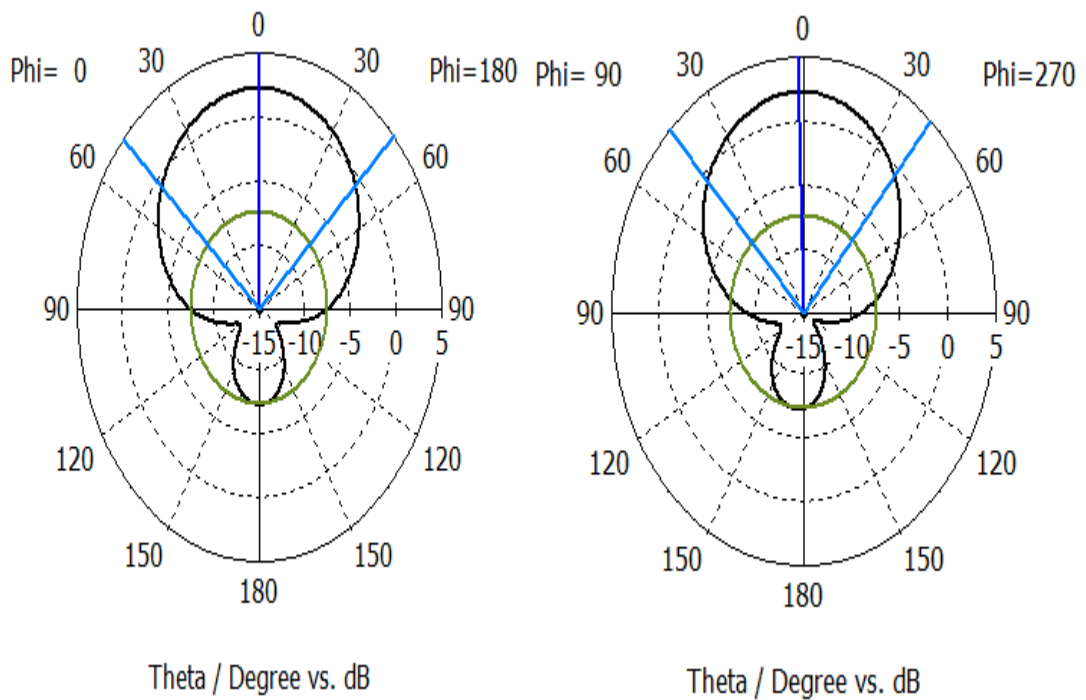


Figure 3.10(a): H- plane radiation pattern Figure 3.10(b): E- plane radiation pattern

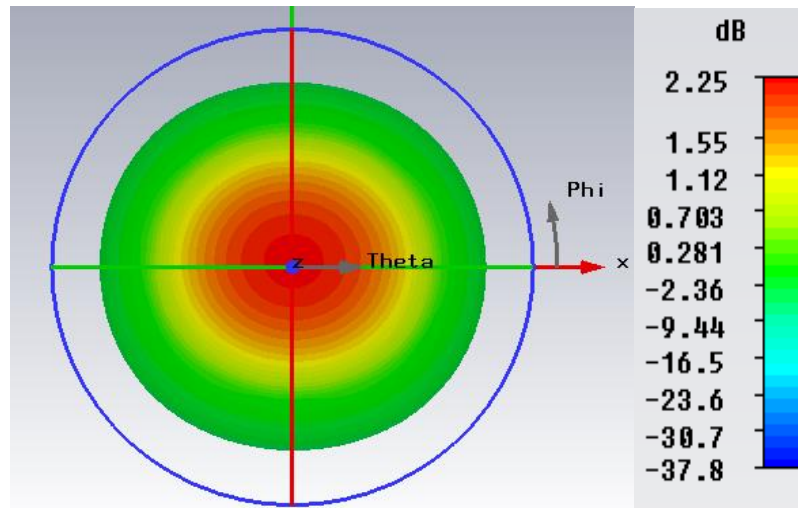


Figure 3.10(c) 3D plot of second iteration radiation pattern

3.1.3 Edge Fed Sierpinski Carpet Third Iteration

All the parameters remain the same as second iteration. From the return loss plot in Figure 3.12, the antenna is resonating at 2.45GHz with return loss of -23dB this shows that the antenna retain its resonating point after third iteration while antenna size further reduced by 17.49%. Figure 3.13(a-c) shows the 3D and polar plot radiation pattern of the antenna in third iteration. From the result, the antenna has similar radiation pattern as the main patch with a gain of 2.37dB.

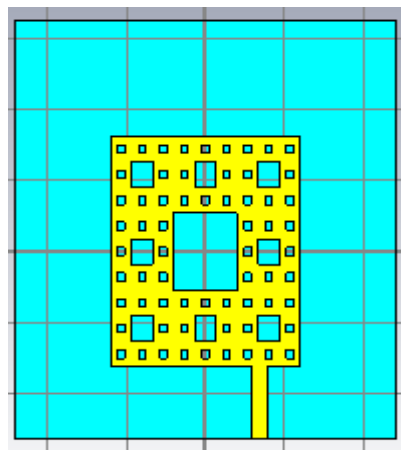


Figure 3.11: Sierpinski Carpet third iteration

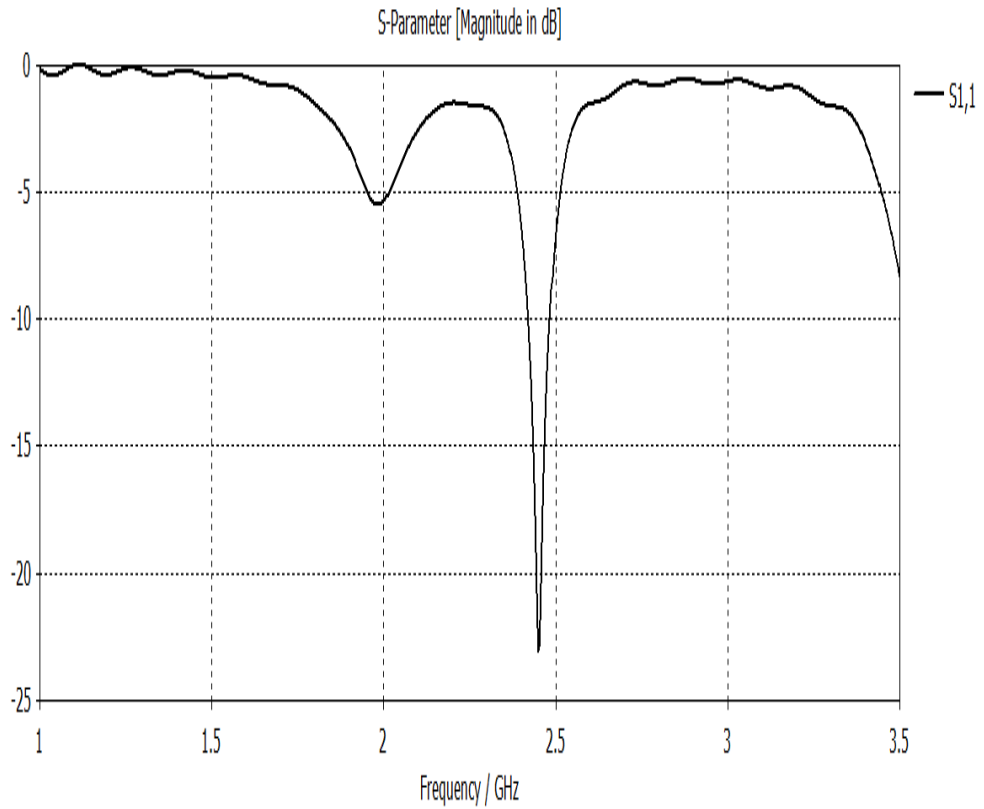


Figure 3.12: Third iteration SCF reflection coefficient

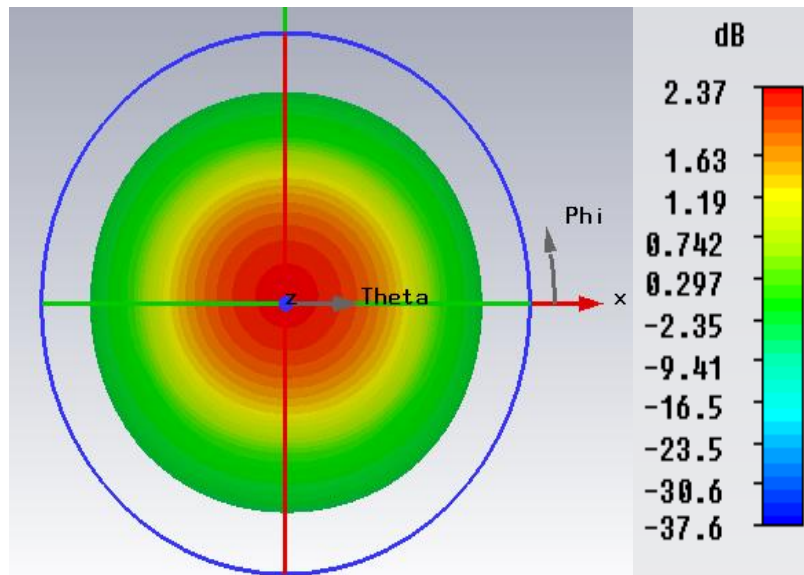


Figure 3.13(a): 3D radiation pattern of third iteration

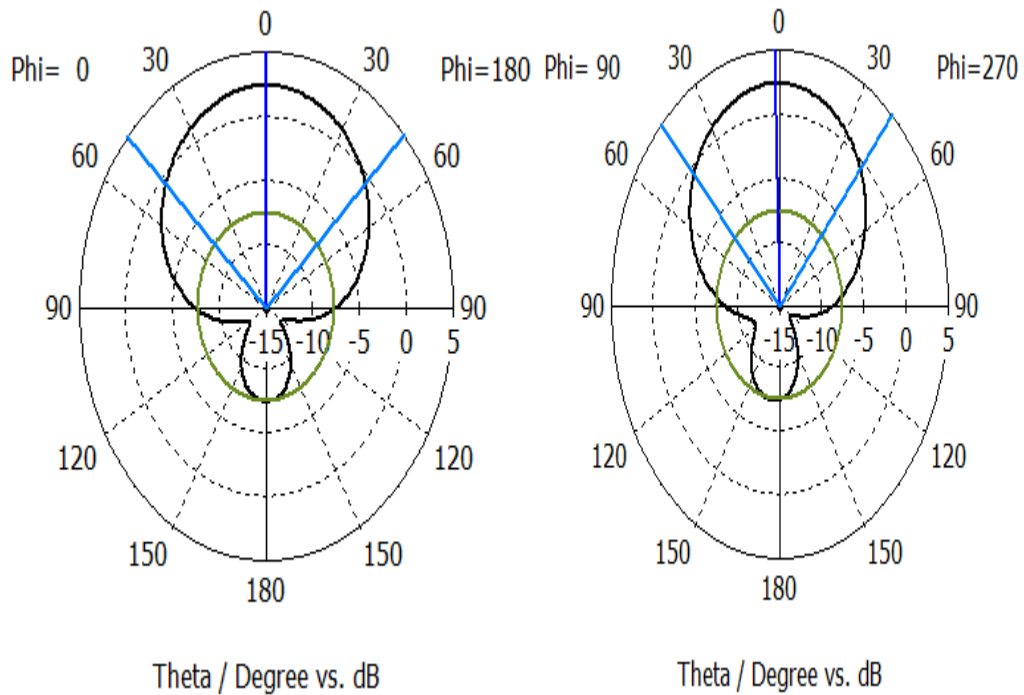


Figure 3.13(b): H- plane radiation pattern Figure 3.13(c): E- plane radiation pattern

So far we have designed an edge fed Sierpinski carpet microstrip fractal antenna in third iteration to achieve size reduction without affecting the resonant frequency. Antenna performance was observed at the designed frequency of 2.45GHz. The resonant frequency was kept constant after the third iteration thereby achieving 17.49% size reduction. This antenna can find applications as wireless sensor.

3.2 Using a Single Slot to Design Miniaturized Patch Antenna

In this section, instead of going through several iterations which involves complex stage we take a simple iteration by using an iteration factor of $\frac{1}{2}$ which will achieve 34.88% reduction of the main patch. To further enhance the antenna performance, a slit was made in the ground plane to increase the bandwidth of the antenna compare to the main patch. Figure 3.14 shows the structure of the modified design.

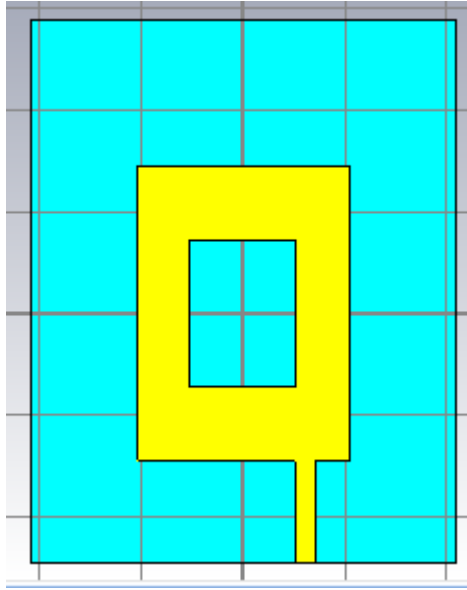


Figure 3.14: Modified Miniaturized Patch Antenna

The length and width of the patch were slightly adjusted while keeping the feed position constant as in first iteration. From the return loss plot in Figure 3.15, the antenna is resonating at 2.45GHz with return loss of -36dB this shows that the antenna retain its resonating point after achieving 34.88% size reduction of the main patch. Figure 3.16(a-c) shows the 3D and polar plot radiation pattern of the antenna in the new modified iteration. From the 3D result, the antenna has a gain of 0.48dB.

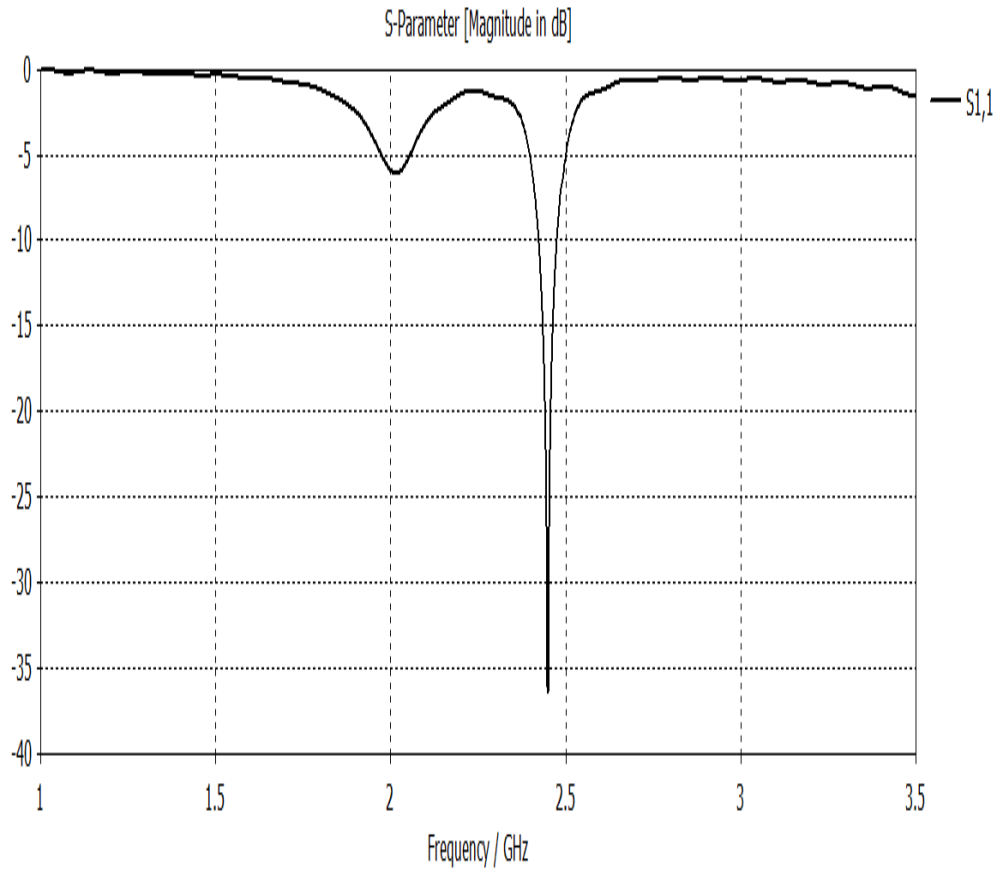


Figure 3.15: Return loss plot for the new modified miniaturized MPA

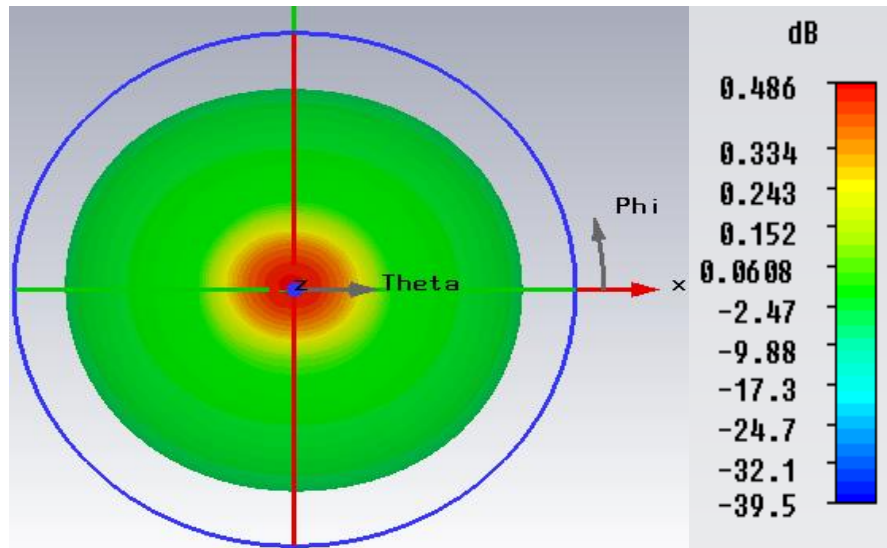


Figure 3.16(a): 3D radiation pattern of the new modified miniaturized MPA

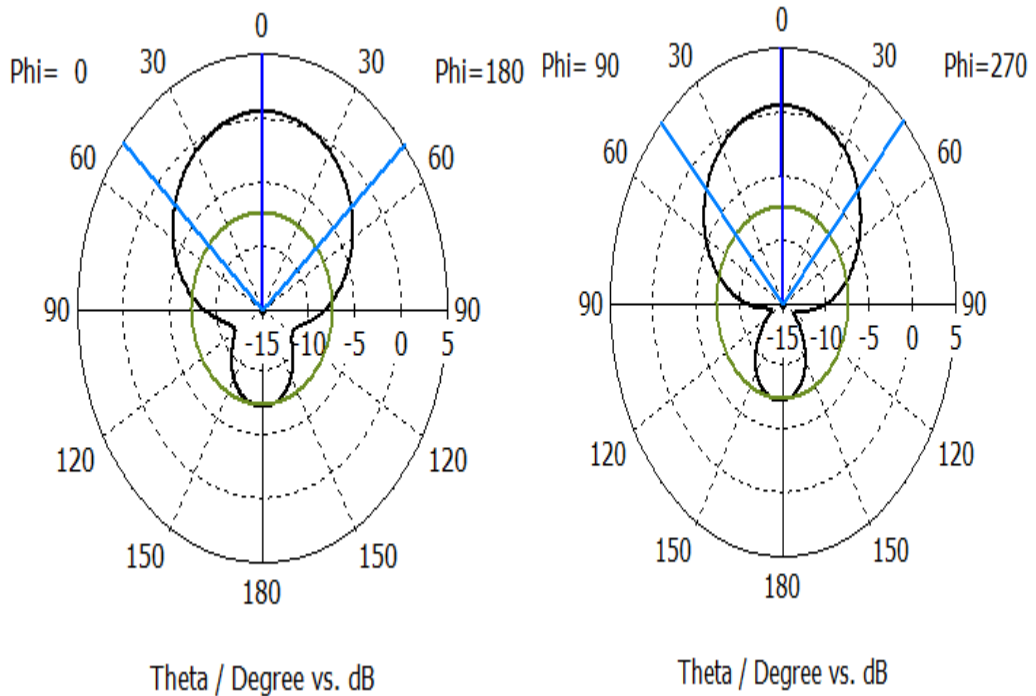


Figure 3.16(b): H- plane radiation pattern Figure 3.16(c): E- plane radiation pattern

So far we have come up with a simple single slot miniaturized microstrip patch antenna design to reduce the patch antenna size by 34.88% without affecting the operating frequency. We will further investigate the effect of cutting the ground plane on the designed antenna.

Without changing any parameter test will be carried out on the ground plane by slightly cutting it from top. Figure 3.17 shows the ground plane reduces by 5mm, 10mm, 15mm and 20mm. The effect on the resonant frequency is shown in Figure 3.18.

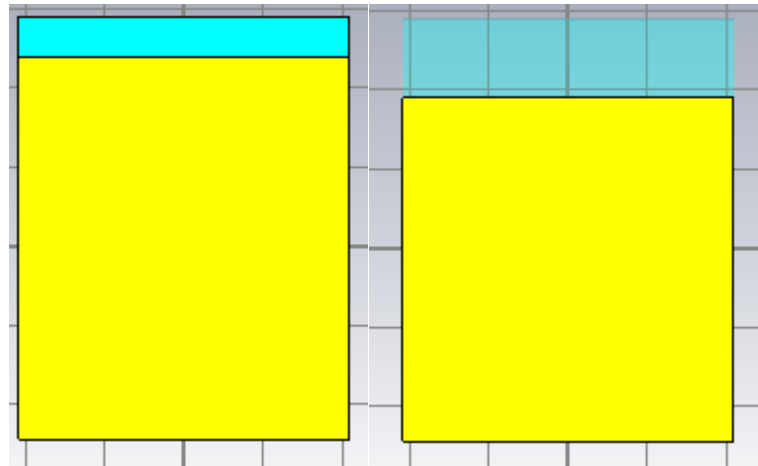


Figure 3.17(a): Lg-5

Figure 3.17(b): Lg-10

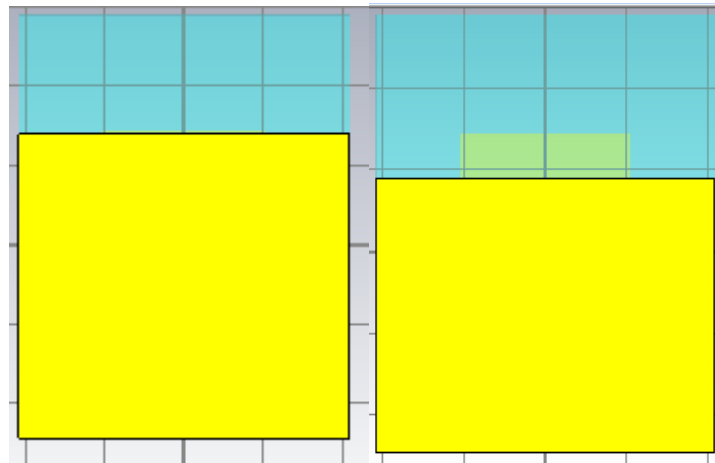


Figure 3.17(c): Lg-15

Figure 3.17(d): Lg-20

Figure 3.17(a-d) above shows the cut made in the ground plane to see the effect on the resonant frequency. From the return loss plot, we can observe that as the ground plane is cut from the top, the resonant frequency shift backward and the return loss graph move upward showing there is increase reflection. The antenna is resonating until the ground cut is below the patch which shows there is high loss in the antenna. From the return loss we observed there is little increment in the bandwidth but since the antenna is not resonating at the desired 2.45GHz frequency, the radiation pattern will not be analysed for this test as we are concerned with the antenna behaviour at 2.45GHz.

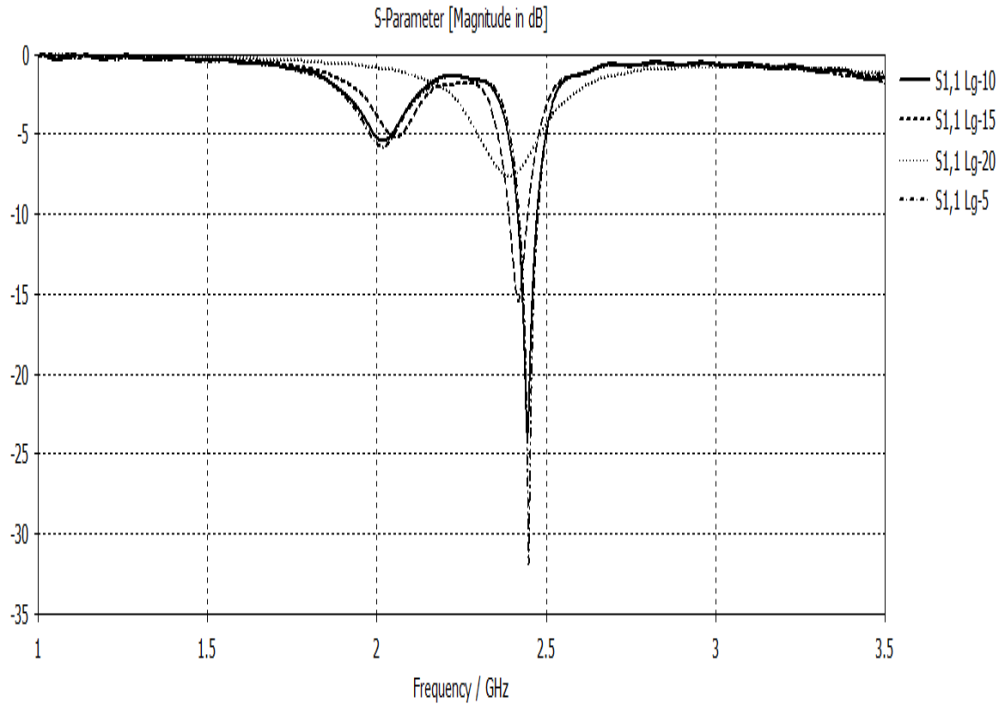


Figure 3.18: Return loss plot for various ground length

3.2.1 Modified Miniaturized Patch Antenna With U Slot Ground To Increase Bandwidth.

From the literature review it was reported that creating a slit in the ground will further increased the bandwidth and overall performance of the antenna [23]. Here a simple U slit is made in the ground plane of the modified miniaturized patch antenna and the result was compared with the main design to see the effect of the U slit. Figure 3.19 show the structure of the modified shape with U slit ground.

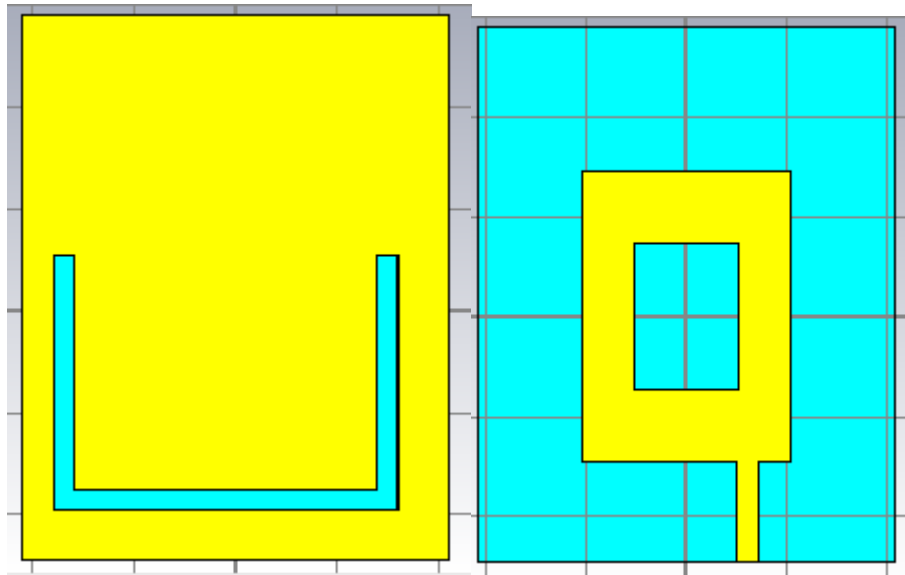


Figure 3.19: Front and back view of the new proposed U slit ground SCF

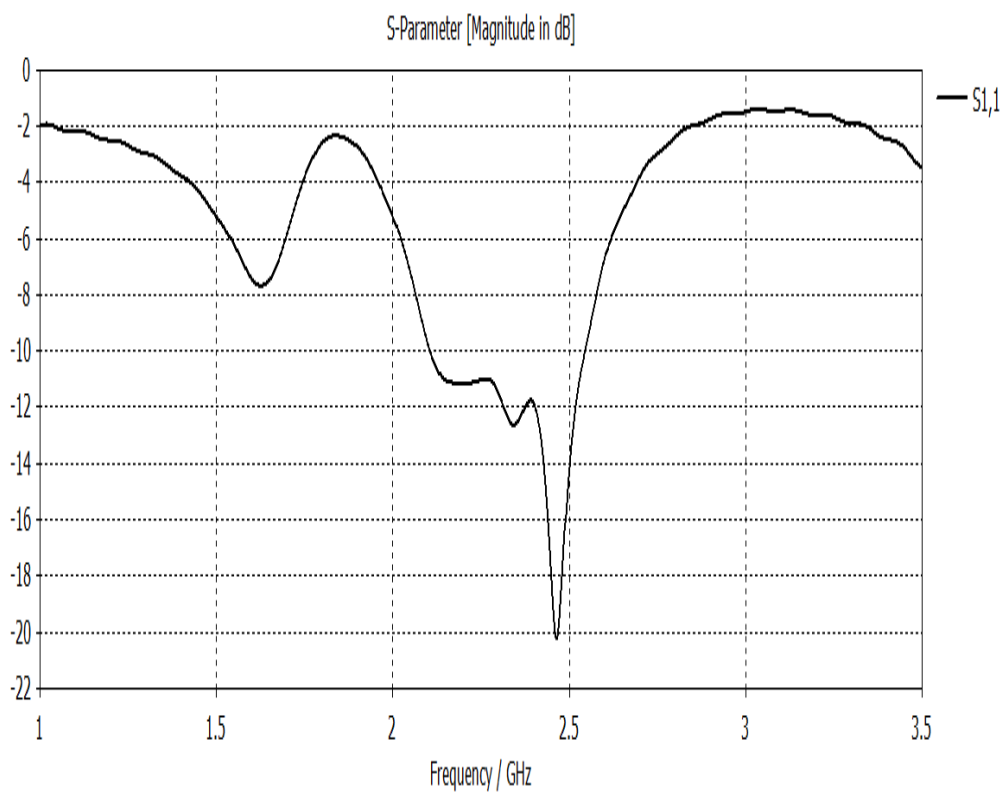


Figure 3.20: Return loss plot for the U slit ground sierpinski carpet

From the return loss plot, we can observe that the antenna has a very wide bandwidth of 442MHz in the frequency range of 2.1GHz-2.54GHz. The bandwidth increment was due to the U slit made in the ground plane. The radiation pattern measured at

2.45GHz shows that the gain of the antenna has increased from 0.486dB to 2.62dB. Using defected ground structure provides wider bandwidth, enhanced gain and higher radiation efficiency [12].

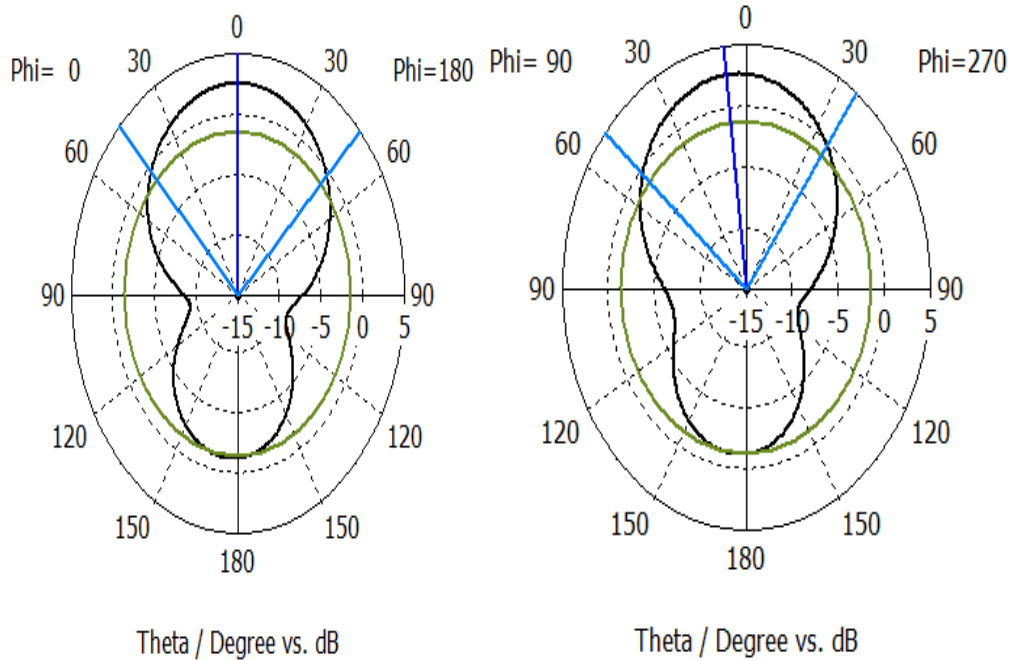


Figure 3.21(a): H- plane radiation pattern Figure 3.21(b): E- plane radiation pattern

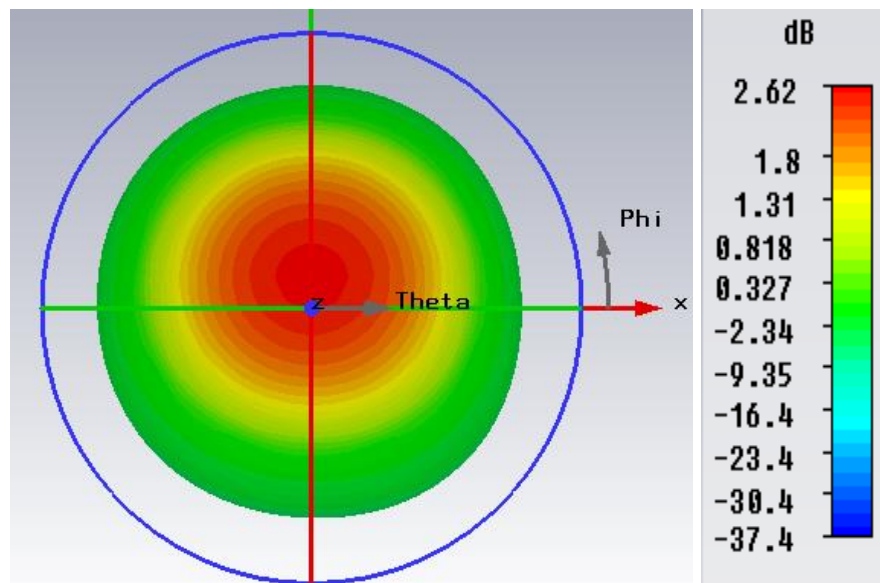


Figure 3.21(b):3D radiation pattern at 2.45GHz

From the radiation pattern plot we can see that the H-plane has main lobe direction at 0° while the E-plane direction is at 7° . The shift in the main lobe direction was due to the U slot introduced in the ground plane. We can therefore conclude that reducing the patch antenna by 34.88% of the original size with U slit in the ground plane enhanced the performance of the patch antenna in terms of gain and bandwidth but shift the E-plane beam direction.

Table 3.3: Performance of the designed antenna

Antenna	Return loss(dB)	Bandwidth (MHz)	Gain (dB)	Area Reduction
Generator	-37	70	3.64	
First iteration	-25	62	2.41	12.67%
Second iteration	-29	69	2.25	17.49%
Third iteration	-23	69	2.37	17.49%
Modified approach	-36	59	0.48	34.88%
Modified approach with U slot	-19	442	2.62	34.88%

The proposed method was compared with result obtained by S. Shretha et'al which is shown in table 3.4

Table 3.4 Comparison of Result

RESULTS	S.Shretha et'al	Proposed Method
Return loss	-38.25dB	-19dB
Bandwidth	60MHz	442MHz
Gain	2.39dB	2.62dB
Size Reduction	17.49%	34.88%

This antenna can find application in wireless sensor, radio frequency application and personal area network.

Chapter 4

SIERPINSKI CARPET FRACTAL FOR MULTIBANDS APPLICATIONS

There is an increasing demand for small size, low cost, multiband and wideband antenna due to advancement in communication technology. Fractal design is a better candidate in meeting this demand. This chapter tends to design a multiband antenna using third iteration Sierpinski Carpet fractal on square microstrip patch antenna.

4.1 Antenna Design

A miniaturized compact antenna was designed based on the well-known Sierpinski Carpet fractal with iteration factor of $1/3$. The antenna was designed up till third iteration to achieve multiband. FR-4 lossy with permittivity of 4.5 of 0.012 loss tangent and thickness of 1.59mm was used as the substrate. Copper was used as the radiating patch and the ground plane. The same procedure described previously was used in designing the antenna.

Same antenna was designed by [8] by taking a square patch of 37mmx37mm but the material used for the radiating patch and the feed position was not stated in [8]. The patch antenna was matched to $Z_0 = 50 \Omega$ transmission lines using quarter wave transformer. The impedance at the edge of the patch antenna $Z_{in} = 247.5 \Omega$ was provided by the program in [27]. The quarter wave line characteristic impedance was calculated as follows:

$$Z_1 = \sqrt{Z_0 Z_{in}} \quad (4.1)$$

The desired length and width of the transmission line were calculated by inserting the appropriate data into transmission line calculator. In this simulation, the antenna was fed at the centre of the patch, as this is the optimum point where resonant was achieved.

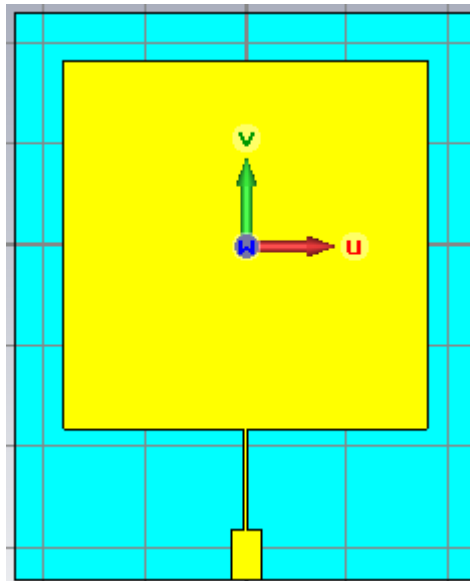


Figure 4.1: MPA geometry

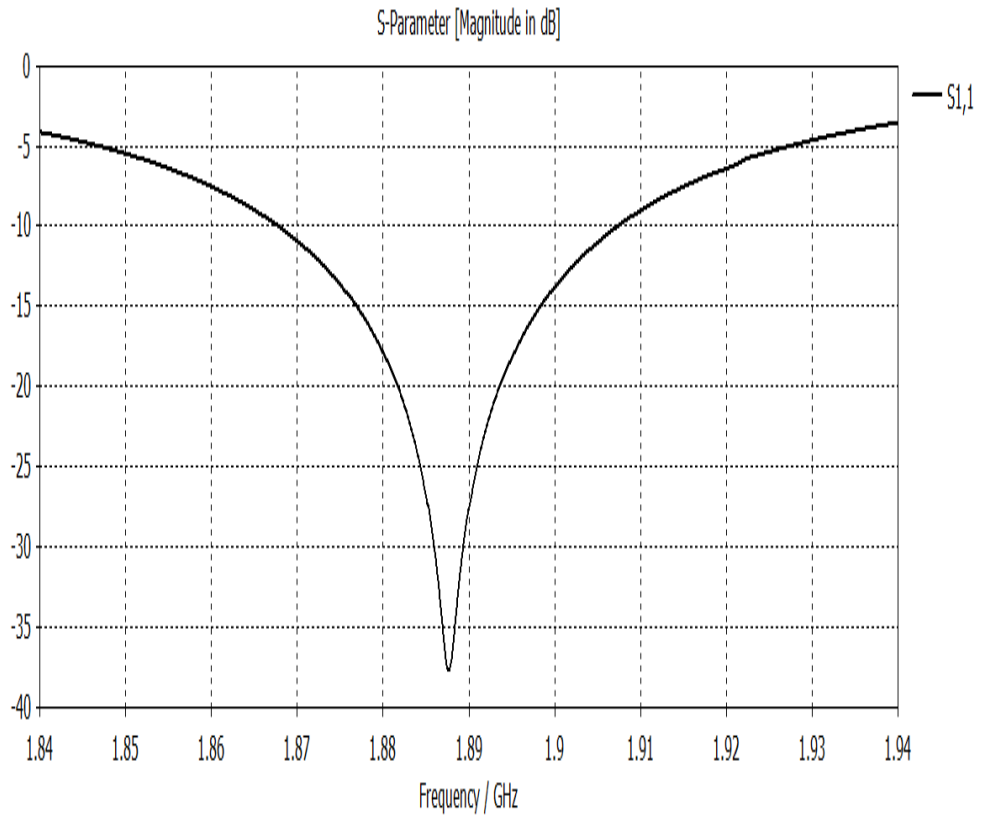


Figure 4.2: MPA reflection coefficient

From Figure 4.2, the antenna is resonating at 1.8877GHz with return loss of -37 dB.

This same antenna was designed by [8] using IE3D and the return loss plot is shown in Figure 4.3.

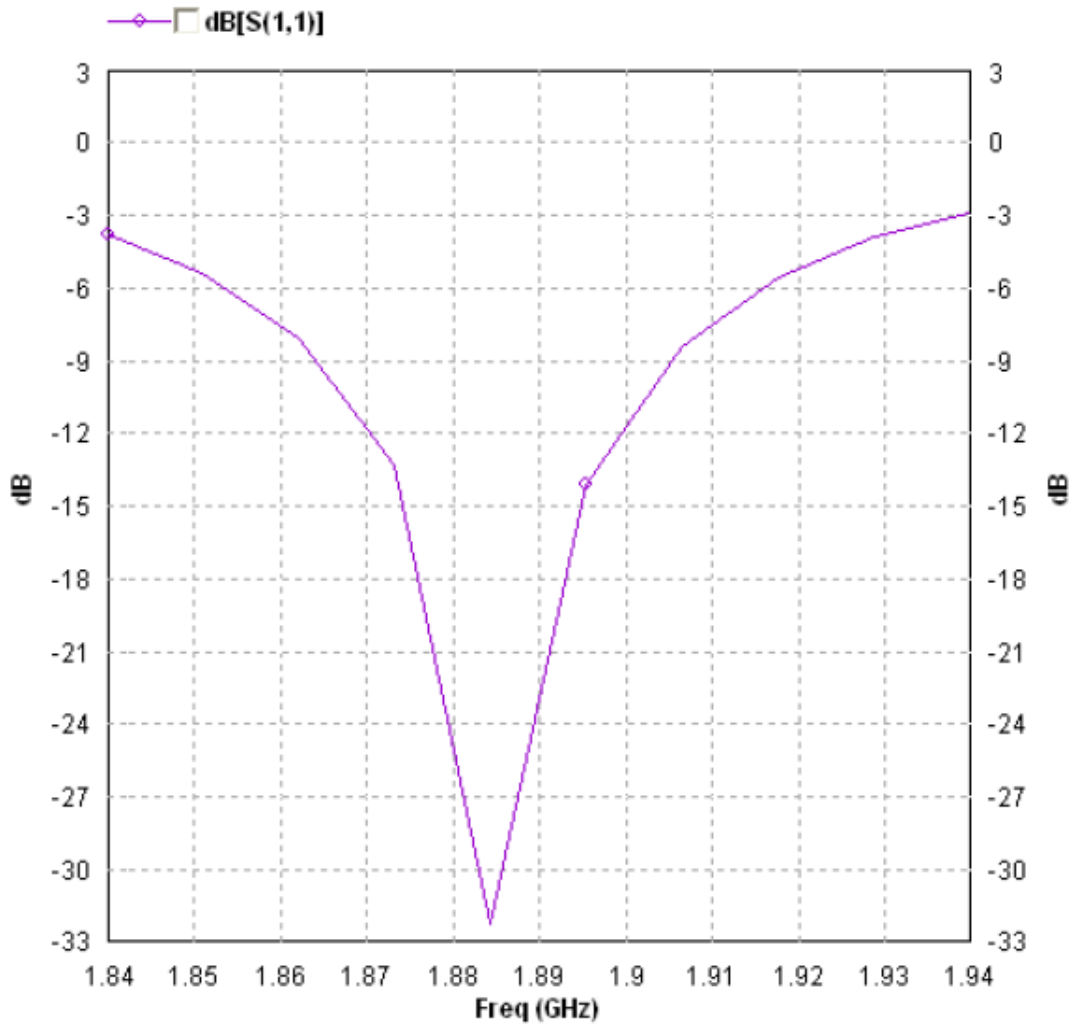


Figure 4.3: MPA reflection coefficient simulated in IE3D [8]

We can see that the antenna is resonating at 1.884GHz with return loss of -32db. From the radiation pattern result, the antenna has a gain of 3.17dB with 59% radiation efficiency. The radiation pattern is shown in Figure 4.4.

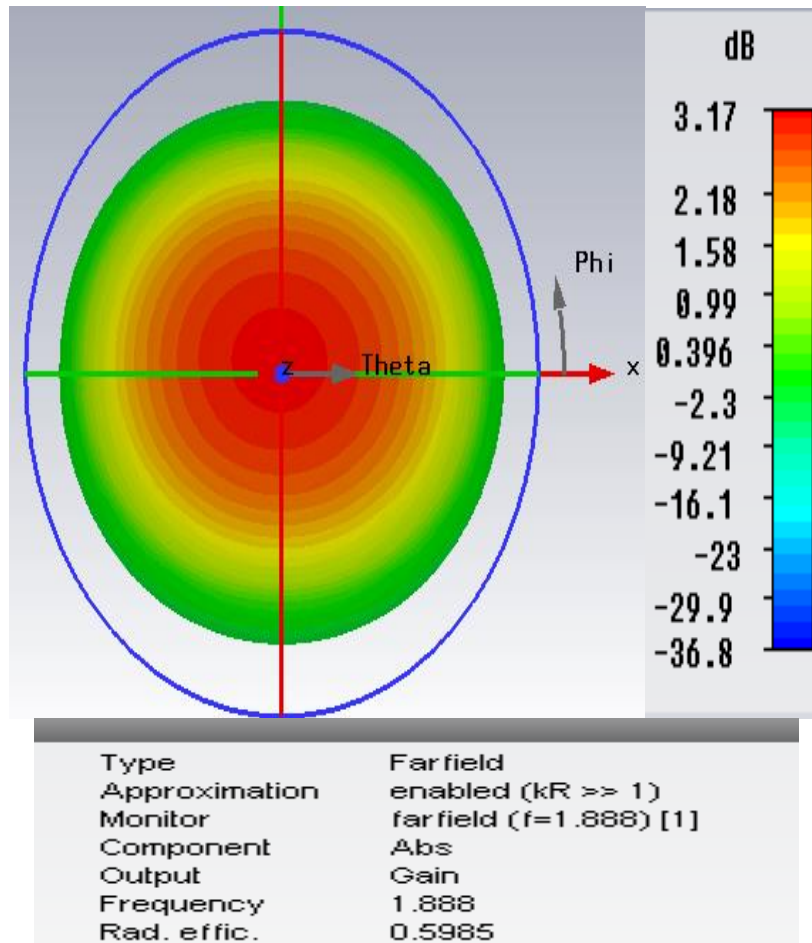


Figure 4.4(a): 3D radiation pattern

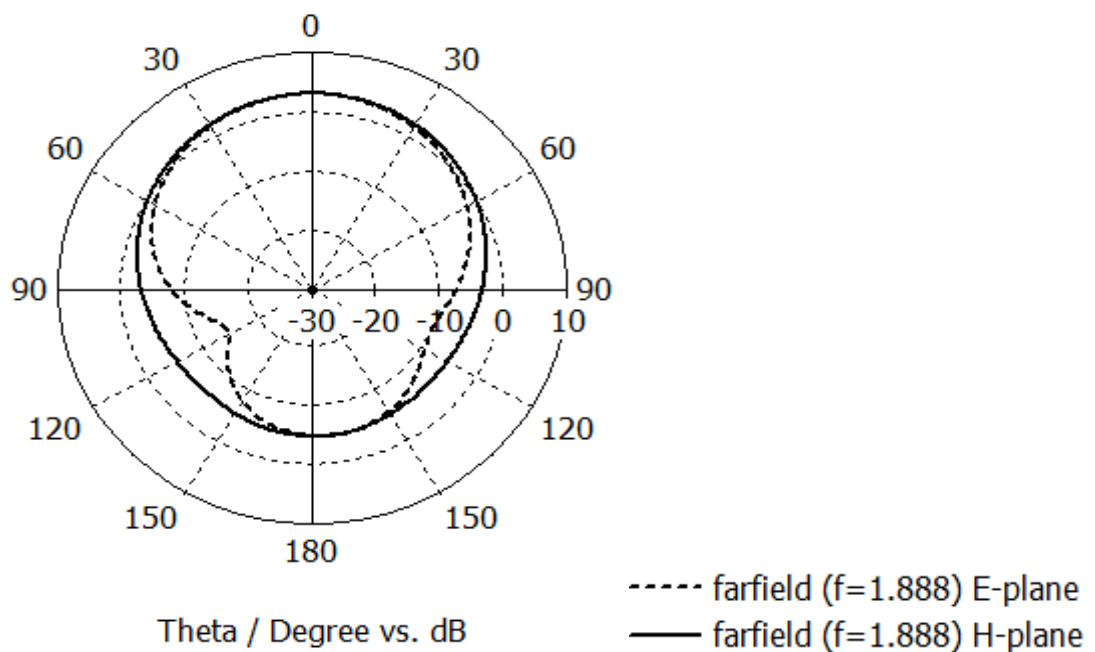


Figure 4.4(b): Polar plot radiation pattern

4.1.1 Sierpinski Carpet First Iteration

The Sierpinski Carpet geometry in the first iteration with the iteration factor of $1/3$ was applied to the antenna without changing any parameter of the patch. This involves dividing both the length and width of the patch by 3 and removing the middle square which will form air gap to achieve the first iteration. The structure is shown in Figure 4.5.

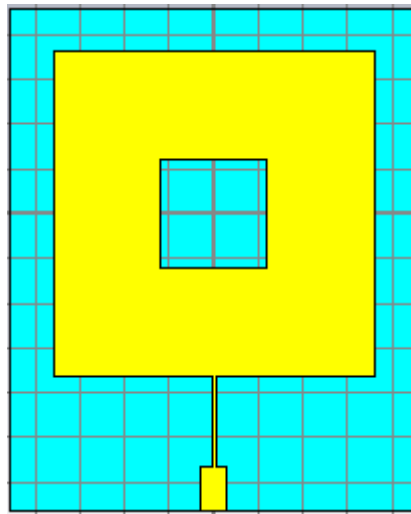


Figure 4.5: Sierpinski carpet first iteration

From figure 4.5, the empty space shows the first iteration. Figure 4.6 shows the return loss plot. The plot shows that the antenna demonstrates a multiband behaviour. The first point of the resonance is at 1.71GHz which is due to the frequency lowering property of the Sierpinski Carpet microstrip patch antenna [7]. Table 4.1 shows the resonating points of the antenna and their characteristics.

Table 4.1: Result of first iteration

Centre Frequency (GHz)	S11 (dB)	Upper Frequency (GHz)	Lower Frequency (GHz)	Bandwidth (MHz)	Gain (dB)	Efficiency (%)
1.71	-22	1.7319	1.6846	47.29	0.1	31
5.83	-20	5.8782	5.7912	86.97	1.87	40
6.73	-31	6.7931	6.6724	120.6	2.06	39
7.69	-23	7.7828	7.6035	179.26	3.21	42
9.28	-15	9.358	9.2057	152.34	6.81	36

As seen from the table above, the antenna shows multiband behaviours with highest bandwidth of 179MHz.

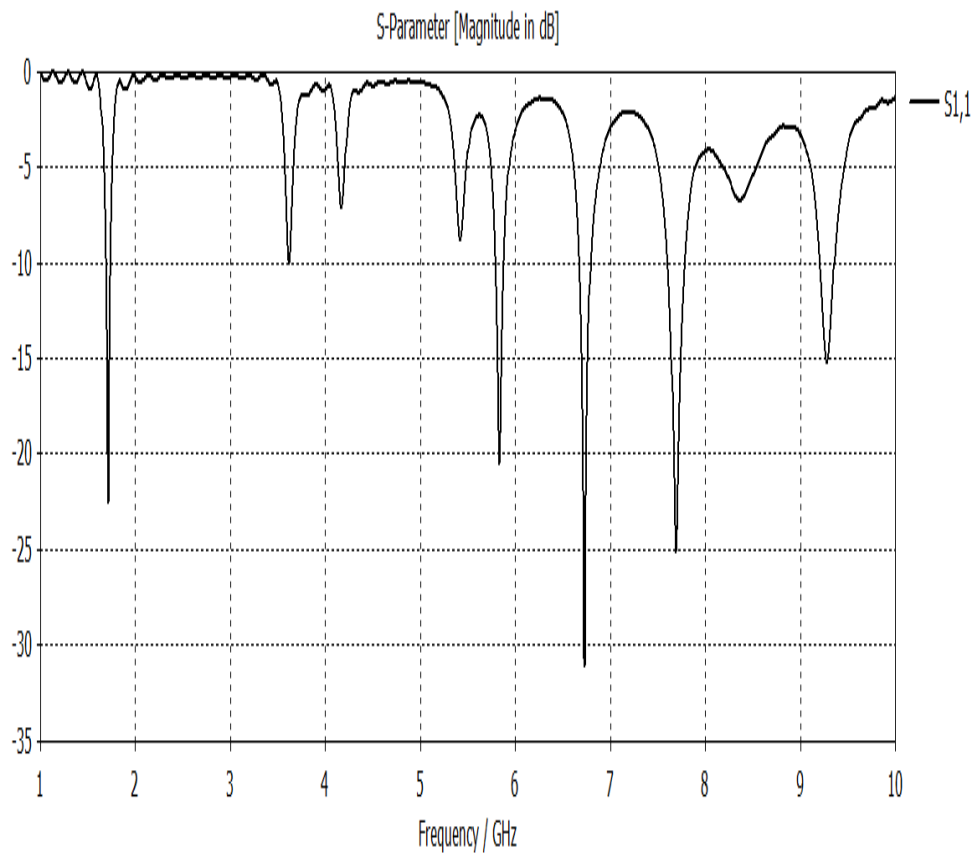
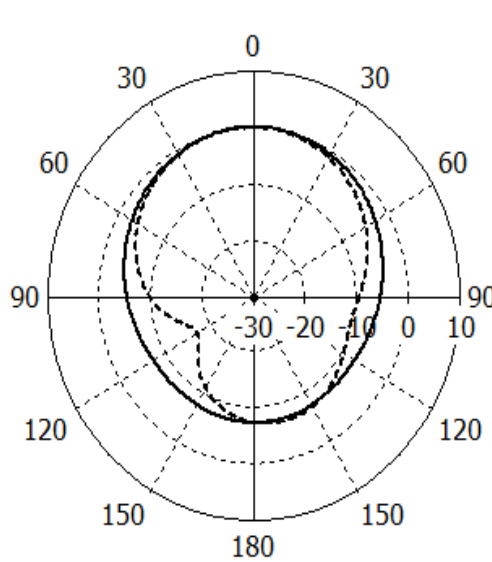


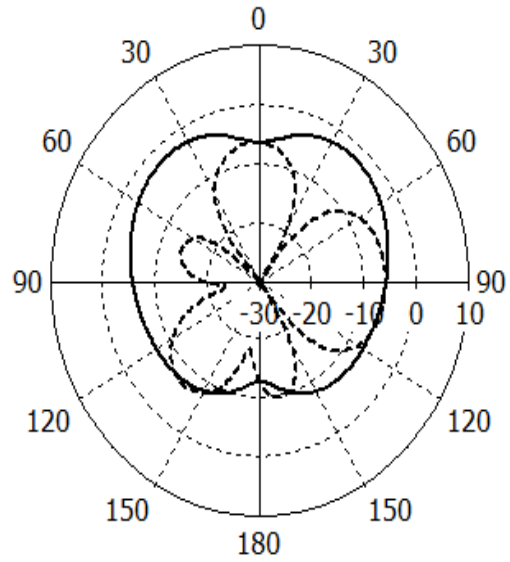
Figure 4.6: First iteration SCF reflection coefficient

Figure 4.7 (a-e) shows the polar plot radiation pattern of the first iteration measured at five resonant frequencies.



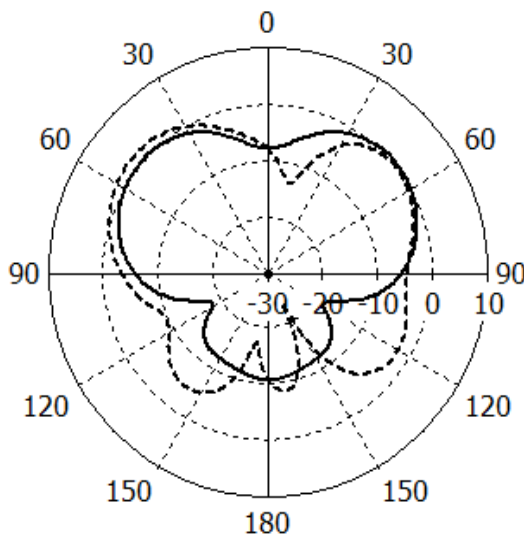
Theta / Degree vs. dB
 ----- farfield (f=1.71) E-plane
 ————— farfield (f=1.71) H-plane

Figure 4.7(a)

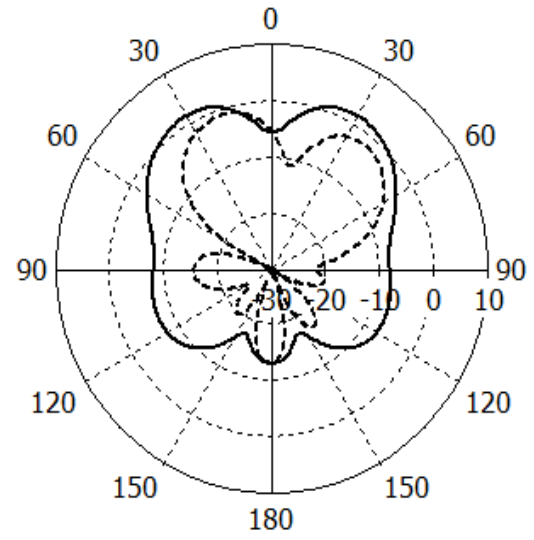


Theta / Degree vs. dB
 ----- farfield (f=5.83) E-plane
 ————— farfield (f=5.83) H-plane

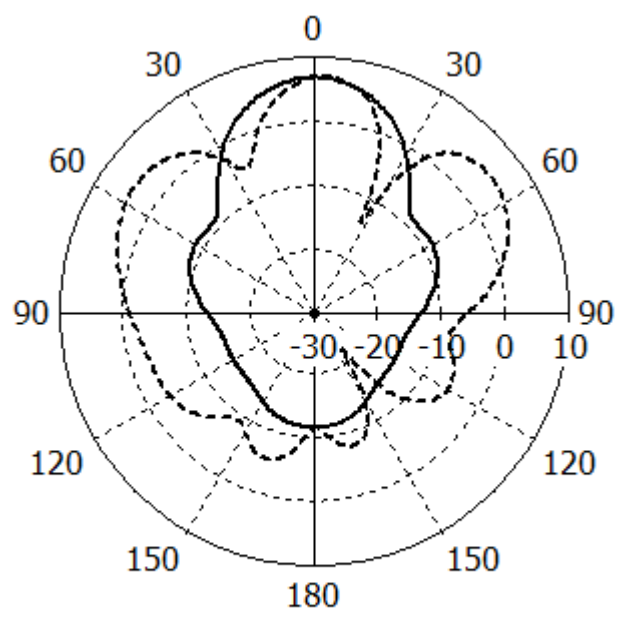
Figure 4.7 (b)



Theta / Degree vs. dB
 - - - - - farfield (f=6.73) E-plane
 ——— farfield (f=6.73) H-plane
 Figure 4.7 (c)



Theta / Degree vs. dB
 - - - - - farfield (f=7.69) E-plane
 ——— farfield (f=7.69) H-plane
 Figure 4.7 (d)



Theta / Degree vs. dB
 - - - - - farfield (f=9.28) E-plane
 ——— farfield (f=9.28) H-plane
 Figure 4.7 (e)

4.1.2 Sierpinski Carpet Second Iteration

Following the design procedure described previously, the second iteration is shown below in Figure 4.8. All the parameters were left unchanged.

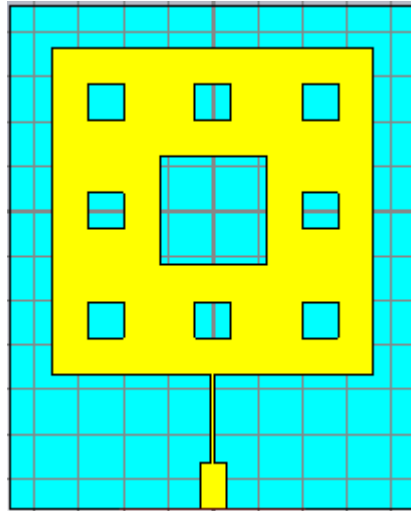


Figure 4.8: Sierpinski Carpet second iteration

The plot of return loss of the designed antenna is shown in Figure 4.9. The plot shows that the antenna demonstrates a multiband behaviour. Again as observed from the plot, the first point of resonance is at 1.7GHz which is due to the frequency lowering property of the Sierpinski Carpet microstrip patch antenna after iteration. Table 4.2 shows the resonating points of the antenna and their characteristics.

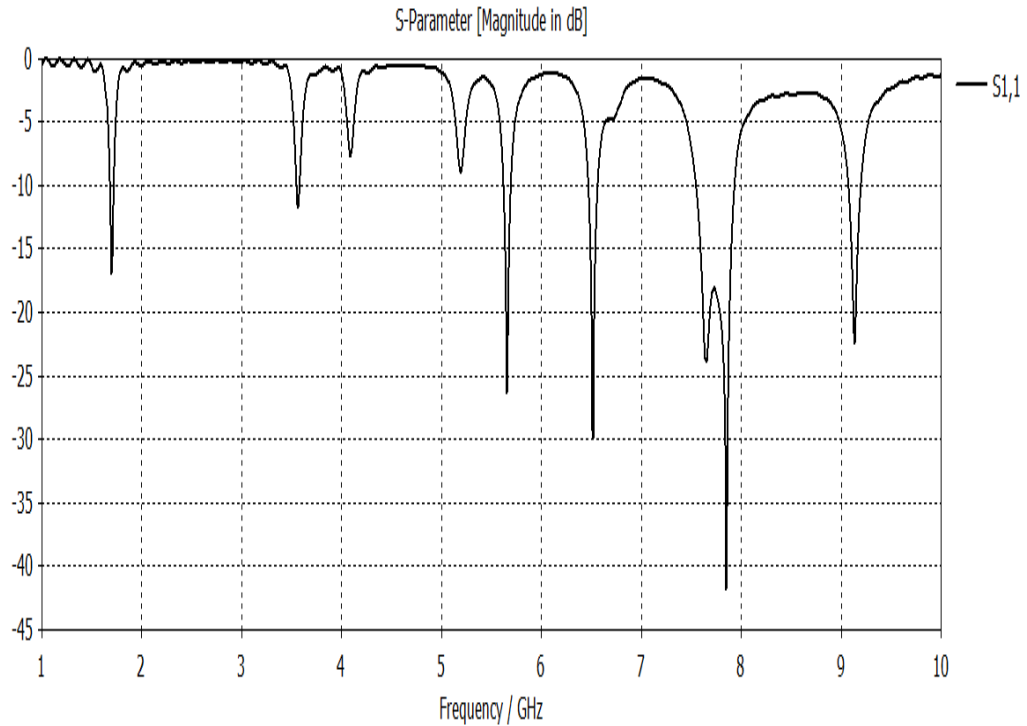
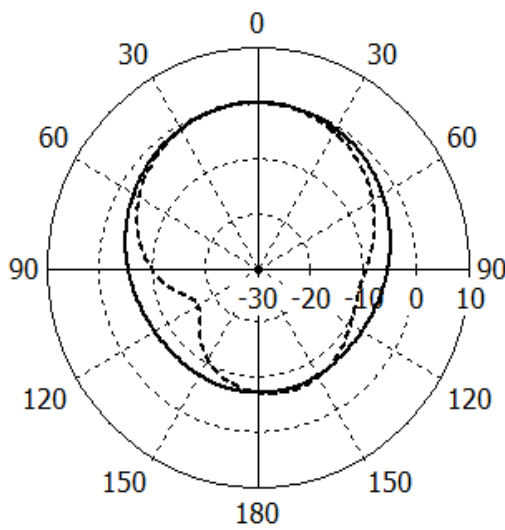


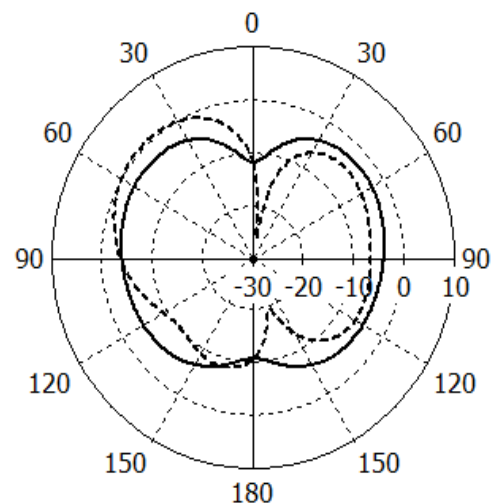
Figure 4.9: second iteration SCF reflection coefficient

Polar plots of radiation patterns for different resonant frequency are shown in Figure 4.10(a-f).



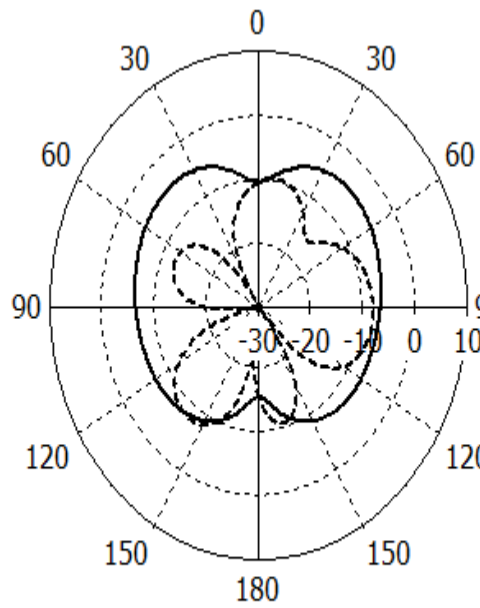
Theta / Degree vs. dB
 - - - - farfield (f=1.7) E-plane
 ——— farfield (f=1.7) H-plane

Figure 4.10(a)



Theta / Degree vs. dB
 - - - - farfield (f=3.57) E-plane
 ——— farfield (f=3.57) H-plane

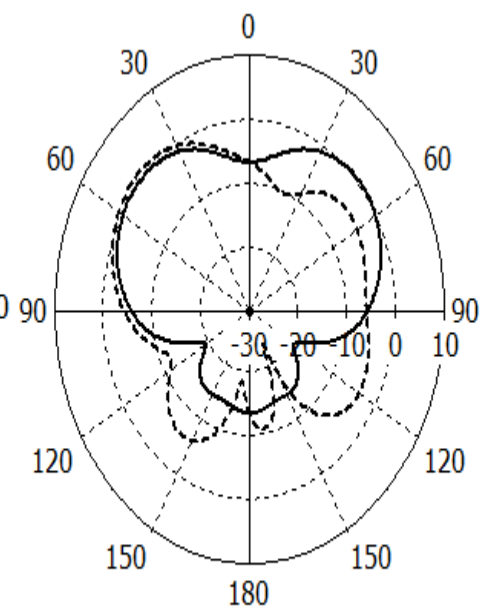
Figure 4.10 (b)



Theta / Degree vs. dB

----- farfield (f=5.66) E-plane
 ——— farfield (f=5.66) H-plane

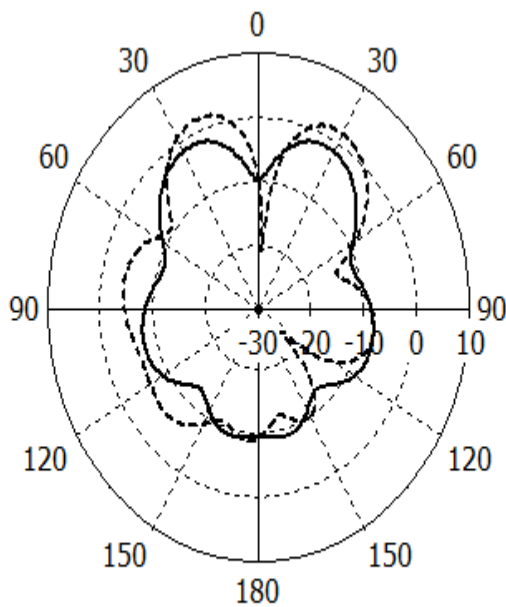
Figure 4.10 (c)



Theta / Degree vs. dB

----- farfield (f=6.53) E-plane
 ——— farfield (f=6.53) H-plane

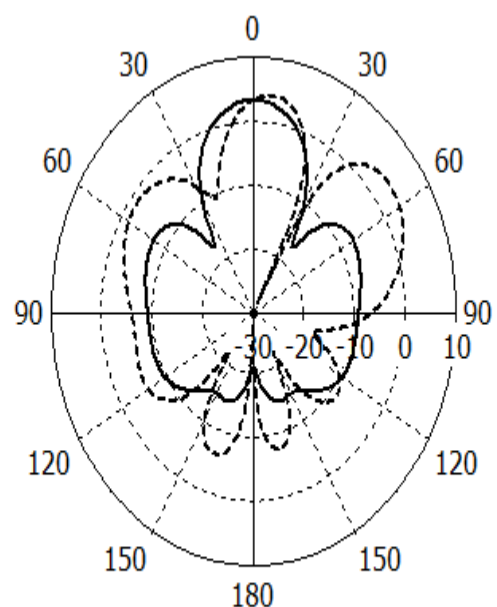
Figure 4.10 (d)



Theta / Degree vs. dB

----- farfield (f=7.85) E-plane
 ——— farfield (f=7.85) H-plane

Figure 4.10 (e)



Theta / Degree vs. dB

----- farfield (f=9.14) E-plane
 ——— farfield (f=9.14) H-plane

Figure 4.10 (f)

Table 4.2: Results of the second iteration.

Centre Frequency (GHz)	S11 (dB)	Upper Frequency (GHz)	Lower Frequency (GHz)	Bandwidth (MHz)	Gain (dB)	Efficiency (%)
1.7	-16	1.7167	1.6767	39.97	0.07	31
3.57	-11	3.579	3.5466	32.3	0.677	30
5.66	-26	5.6173	5.6941	76.8	1.03	32
6.53	-29	6.5619	6.4679	94.02	1.56	34
7.85	-41	7.9349	7.552	382.9	1.76	20
9.14	-23	9.201	9.0709	130.14	4.03	25

From Table 4.2, we can observe that the antenna have six different resonant frequencies with highest bandwidth of 382.9MHz. The antenna gain keeps decreasing as the number of iteration increases.

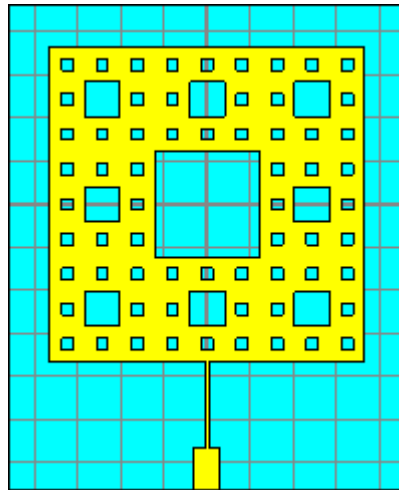


Figure 4.11: Sierpinski Carpet third iteration model

Further iteration is made to see the effect on antenna performance. From the return loss plot in Figure 4.12, the antenna shows a multiband behaviour almost similar to the second iteration.

Table 4.3: Results of third iteration.

Centre Frequency (GHz)	S11 (dB)	Upper Frequency (GHz)	Lower Frequency (GHz)	Bandwidth (MHz)	Gain (dB)	Efficiency (%)
1.69	-21	1.7151	1.6679	47.11	-0.506	30
3.57	-11	3.5721	3.5413	30.73	0.527	30
5.64	-24	5.6839	5.6062	77.75	0.828	31
6.5	-35	6.5526	6.4574	95.20	1.22	32
7.85	-30	7.929	7.5445	384.4	1.55	20
9.14	-23	9.1947	9.0686	126.15	3.91	25

From the result we can conclude that after third iteration, the antenna performance in terms of gain and efficiency start diminishing but with bandwidth increment. Figure 4.13 (a-f) shows polar plot radiation pattern of the antenna in third iteration.

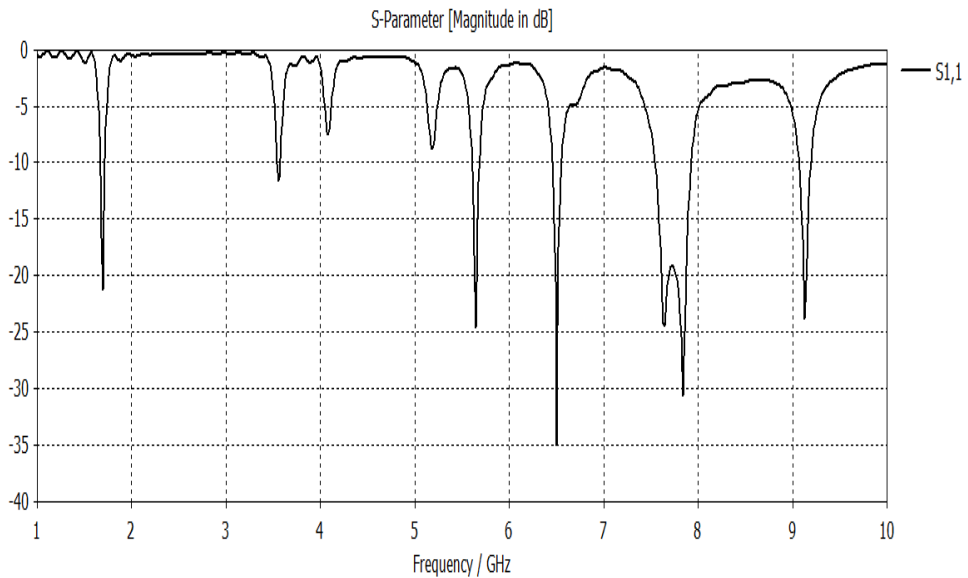
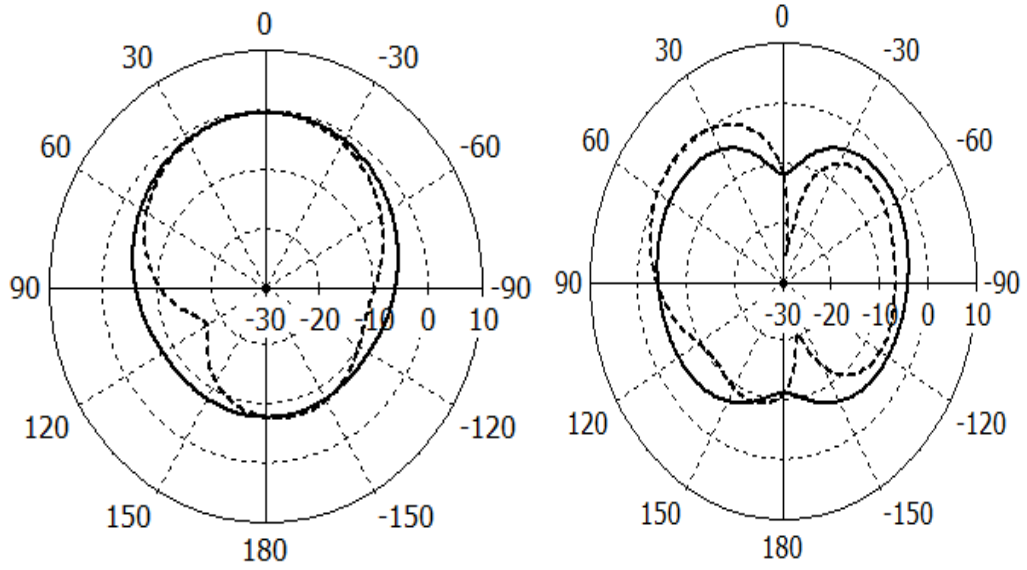


Figure 4.12: Third iteration SCF reflection coefficient

The plot of radiation pattern at each of the resonant frequency is display in Figure 4.13 (a-f).

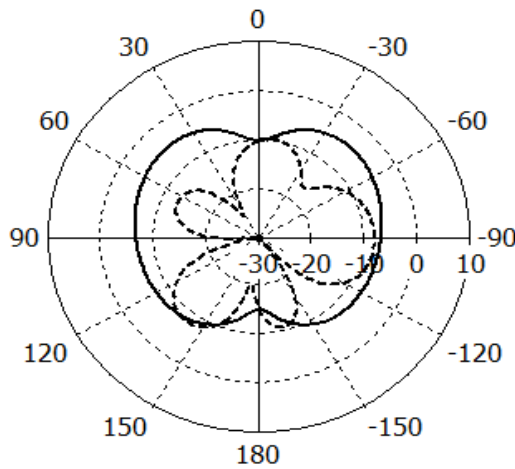


Theta / Degree vs. dB
 ----- farfield (f=1.69) E-plane
 ——— farfield (f=1.69) H-plane

Figure 4.13 (a)

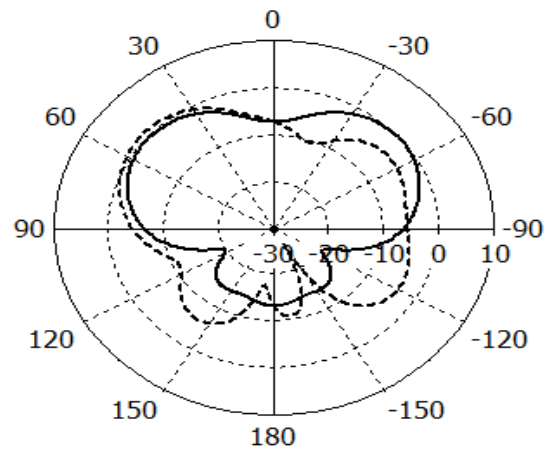
Theta / Degree vs. dB
 ----- farfield (f=3.57) E-plane
 ——— farfield (f=3.57) H-plane

Figure 4.13 (b)



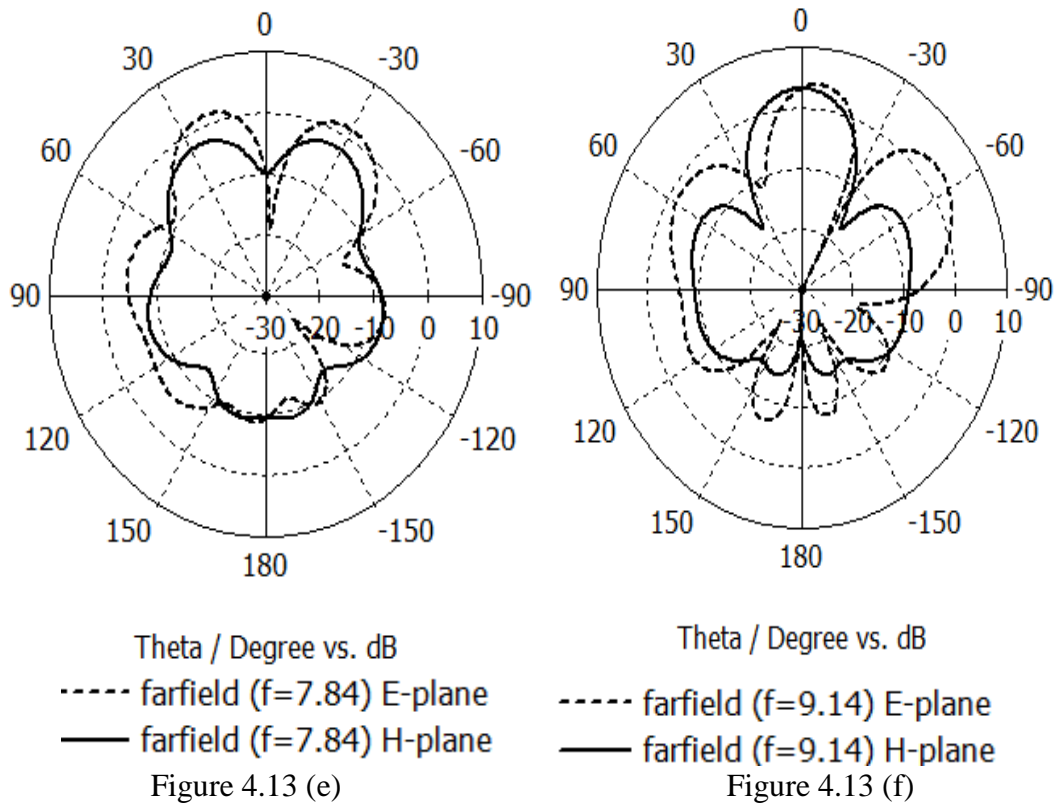
Theta / Degree vs. dB
 ----- farfield (f=5.64) E-plane
 ——— farfield (f=5.64) H-plane

Figure 4.13 (c)



Theta / Degree vs. dB
 ----- farfield (f=6.5) E-plane
 ——— farfield (f=6.5) H-plane

Figure 4.13 (d)



So far we have designed a third order Sierpinski Carpet square patch antenna for multiband application with six different resonant frequencies. As the number of iteration increases, the gain of the antenna reduces which is due to the fractal cut made in the antenna and associated antenna losses. After the third iteration with six resonant frequencies, only two of the resonant frequencies have the same main lobe direction as the direction of the design frequency while other frequencies has different beam directions. This same antenna was designed in Chapter 5 by using a circular fractal shape with partial ground plane to further enhance the performance in terms of the gain, bandwidth and efficiency.

Chapter 5

CIRCULAR FRACTAL ANTENNA WITH PARTIAL GROUND PLANE

This chapter aims at designing a circular fractal antenna with partial ground structure for multiband and wideband application. Due to modern wireless communication system requirement of antenna with improved performance, there is an increase in extensive research of compact antennas [19]. This system requires antenna that possess some characteristics like small size, very light in weight and low cost in other for the antenna to be incorporated inside a mobile telephone without extending out [20]. Microstrip antenna is suitable for this requirement due to its characteristics like small size, light in weight and low cost. Although the microstrip antenna also has limitation such as narrow bandwidth. With the conventional antenna design using infinite ground plane, this narrower bandwidth limitation cannot be curtailed as the bandwidth can only be increase by a small percentage. Several literatures have employed different technique such as the use of truncated ground plane and a rectangular patch tapered from the microstrip feed [21], also using of defected ground structure [22] to enhance the bandwidth of the microstrip antenna. In this work, a circular fractal antenna with partial ground plane is designed to meet the modern wireless communication demand of compact, light, multiband and wideband.

5.1 Antenna design

In circular patch antenna mode, the ground plane, patch and the material between them are treated as two circular cavities. The substrate height of the circular patch is

small ($h \ll \lambda$). Unlike the rectangular patch antenna which is controlled by length and width, the circular patch has only one degree of freedom to control the patch which is the patch radius [1]. By changing the radius of the patch, the patch resonant frequency also changes but without having effect on the patch mode. Analysis of the circular patch antenna can be conveniently carried out using the cavity model. The actual radius of the patch can be obtained using the given equation [1]:

$$R = \frac{F}{\sqrt{1 + \frac{2h}{\pi\epsilon_r F} [\ln\left(\frac{\pi F}{2h}\right) + 1.7726]}} \quad (5.1)$$

Where R is the radius of the patch, h is the substrate height and ϵ_r is the relative permittivity.

$$F = \frac{8.791 \times 10^9}{f_r \sqrt{\epsilon_r}} \quad (5.2)$$

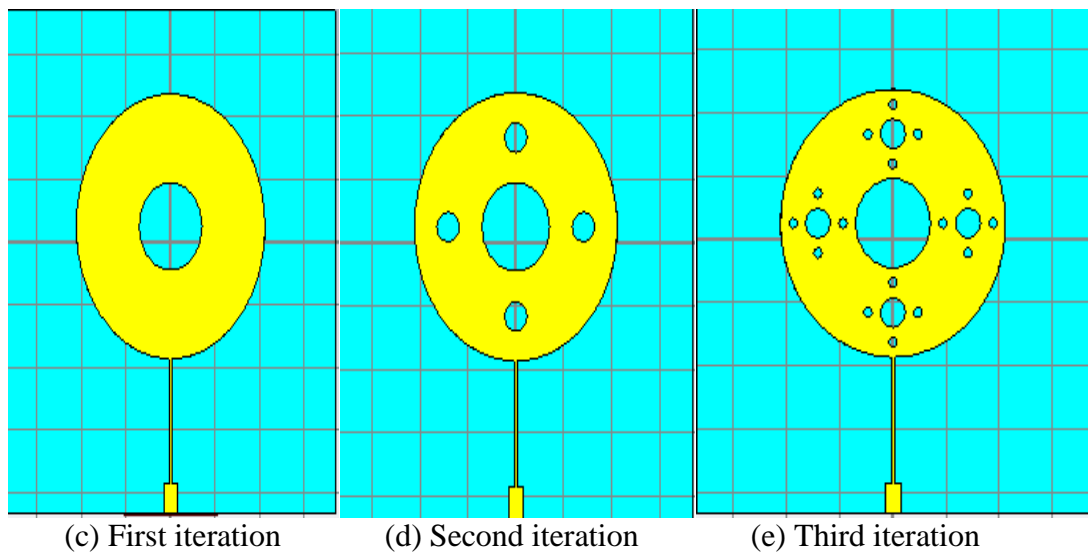
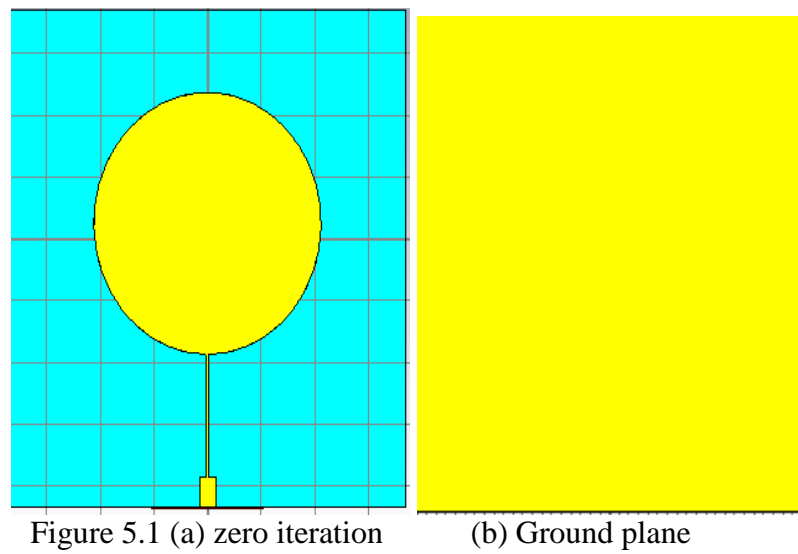
Where f_r is the resonant frequency.

The proposed antenna was previously designed in chapter 4 using square patch with Sierpinski Carpet in third iteration. The same antenna has been designed using circular fractal with partial ground plane. The circular patch was designed with a radius of 21.2mm on a FR-4 lossy substrate with relative permittivity of 4.5 and loss tangent of 0.012. This is called the initial stage without iteration (zero iteration).

The first iteration was achieved by creating a circle of radius R/3 using sierpinski iteration factor of $(1/3)^n$ whose centre lies on the diameter of the main radiating patch. This middle circle was subtracted from the main patch and this is called the first iteration. The second iteration was achieved by creating four circles of radius

$R/9$ and subtracted from the main patch. The third iteration was formed by creating circles of radius $R/27$ and subtracted from the main patch. The same feeding technique employed in chapter 4 was used here to achieve resonance at the desired frequency.

The design antenna is shown in Figure 5.1 below



As we can see from figure above, Figure 5.1(a) shows the circular patch in its conventional form where the ground plane size is the same as the substrate. The first, second and third iteration were shown in Figure 5.1(c-e).

The simulation result of the above figure from zero to third iteration is shown in the next figures.

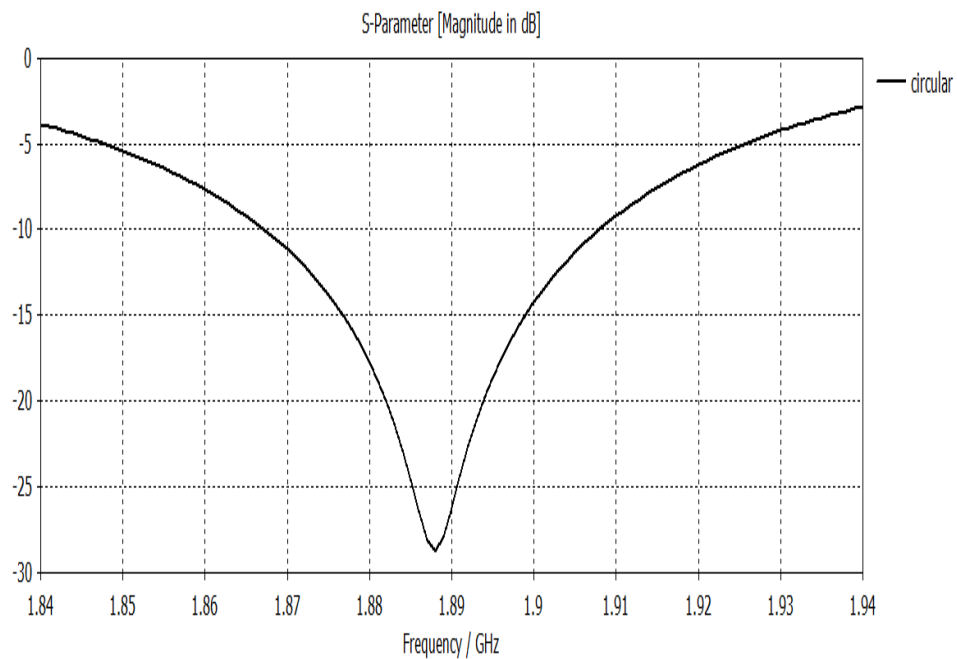
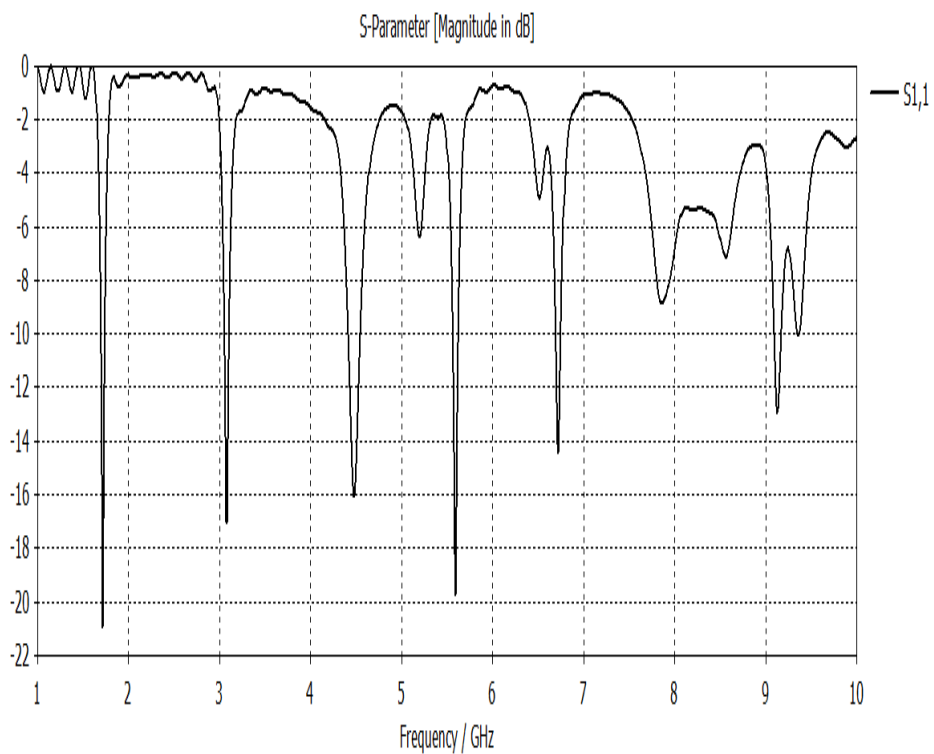
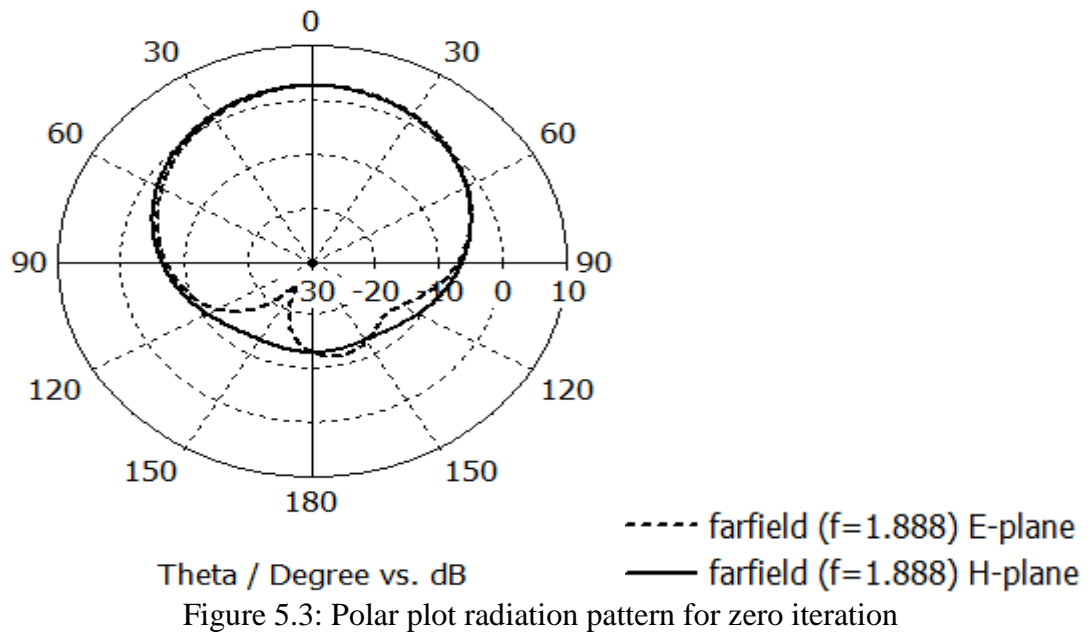


Figure 5.2: Return loss plot of zero iteration

In its conventional form, the zero iteration circular patch antenna is resonating at frequency of 1.888GHz with bandwidth of about 41MHz. The antenna has a gain of 2.59dB with efficiency of 41%. The radiation pattern is shown below.



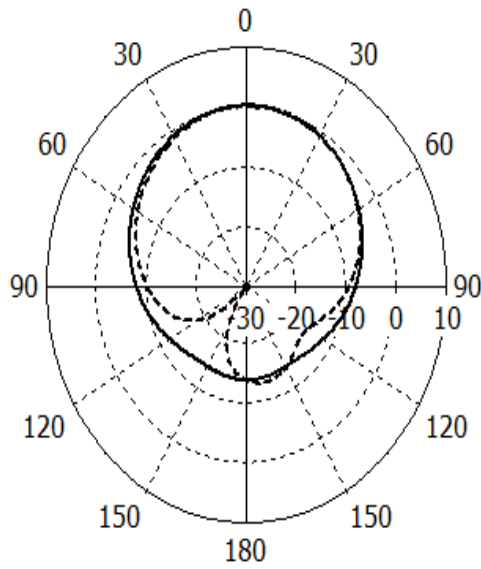
The first iteration was simulated at higher frequency to see the multiband behaviour. The antenna is resonating at six different frequencies with first resonant occurring at

1.71GHz with return loss of -20.7dB. Table 5.1 shows the behaviours exhibit by the antenna in first iteration.

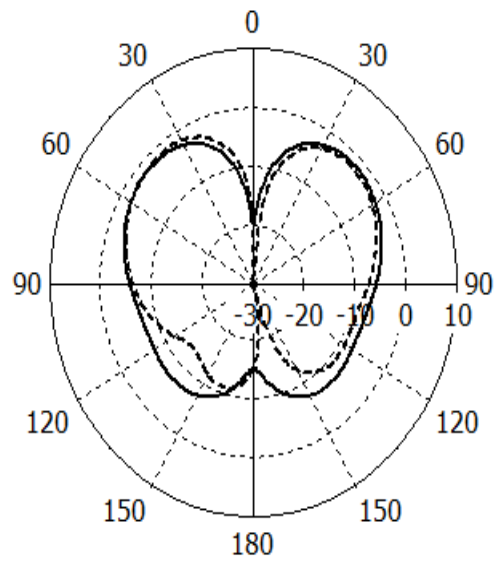
Table 5.1: Results of the circular patch first iteration.

Centre Frequency (GHz)	S11 (dB)	Upper Frequency (GHz)	Lower Frequency (GHz)	Bandwidth (MHz)	Gain (dB)	Efficiency (%)
1.71	-20.7	1.735	1.6918	43	0.166	25
3.07	-17	3.1012	3.0496	51	-1.38	25
4.48	-16	4.546	4.412	134	3.59	51
5.59	-19.7	5.6184	5.5578	60	-2.48	15
6.72	-14.5	6.7497	6.693	55	-0.914	13
9.12	-12.9	9.1704	9.092	78	4.44	44

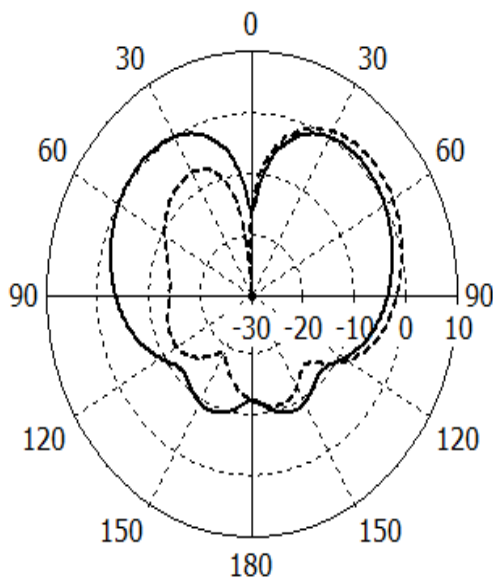
From the result shown above we can see that the first iteration demonstrate multiband behaviour resonating at six frequencies. The antenna has highest efficiency of 51% occurring at 3.59GHz. The radiation patterns for the resonant frequencies are shown in Figure 5.5(a-f)



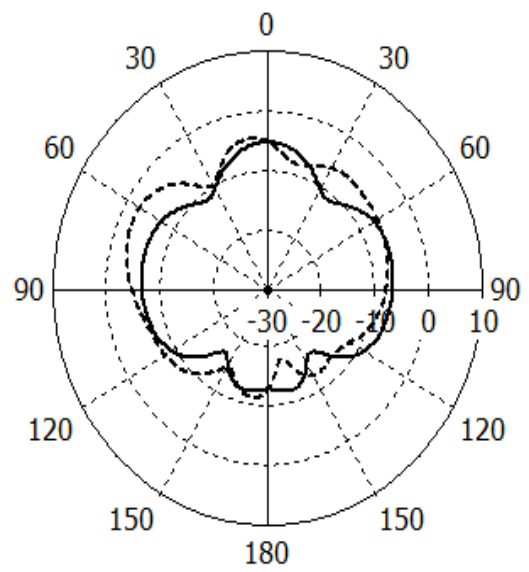
Theta / Degree vs. dB
 ----- farfield (f=1.71) E-plane
 ————— farfield (f=1.71) H-plane
 Figure 5.5(a)



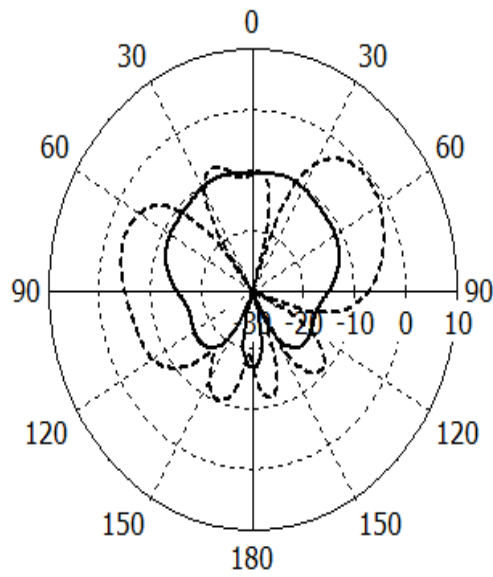
Theta / Degree vs. dB
 ----- farfield (f=3.07) E-plane
 ————— farfield (f=3.07) H-plane
 Figure 5.5(b)



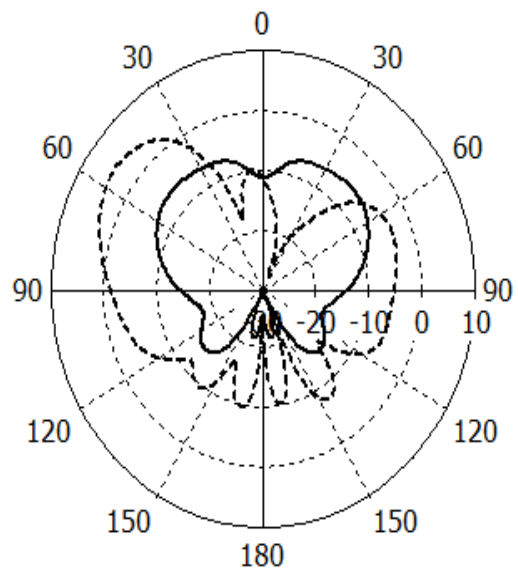
Theta / Degree vs. dB
 ----- farfield (f=4.48) E-plane
 ————— farfield (f=4.48) H-plane
 Figure 5.5(c)



Theta / Degree vs. dB
 ----- farfield (f=5.59) E-plane
 ————— farfield (f=5.59) H-plane
 Figure 5.5(d)



Theta / Degree vs. dB
 - - - - farfield (f=6.72) E-plane
 ——— farfield (f=6.72) H-plane
 Figure 5.5(e)



Theta / Degree vs. dB
 - - - - farfield (f=9.12) E-plane
 ——— farfield (f=9.12) H-plane
 Figure 5.5(f)

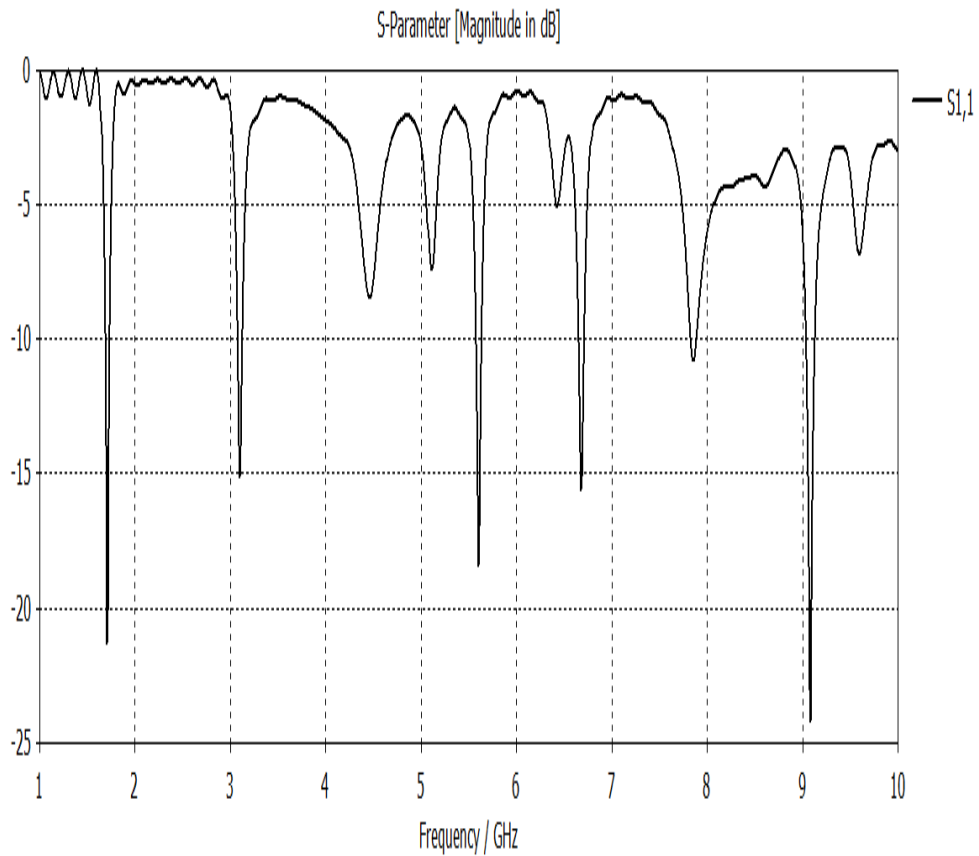


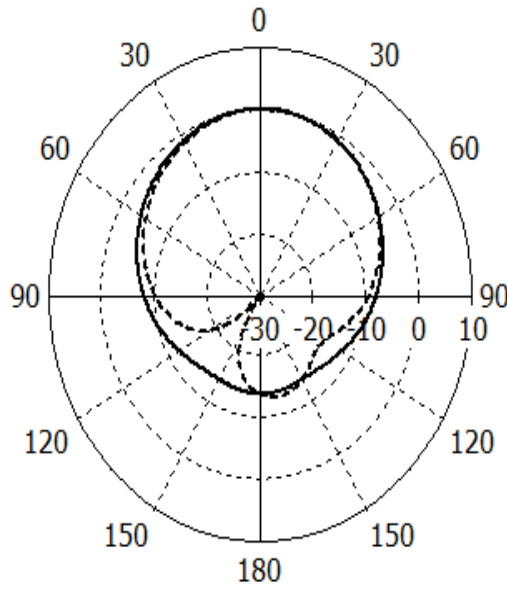
Figure 5.6: Return loss for the second iteration

The second iteration which was simulated up till 10GHz has a multiple band of operation with six different resonant frequencies.

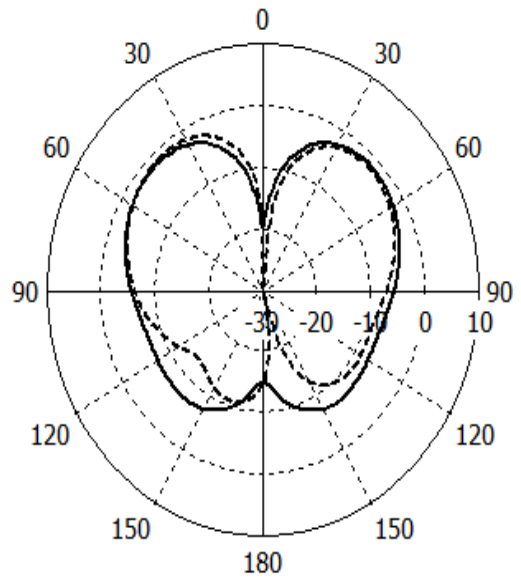
Table 5.2: Results of the circular patch second iteration.

Centre Frequency (GHz)	S11 (dB)	Upper Frequency (GHz)	Lower Frequency (GHz)	Bandwidth (MHz)	Gain (dB)	Efficiency (%)
1.7	-21.2	1.7284	1.6849	43	0.12	27
3.09	-15	3.1234	3.0729	50	-1.23	25
5.6	-18	5.6308	5.5713	59	-0.213	16
6.79	-15.4	6.7112	6.652	59	-2.24	13
7.85	-10.8	7.8886	7.8241	64	-1.6	10
9.08	-24	9.128	9.0327	95	-0.172	11

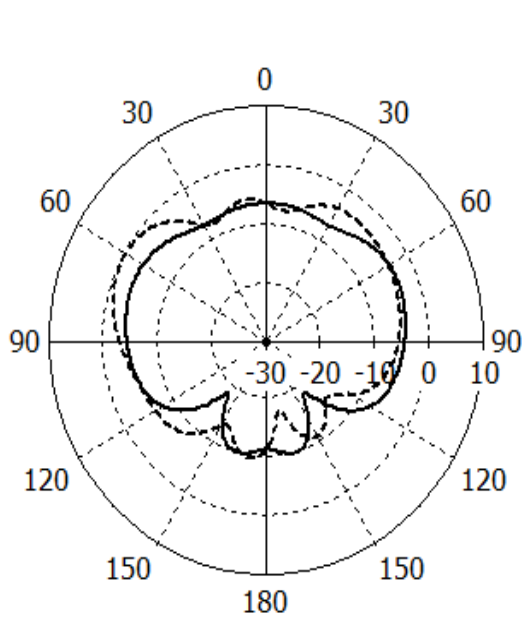
From the above tabulated results, it can be observed that after the second iteration, the antenna performance start diminishing. The antenna shows low gain and low efficiency. This might be due to antenna losses and also fractal cuts made in the antenna. The far field radiation patterns at the resonant frequencies are display below in Figure 5.7(a-f).



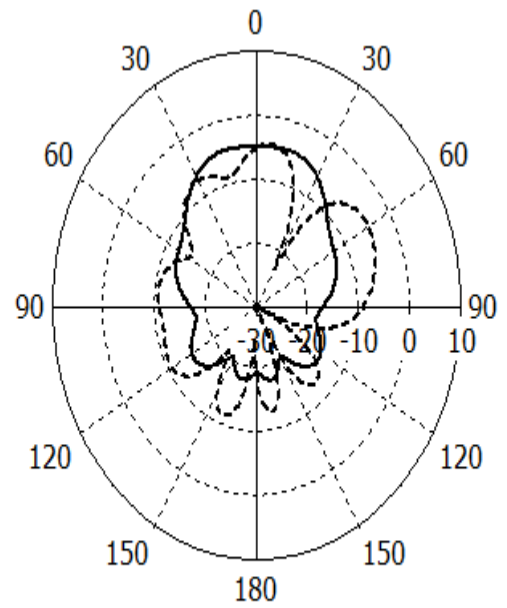
Theta / Degree vs. dB
 ----- farfield (f=1.7) E-plane
 ——— farfield (f=1.7) H-plane
 Figure 5.7(a)



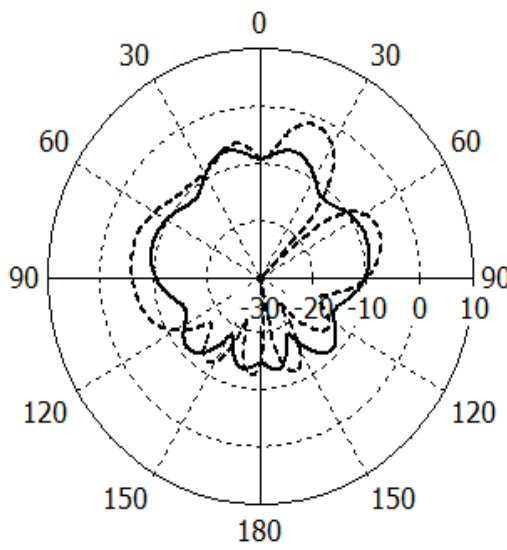
Theta / Degree vs. dB
 ----- farfield (f=3.09) E-plane
 ——— farfield (f=3.09) H-plane
 Figure 5.7(b)



Theta / Degree vs. dB
 ----- farfield (f=5.6) E-plane
 ——— farfield (f=5.6) H-plane
 Figure 5.7(c)



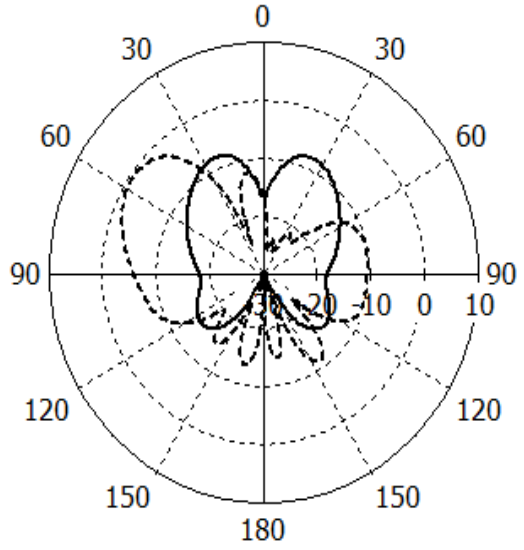
Theta / Degree vs. dB
 ----- farfield (f=6.79) E-plane
 ——— farfield (f=6.79) H-plane
 Figure 5.7(d)



Theta / Degree vs. dB

----- farfield (f=7.85) E-plane
 ——— farfield (f=7.85) H-plane

Figure 5.7(e)



Theta / Degree vs. dB

----- farfield (f=9.08) E-plane
 ——— farfield (f=9.08) H-plane

Figure 5.7(f)

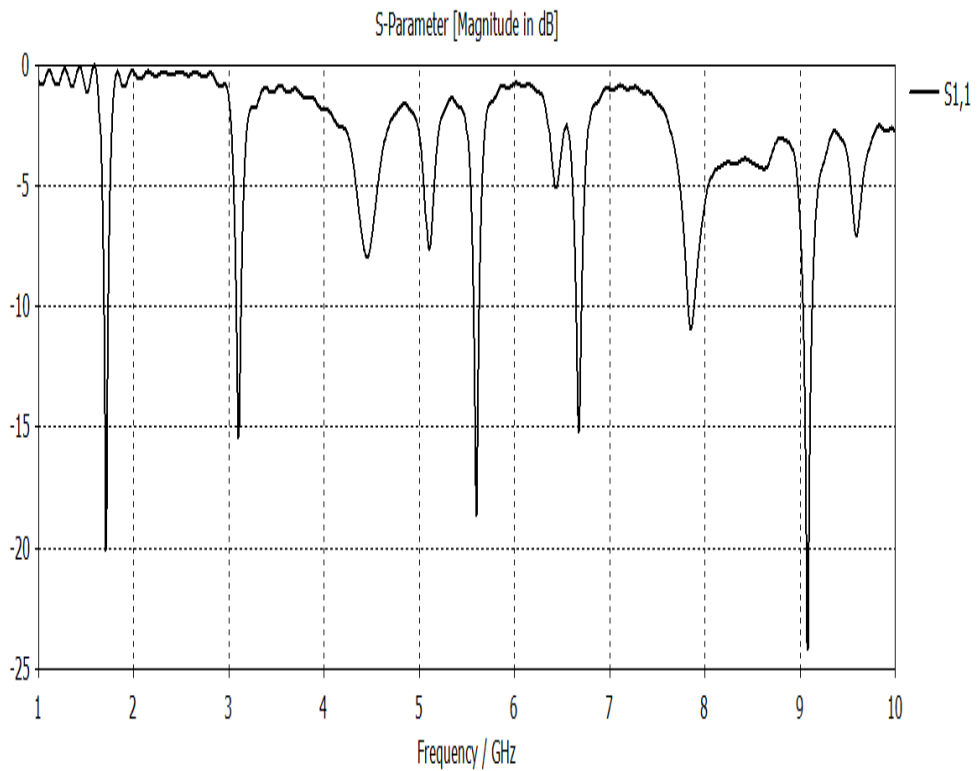
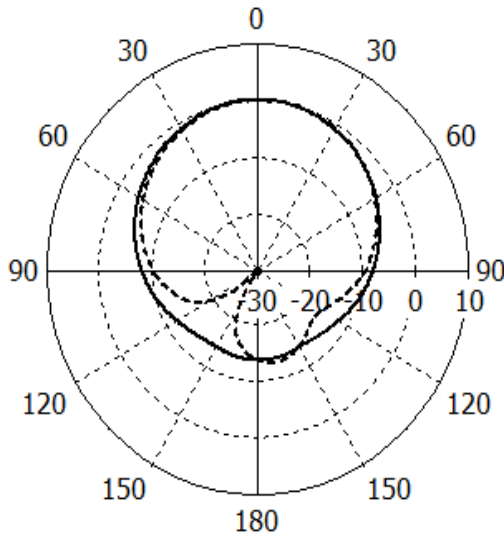


Figure 5.8: Return loss for third iteration

Table 5.3: Results of the circular patch third iteration.

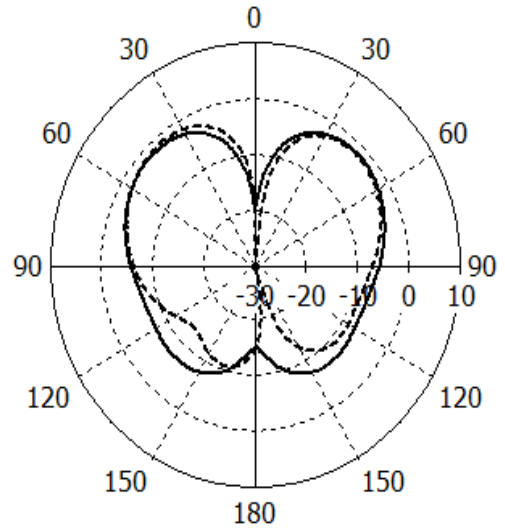
Centre Frequency (GHz)	S11 (dB)	Upper Frequency (GHz)	Lower Frequency (GHz)	Bandwidth (MHz)	Gain (dB)	Efficiency (%)
1.7	-20	1.7278	1.6828	44	0.107	27
3.09	-15.2	3.1272	3.0748	52	-1.27	25
5.6	-18.5	5.6668	5.627	60	-0.32	16
6.65	-15.5	6.7078	6.649	58	-2.5	13
7.85	-10.8	7.8886	7.8241	64	-1.63	10
9.08	-24	9.1288	9.0294	99	-0.03	15

From the tabulated results of third iteration, we can observed that the third iteration has almost similar result to the second iteration in terms of return loss and bandwidth but with some reduction in gain and efficiency due to fractals cut and losses in the antenna. The far field radiation patterns at the resonant frequencies are display below in Figure 5.9(a-f).



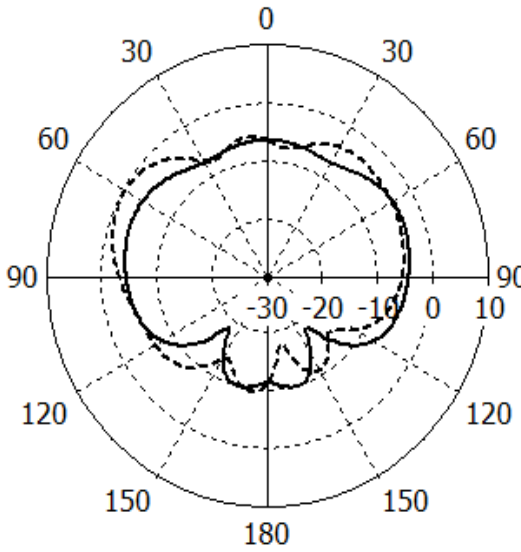
Theta / Degree vs. dB
 - - - - farfield ($f=1.7$) E-plane
 ——— farfield ($f=1.7$) H-plane

Figure 5.9(a)



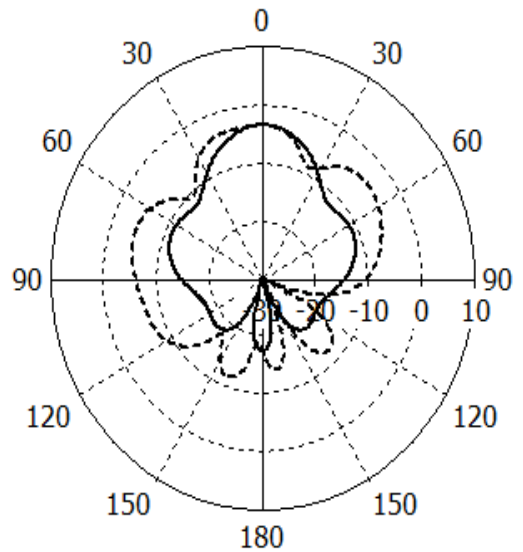
Theta / Degree vs. dB
 - - - - farfield ($f=3.09$) E-plane
 ——— farfield ($f=3.09$) H-plane

Figure 5.9(b)



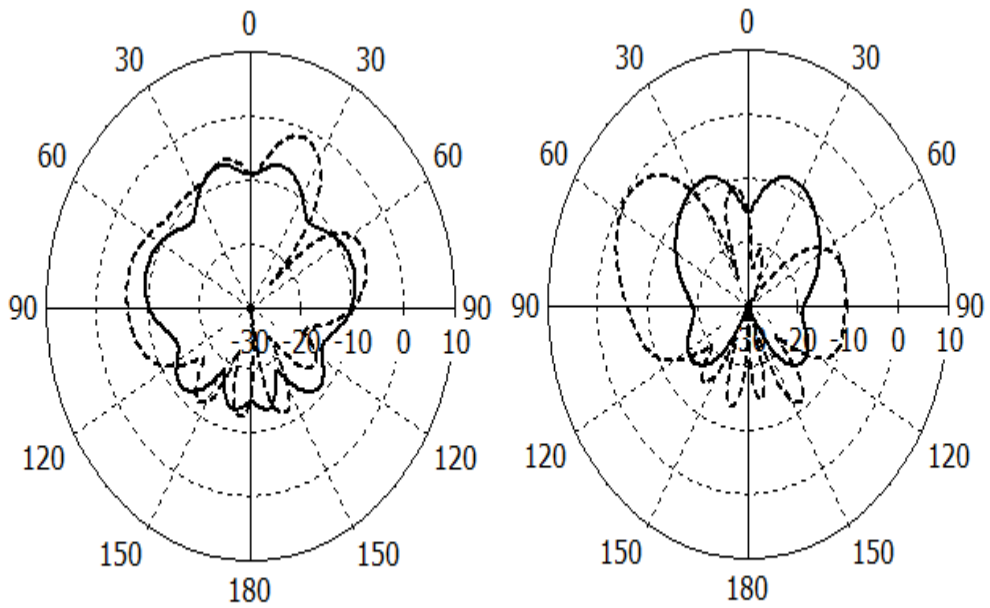
Theta / Degree vs. dB
 - - - - farfield ($f=5.6$) E-plane
 ——— farfield ($f=5.6$) H-plane

Figure 5.9(c)



Theta / Degree vs. dB
 - - - - farfield ($f=6.65$) E-plane
 ——— farfield ($f=6.65$) H-plane

Figure 5.9(d)



Theta / Degree vs. dB
 ----- farfield (f=7.85) E-plane
 ————— farfield (f=7.85) H-plane

Figure 5.9(e)

Theta / Degree vs. dB
 ----- farfield (f=9.08) E-plane
 ————— farfield (f=9.08) H-plane

Figure 5.9(f)

We can see that the antenna shows a multiband behaviour after third iteration. When compared with the Third iteration Sierpinski Carpet using square patch, the circular patch has lower gain, lower bandwidth and efficiency after the third iteration. This problem of low gain, Bandwidth and efficiency will be tackled by using partial ground plane.

5.2 Circular Fractal with Partial Ground Plane.

In most common form of microstrip patch antennas, the metal patch is on the top of grounded dielectric substrate. When the patch antenna is energized, it radiates Electromagnetic waves in all directions and the Electromagnetic waves that travel in the substrate is known as surface waves. Losses due to these surface waves is known as surface wave losses, this is the main loss associated with microstrip patch antennas that reduce the gain of microstrip patch antennas [28]. For suppression of

surface wave, metallic ring was introduced on to the radiating patch with defected ground structure in [28] to enhance the gain of the patch antenna. The surface waves were provided with an in phase excitation rather than suppressing them and this was achieved by introducing parasitic patches at the partial ground plane [29]. In this study, partial ground plane comprising of circular and slotted rectangular structure placed above and below the feed line was used in enhancing the gain and achieving ultra-wideband behaviour. The structure of the antenna is shown in Figure 5.10.

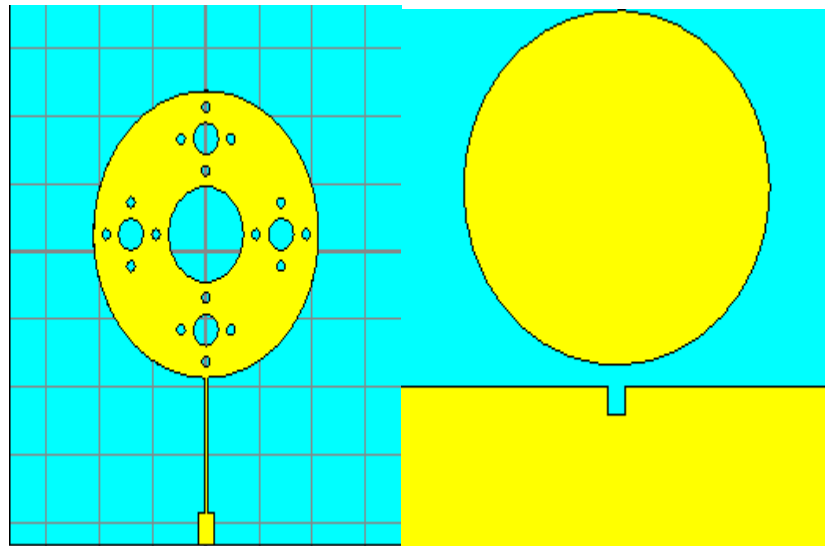


Figure 5.10: Front and back view of third iteration with partial ground plane

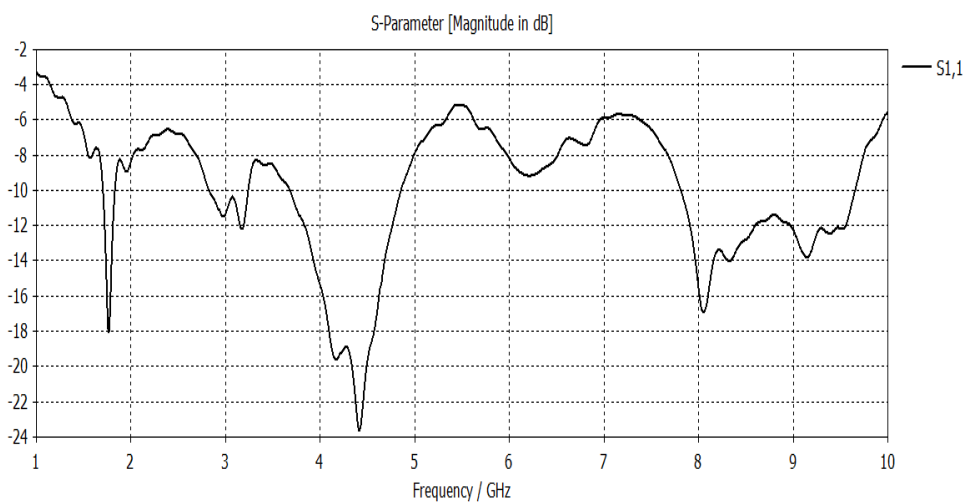


Figure 5.11: Return loss plot for partial ground third iteration

From the return loss plot, we can see that the antenna shows multiband and wideband behaviour with highest bandwidth of 1.86GHz at centre frequency of 8GHz. To further enhance the bandwidth of the antenna in order to cover the ultra-wide band range of (3-10)GHz, quarter wave transformer is used to match the load to 50Ω microstrip. The proposed designed is shown in Figure 5.12.

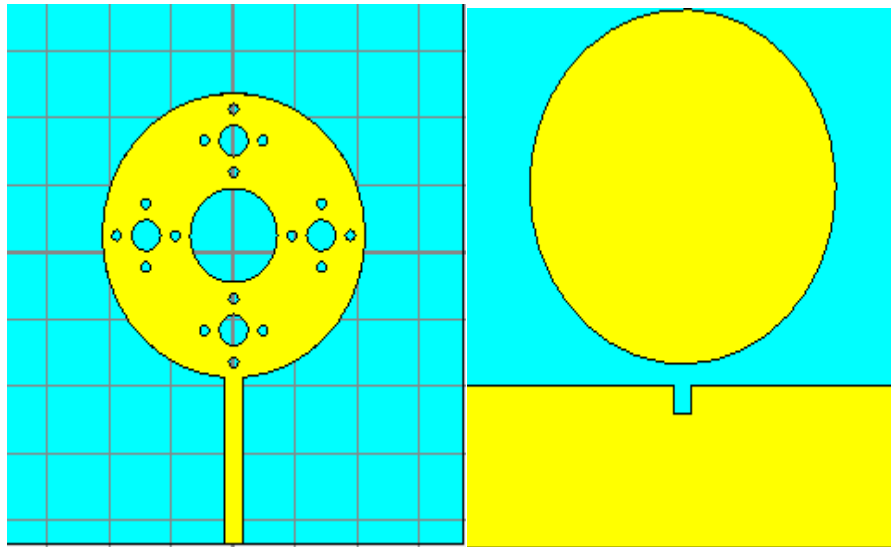


Figure 5.12: showing front and back view of proposed design

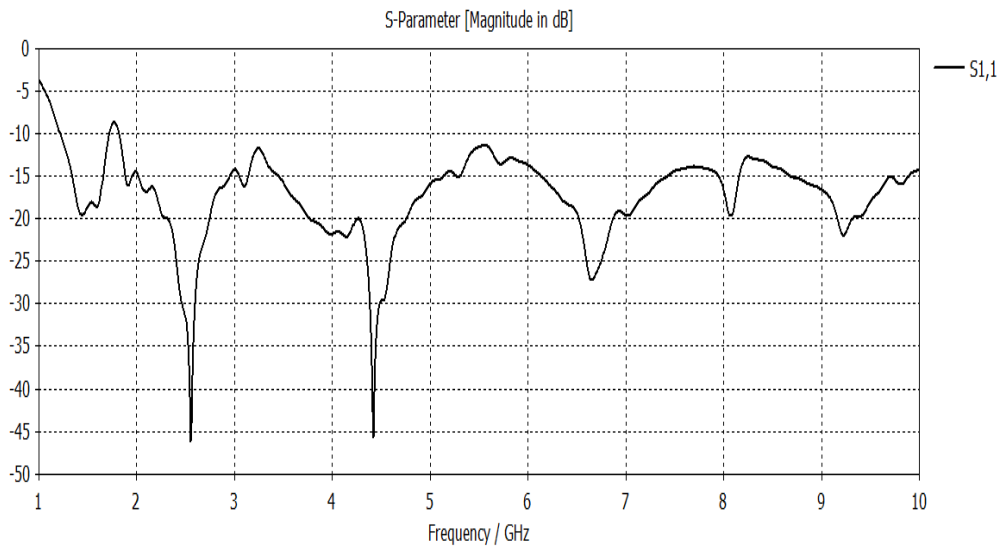


Figure 5.13: Return loss plot of the proposed Design

From the return loss plot, the antenna shows multiband with ultra-wideband behaviour having a bandwidth of 8.18GHz in the frequency range of 1.81GHz-10GHz with centre frequency of 2.54GHz.

Table 5.4: Results of the Proposed Design.

Centre Frequency (GHz)	S11 (dB)	Upper Frequency (GHz)	Lower Frequency (GHz)	Bandwidth (MHz)	Gain (dB)	Efficiency (%)
1.88	-15	10	1.8196	8180	2.67	83
2.54	-45	10	1.8196	8180	3.49	95
3.0	-15	10	1.8196	8180	5.06	94
4.45	-45	10	1.8196	8180	3.85	86
5.18	-15	10	1.8196	8180	5.42	86
6.65	-15.5	10	1.8196	8180	3.8	87
7.85	-10.8	10	1.8196	8180	3.49	86
9.08	-24	10	1.8196	8180	5.66	82

With the use of partial ground, we can see that the antenna exhibit wide band and multiband behaviour compared to the conventional circular patch in the previous iterations. Comparisons were made between the proposed circular fractal and the Square patch Sierpinski Carpet fractal. From the simulation result, the return loss plot shows that at the initial stage, both square and the circular patch have same resonant. With the use of partial ground on the circular fractal shape, performance enhancement in terms of bandwidth, gain and efficiency were achieved which is better than the third other Sierpinski carpet using square patch. Furthermore, the square patch antenna was originally designed at 1.88GHz .After the Sierpinski

iteration, the antenna no longer has resonant at the designed frequency but with the case of partial ground circular fractal the antenna still operate at the original designed frequency.

Polar plot and 3D radiation patterns of the proposed antenna measured at some frequencies were shown in Figure 5.14. From 1.88GHz-3GHz the antenna H- plane radiation pattern has main lobe magnitude along the zero degree. At higher frequencies, the pattern becomes directional.

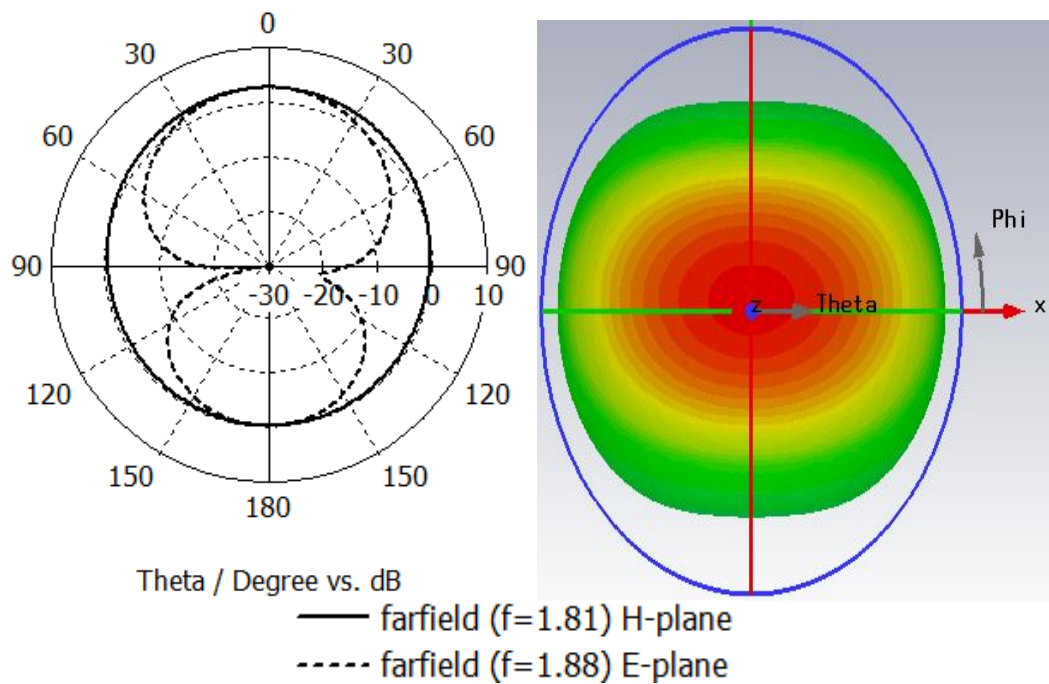


Figure 5.14(a): Polar plot and 3D radiation pattern at f=1.88GHz

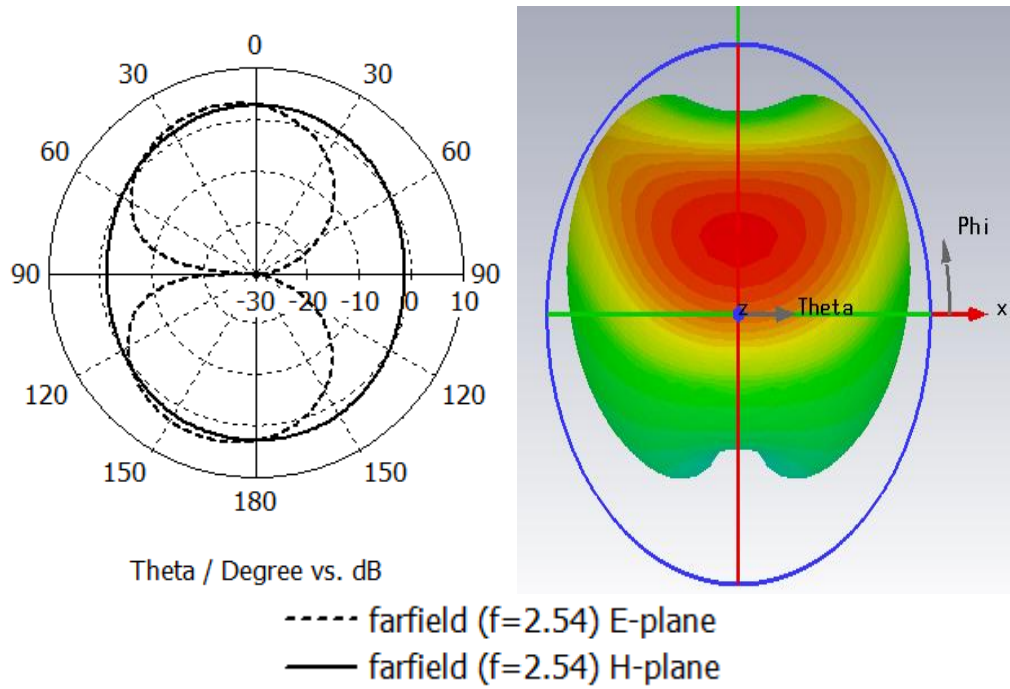


Figure 5.14(b): Polar plot and 3D radiation pattern at f=2.54GHz

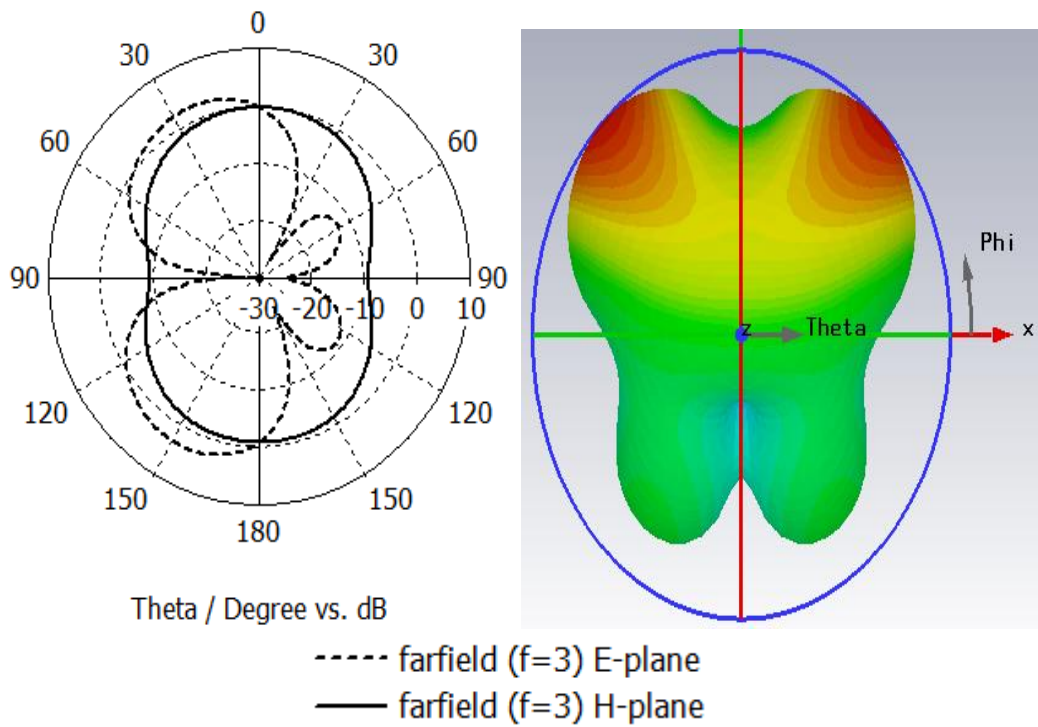


Figure 5.14(c): Polar plot and 3D radiation pattern at f=3GHz

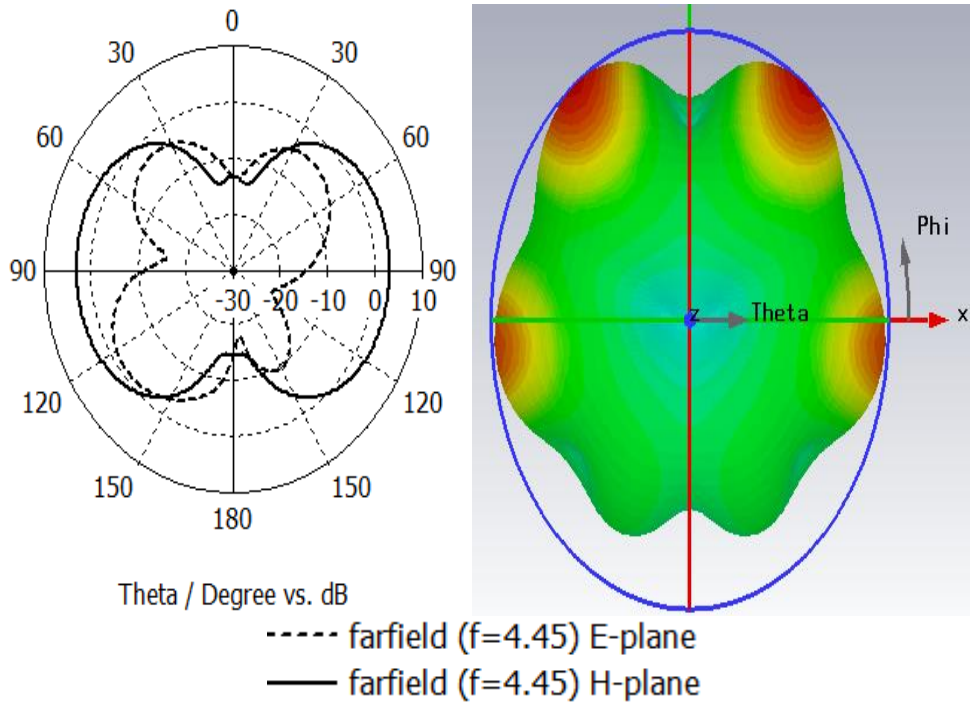


Figure 5.14(d): Polar plot and 3D radiation pattern at f=4.45GHz

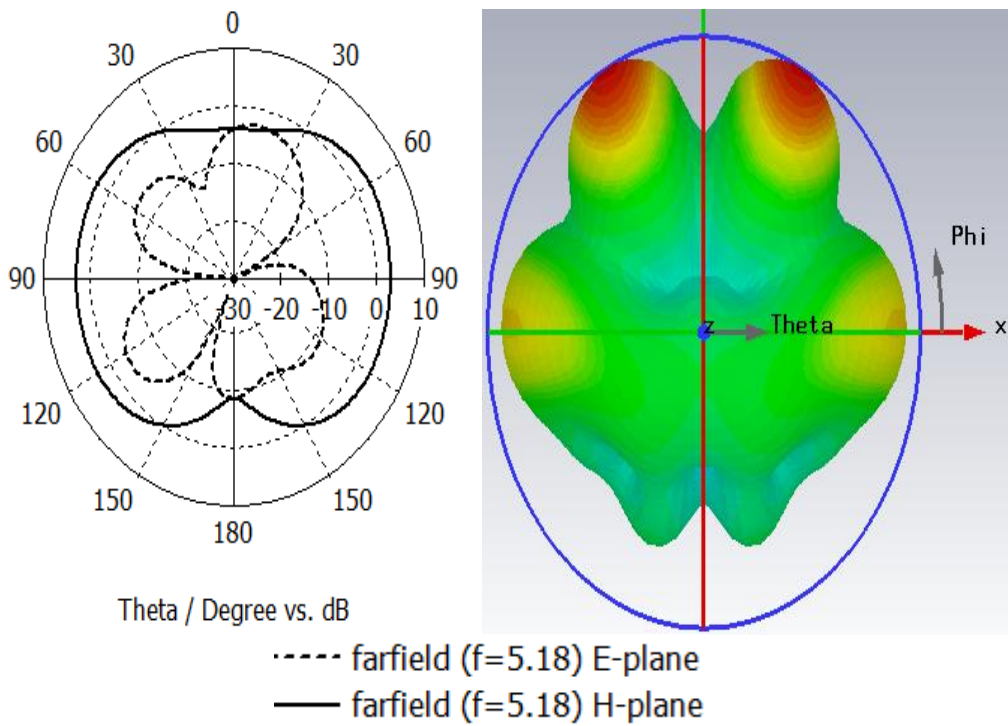


Figure 5.14(e): Polar plot and 3D radiation pattern at f=5.18GHz

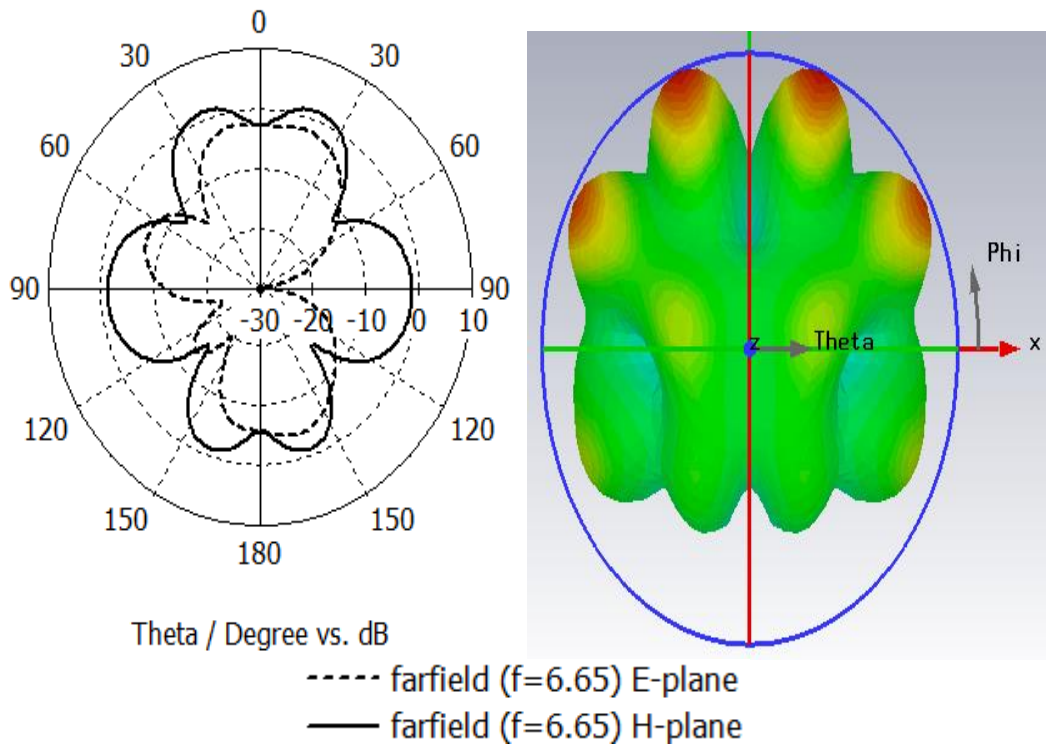


Figure 5.14(f): Polar plot and 3D radiation pattern at f=6.65GHz

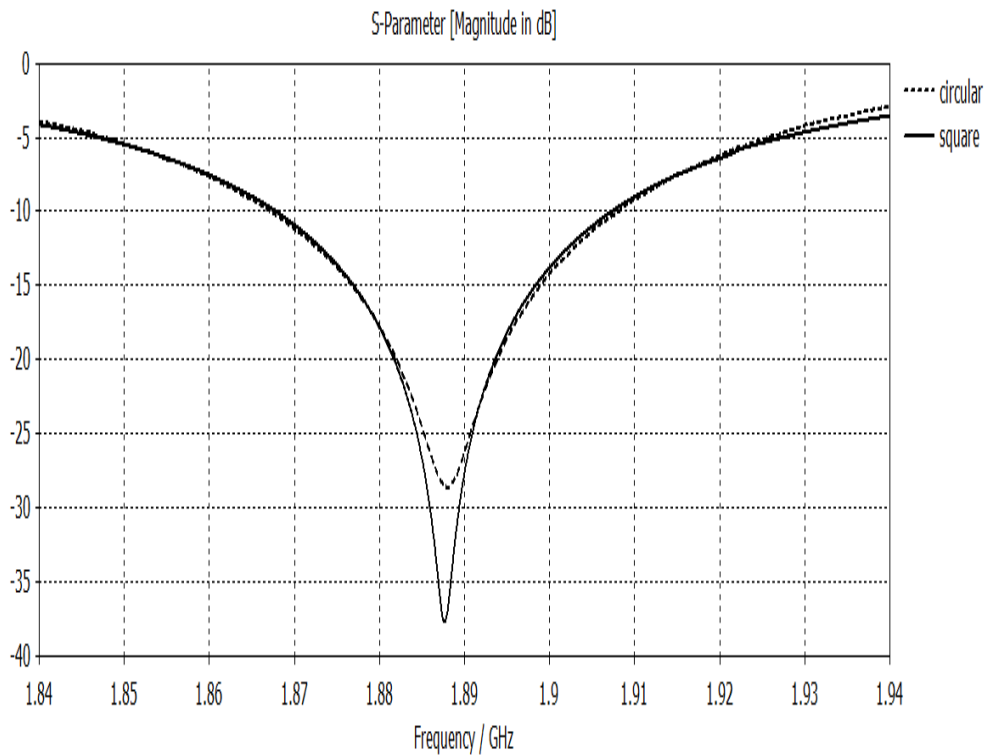


Figure 5.15: Return loss plot of square and circular patch antenna without iteration

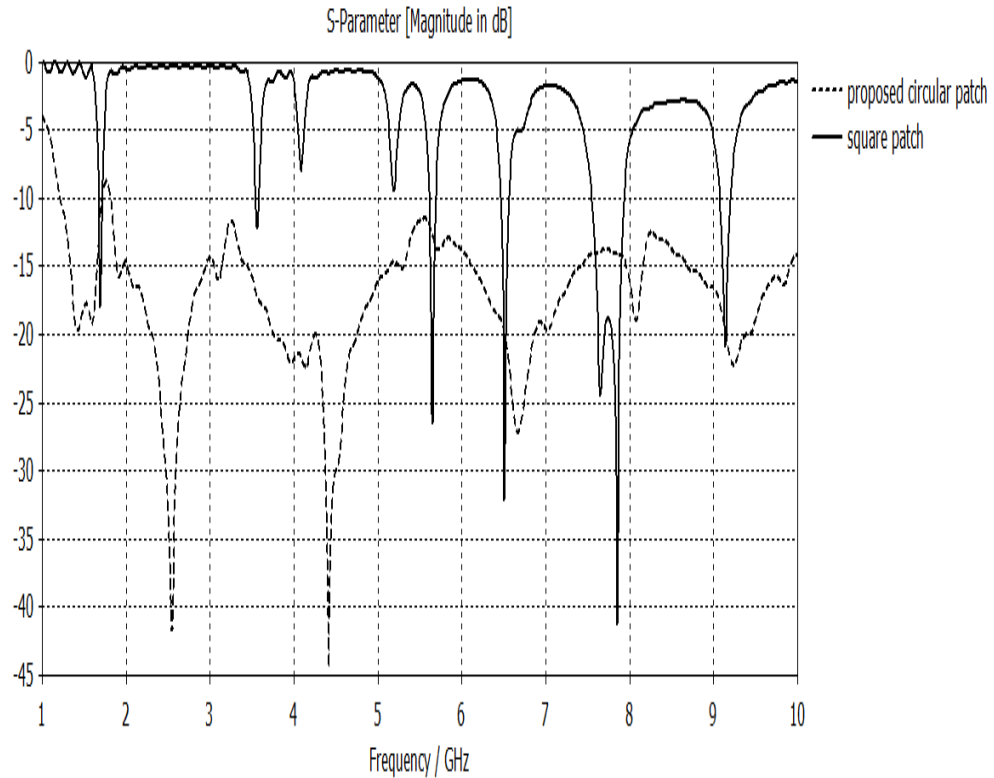


Figure 5.16: Return loss plot of third iteration sierpinski carpet and proposed Partial ground circular fractal

As we can see from the range of frequencies covered by the proposed antenna, this antenna can find applications in several areas like WLAN, WIMAX, Microwave landing systems, Radio determination applications, Aeronautical telemetry, Passive sensors, Radar Imaging Technology, Real Time Location System, Active sensors. Defence systems etc.

Chapter 6

CONCLUSION AND FUTURE WORK

6.1 Conclusion

In this thesis, fractal geometry was applied to rectangular, square and circular microstrip patch antenna. A rectangular antenna was fed at the edge using Sierpinski Carpet fractal geometry up to third iteration to achieve 17.96% size reduction. A new modified miniaturized patch antenna was designed incorporated with U shape defected ground structure. Miniaturization by 34.88% size reduction and a bandwidth enhancement were achieved without affecting the operating frequency of the antenna. A multiband third order Sierpinski carpet square patch antenna having six different resonant frequencies was designed. A new circular fractal antenna was designed up to third iteration. The designed circular fractal antenna has a low gain, low bandwidth and low efficiency. A new approach using a partial ground plane technique was proposed to enhance the gain, bandwidth and the efficiency of the circular fractal antenna. The proposed antenna was able to achieve up to 8.18GHz of bandwidth at centre frequency of 2.54GHz. Also, the gain and efficiency was enhanced by achieving up to 95% radiation efficiency. The objective of the thesis to design a fractal antenna with small size, multiband and wideband behaviour was achieved at the end of the thesis.

6.2 Future Work

As we know that fractal antenna area is still in its early stage. There is still a lot of future configuration to be made. Future work will involve incorporating a reconfigurable technique to make the antenna suitable for switching to desired band of operation.

REFERENCES

- [1] A. Balanis, *Antenna Theory Analysis and Design* (3rd ed.), New York: New Jersey: John Wiley & Sons, Inc., 2005.
- [2] B. Shi, Z. Long, J. Wang and L. Yang, "Design and analysis of a modified Sierpinski Carpet fractal antenna for UWB applications," *Proceedings of the International Symposium on Antennas & Propagation (ISAP)*, vol.1, pp. 99- 102, 2013.
- [3] M. Hayder, R. Uyguroglu, "Multiband Wideband Antenna Design", Master's Thesis, Eastern Mediterranean University, 2013.
- [4] N. Lu and X. Xu, "Sierpinski carpet fractal antenna in third iteration," *IEEE International Conference on Microwave Technology & Computational Electromagnetics (ICMTCE)*, pp. 164- 167, 2013.
- [5] V. Dinesh and G. Karunakar, "Analysis of microstrip rectangular carpet shaped fractal antenna," *International Conference on Signal Processing and Communication Engineering Systems (SPACES)*, pp. 531- 535, 2015.
- [6] S. S. Mohammed, K. Ramasamy, T. Shanmuganatham, "A 2.45GHz Sierpinski Carpet edge-fed microstrip patch fractal antenna for WPT rectenna," *7th International Multi-Conference on Signals Systems and Devices (SSD)*, pp. 1-4, 2010.

- [7] W. Chen and G. M. Wang, "Small Size Edge-Fed Sierpinski Carpet Microstrip Patch Antenna," *Progress in Electromagnetics Researches*, vol. 3, pp. 195-202, 2008.
- [8] R. Mohanamurali and T. Shanmuganatham, "Sierpinski Carpet Fractal Antenna for Multiband Applications," *International Journal of Computer Applications*, vol. 39, pp. 19-23, 2012.
- [9] S. Shrestha, J. J. Park, S. K. Nouh and D. Y. Choi, "Design of 2.45 GHz Sierpinski Fractal Based Miniaturized Microstrip Patch Antenna" *IEEE 18th Asia-Pacific Conference on Communications (APCC)*, pp. 36-41, 2012.
- [10] R. Roopa, M. Sarka and T. S. Jayadeva, "Optimization of Sierpinski Carpet Fractal Iteration," *International Journal of Advanced Research in Computer Science and Software Engineering*, vol. 5, no. 2, pp. 835-839, 2015.
- [11] A. Khanna, D. K. Srivastava, J. P. Saini, "Bandwidth enhancement of modified square fractal microstrip patch antenna using gap-coupling," *Engineering Science and Technology, an International Journal*, vol. 18, pp. 286-293, 2015.
- [12] R. Saini and D. Parkash, "Design and Simulation of CPW fed Slotted Circular Microstrip Antenna with DGS for Wireless Applications," *Int. Journal of Applied Sciences and Engineering Research*, vol. 3, no. 1, pp. 82-90, 2014.
- [13] O. Kaka, M. Toycan and V. Bashiry, "Modified Hilbert fractal geometry, multiservice, miniaturized patch antenna for UWB wireless communication,"

The International Journal for Computation and Mathematics in Electrical and Electronic Engineering, vol. 31, no. 6, pp. 1835-1849, 2012.

- [14] Y. J. Sung, "Bandwidth enhancement of a wide slot using fractal-shaped Sierpinski," *IEEE Transactions on Antennas and Propagation*, vol. 59, no. 8, pp. 3076-3079, 2011.
- [15] R. Mishra, R. Ghatak and D. Poddar, "Design formula for sierpinski gasket pre fractal planar monopole antennas," *IEEE Antennas and Propagation Magazine*, vol. 50, no. 3, pp. 104-107, 2008.
- [16] Y. Kumer, S. Kumer and R. Jyoti, "Sectorial sierpinski gasket fractal antenna for wireless LAN applications," *International Journal of RF and Microwave Computer Aided Engineering*, vol. 22, no. 1, pp. 68-74, 2012.
- [17] L. Chen, Y. Chang and H. Xie, "Minkowski fractal patch antenna for size and radar cross section reduction," *IEEE CIE International Conference*, vol. 2, pp. 1406-1409, 2011.
- [18] A. Younas, "A new directivity fractal antenna based on modified Koch snowflake geometry," *Asia-Pacific Microwave Conference Proceedings (APMC)*, pp. 191-194, 2010.
- [19] A. Tiwari, B. Sharma, D. Bhatnagar, V. Sharma, and S. Chakrabarti, "Design of compact wideband key-slotted circular microstrip patch antenna with modified ground plane", *Applied Electromagnetics Conference (AEMC)*, pp. 1-2, 2013 .

- [20] G. Debatosh and M. M. Yahia , *Microstrip and Printed Antennas New Trends, Techniques and Applications*, Wiley Int. Sc., U.K., 2011.
- [21] K. Baskaran , C.P. Lee and K.C. Chandan, “A Compact Microstrip Antenna for Ultra-wideband Applications,” *European Journal of Scientific Research*, ISSN 1450-216X vol.67, no.1, pp. 45-51, 2011.
- [22] C. Y. Pan, J. H. Duan and J. Y. Jan, “Coplanar Printed Monopole Antenna using Coaxial Feed line for DTV Application,” *Progress In Electromagnetics Research Letters*, vol. 34, pp.21 - 29, 2012.
- [23] “Square Microstrip Patch Antenna Aperture Coupling Feed,” available at <http://lib.znate.ru/docs/index-149720.html?page=4>, last accessed June 2015.
- [24] “Koch Curve Fractal Iteration,” available at <http://www.vanderbilt.edu/AnS/psychology/cogsci/chaos/workshop/Fig4.7.GIF>, last accessed June 2015.
- [25] “Sierpinski Gasket Fractal Iteration,” available at <http://math.bu.edu/DYSYS/chaos-game/sierp-det.GIF>, last accessed June 2015.
- [26] S.Gupta and S. Singh, “Bandwidth Enhancement in Multilayer Microstrip Proximity Coupled Array,” *International Journal of Electronics and Computer Science Engineering*, vol.1, no.2, pp. 287-293, 2012.
- [27] “Microstrip Patch Antenna Calculator,” available at

<http://www.emtalk.com/mpacalc.php>, last assessed June 2015.

- [28] A. kumar and M. Kumar, "Gain Enhancement in Microstrip-Feed Patch Antenna Using Metallic Ring and DGS," *International Journal of Electronics and Computer Science Engineering*, vol. 3, no. 3, pp. 332-338, 2014.
- [29] G. S Reddy, S. K. Mishra, S. Kharche, and J. Mukherjee, "High gain and low cross-polar compact Printed elliptical monopole UWB antenna loaded with partial ground and parasitic Patches," *Progress in Electromagnetics Researches B*, vol. 43, pp. 151-167, 2012.